The Design, Manufacture and Testing of a Composite Polysialic Acid Mimetic Peptide Loaded Collagen Nerve Graft for Use in Peripheral Nerve Repair

A thesis submitted to the National University of Ireland Galway

for the

Degree of MD in Surgery

By

Mr. Jaime Patrick Doody MRCSI, BCh, MB, BAO, BA

Network of Excellence for Functional Biomaterials

National University of Ireland Galway

December 2014

Research Supervisors: Professer Jack Kelly, Professor Abhay Pandit

Table of Contents

List of Figures

List of Tables

Acknowledgements

To my parents, I would like to thank you for supporting me all through my career and encouraging me to be the best person and doctor I can possibly be. You are my rock and my shelter and have always been there for me at every single step of my life. We always knew the path to success would be bumpy but because of your love and advice I never lose hope and know that anything is possible. I dedicate this thesis solely to you.

To Katie, you have no clue how thankful I am for you putting up with me and my thesis writing over the last few months. Your advice, support, encouragement and occasional butt-kicking have been instrumental in me completing this immense task. After this, I know there is no feat too great we cannot complete together. Onwards, upwards and westwards!

I would like to thank Bill Daly. For my time in Galway, Bill, you were my lab partner, housemate and, most importantly, friend. This would not have happened without you man.

I would like to thank Jacqui O'Connor. You were a source of much needed support and friendship during the highs and lows of my research years.

I would like to thank Ciarstan McArdle, my "cell-mate". We both entered into the world of research at the same time, not really knowing what to expect be they highs, lows or anything else in between. Ciarstan, only you will ever fully appreciate what went into this research and are the only person that will ever understand the sacrifice and cost of those research years.

To Ailbhe McDermott, you are a legend.

I am especially grateful to Professor Jack Kelly. Your eternal optimism and sound advice gave me the encouragement I needed to see this project through. I would also like to extend my gratitude to Professor Abhay Pandit for taking me into his group and allowing me conduct my research with every amenity at my disposal.

I would also like to express my gratitude to Graeme Kelly and Marc DeVocelle for allowing me work in their lab in RCSI. They were incredibly accommodating and extended every courtesy to this surgical "shoo-in".

Lastly, to all the staff of the NFB: Oliver Carroll, Dimitrios Zeugolis, Michael Monaghan, Carolyn Halliday, Estelle Collin, Tara Cosgrove and all the gang. Thanks for your help, it was all greatly appreciated.

Abstract

Peripheral nerve injuries can be debilitating for patients. The current gold-standard technique for peripheral nerve repair is autograft. This procedure involves harvesting a non-critical nerve from a donor site from the same individual before using this autogenous neural tissue to repair the injured area. There are several disadvantages associated with this technique and outcomes vary. The field of biomedical engineering has yielded several alternatives to autograft, but none of which are ideal and very few of which have been carried over into clinical practice. The "ideal graft" would be inexpensive, easy to make, easy to handle, have low antigenicity, good biodegradability and promote neural regeneration better than autograft. Resaerch has shown that physical cues and biochemical cues play important roles in neural graft design. Collagen is an excellent substance for use as a grafting material. It is versatile. It has low antigenicity. It is also relatively inexpensive and has shown experimentally to be useful in nerve grafting. Polysialic acid (PSA) is a polypeptide that has been linked to peripheral nerve growth, maintenance and repair. It is a difficult substance to work with. Polysialic mimetic peptides have been shown to exert identical effects to native PSA in biological systems. In this project, a nerve graft was designed and manufactured to take advantage of the neural regenerative physical cues afforded by a collagen fibre packed nerve conduit and the chemical cues provided by a PSA mimetic. This conduit was tested in live subjects and was shown to perform as good as autograft across several difference morphometric criteria. In the course of this project, a novel method was developed for chemically modifying collagen, a notoriously inert substance.

1 Introduction

Peripheral nerve injury and its subsequent repair are commonplace. Over 50,000 nerve repair procedures were performed in the USA in 1995 (National Center for Health Statistics based on Classification of Diseases, 9th Revision, Clinical Modification for the following categories: ICD-9 CM Code: 04.3, 04.5, 04.6, 04.7). This figure is thought to underestimate the total number of nerve injuries [1]. Many peripheral nerve injuries are diagnosed but repair is not possible due to the limitation of current therapies.

Figure 1.1 Compound injury to right hand with extensive neural tissue loss. Courtesy of Prof. Jack Kelly, FRCS, UCHG Galway.

Among the most challenging peripheral nerve injuries to treat are those involving loss of neural tissue, leaving a so-called "nerve gap". For the nerve to heal correctly, it must bridge the nerve gap during its regeneration. At the Network of Excellence for Functional Biomaterials we are at the forefront of research into finding suitable biomaterial solutions to the problem of bridging the nerve gap.

Peripheral nerve injuries can be severely disabling and interfere greatly with a patient's quality of life. This project is based on the clinical experience of operating on these patients in the acute phase after injury and seeing the problems associated with poor surgical outcome due to the limitations of current techniques and materials. The cost of

these injuries to the economy is significant [2] but the personal and emotional cost of a person being burdened with a lifelong disability is immeasurable.

The current "gold standard" repair for peripheral nerve injury involving loss of neural tissue is autografting [3-4]. The use of autograft is not ideal as it involves the morbidity of two surgical sites (the injured site itself as well as the donor tissue site), is limited by the availability of suitable donor tissue and is associated with its own complications (e.g. neuroma formation). Large scale studies reviewing patients with peripheral nerve injury treated by autografting show that only around 50 % of patients achieve optimal function under ideal conditions [5] with full function rarely being achieved [6].

Current techniques are limited, in both application and outcome. The "ideal" grafting material should be exogenous. This would remove the need for a second operative site for graft harvesting and mean a limitless supply of grafting material. The "ideal" graft should be safe, efficacious and illicit few side effects (e.g. neuroma formation or graft rejection).

In this project we attempted to bridge a nerve gap using a modified synthetic collagen conduit whose structural topography provided a physical cue to promote neuronal regeneration. The conduit also contained a polysialic acid peptide mimetic. This has been shown to promote neuronal regeneration and provides a chemical cue for regenerating axons. The ultimate objective of these studies is the fabrication a nerve grafting material that surpasses autograft and aspires to the "ideal" grafting material. One of our goals was to successfully synthesise a PSA mimetic peptide and incorporate it into a collagen scaffold. We synthesised different PSA mimetic peptides and developed different methods for binding them to collagen. We also devised novel ways to quantify the addition of peptide to collagen scaffolds. We also studied the effects of a collagen scaffold loaded with PSA mimetic on an *in vivo* rat sciatic nerve model.

In order to chemically tether our synthetic peptide to collagen, we developed a *de novo* method for the selective chemical activation of collagen. Collagen is quite an inert molecule. The main targets for chemical activation are the terminal amine and carboxyl groups located on its amino acid residues. Non-specific chemical activation of the collagen molecule is easy to achieve using well established methods (e.g. EDC). However for our purposes we needed to develop a means of activating collagen in a controlled and 'stepwise' fashion in order to ensure our synthetic peptide retained its inherent characteristics after tethering.

The nerve conduit was then tested *in vivo* using the rat sciatic nerve model. Neuronal regeneration was measured using histological methods as well as retrograde nerve tracing.

2 Literature Review

2.1 Peripheral Nerve Structure

When trying to formulate a solution to the problem of peripheral nerve injury an understanding of the anatomical structure of the peripheral nerve is crucial. A normal nerve fibre consists of three distinct layers surrounding central axons: epineurium, perineurium and endoneurium [7-8]. The epineurium is the connective tissue layer of the nerve. It runs around and between the neural fascicles. The outer epineural surfaces condense into a protective sheath. A fascicle is a bundle of nerve fibres and each of these fascicles is surrounded by a perineural sheath, which imparts tensile strength to nerve tissue. The innermost layer, called endoneurium, runs around and within the fascicles, providing structural support and nutrition to the axons [9].

Figure 2.1 A schematic showing the cross-sectional anatomy of a normal peripheral nerve. The left inset shows an umyelinated fibre, the bottom inset shows a myelinated fibre. *From Lee SK, Wolfe SW. Peripheral nerve injury and repair. J Am Acad Orthop Surg. Jul-Aug 2000;8(4):244.*

2.2 Peripheral Nerve Injury Classification & Pathophysiology

Classification of peripheral nerve injury was first attempted by Seddon in 1943 when he coined the terms “neurapraxia”, “axonotmesis”, and “neurotmesis” [10]. Neurapraxia is a crushing type injury without any axonal disruption and complete spontaneous recovery occurs within days. Axonotmesis occurs when axonal disruption occurs within the connective tissues. Neurotmesis, the most severe form of injury on the Seddon scale, occurs when the nerve is completely divided with disruption of the epineurium. The prognosis of spontaneous recovery is very poor without surgical intervention in cases of neurotmesis [11].

The Seddon System was modified by Sunderland in 1951. Instead of three levels of injury, Sunderland devised his system to include five “degrees” of nerve injury [12].
A first degree injury is caused by compression and is characterized by segmental demyelination. It is equivalent to Seddon’s “neurapraxia”. This results in an anatomically intact but functionally inactive nerve incapable of nerve transmission and because it is associated with a transient conduction block the resultant pathological changes are either mild or absent. Motor fibres are more susceptible to first degree injury than sensory fibres [13]. A “Saturday Night Palsy” would be the classic example of a first degree injury; it is caused by compression of the radial nerve at the level of the humerus [14] which results in wrist drop and reduced sensation to dorsum of the hand and wrist. First degree injuries heal spontaneously with a variable recovery time ranging from three to six months [15] (Table 2.1).

Table 2.1 Classification of nerve injury. From Pabari A, Yang SY, Seifalian AM, Mosahebi A. Modern surgical management of peripheral nerve gap. J Plast Reconstr Aesthet Surg. Dec 2010;63(12):1941-1948

More severe injuries (such as laceration, severe compression or stretching) can lead to actual disruption of the nerve trunk and destruction of its anatomy i.e. axonotmesis. Sunderland took Seddon's concept of axonotmesis and divided it into three subdivisions. A second degree injury involves severing of the axon but the endoneurium remains intact. A third degree injury features axonal and endoneural tube discontinuity but the perineurium and fasciculi are spared. Discontinuity of axon, endoneural tube, perineirum and fasiculi are present in a fourth degree injury but the epineurium persists. In a fifth degree injury the nerve trunk is severed entirely. In an amendment to Sunderland's five degrees, a sixth term was proposed by MacKinnon and Dellon in 1988 which described a mixed nerve injury which was a combination of the other degrees [16].

Wallerian degeneration occurs in axonal disruption and is therefore seen in all second, third, fourth and fifth degree injuries [17]. Waller first observed this a process in 1850 during his experiments on frog hypoglossal nerves [18]. When an axon is severed, the distal stump degenerates and fragments in a predictable fashion. Myelin breaks up into its constituent components and is phagocytosed by macrophages. Degenerating myelin sheaths form ovoid shaped "digestion chambers" which are gradually digested [19]. Usually degeneration ceases at the first internode proximal to the site of injury but can extend beyond this with more severe insults. The axonal ends either side of the injury seal over in a very short period of time. Over the coming days, the proximal and distal stumps swell due to persisting axonal transport into the blind ends of the severed axon [20]. The resealing of the disrupted ends is a key prelude to regeneration proper and is

dependent on high levels of Ca^{2+} accumulating in the vicinity [21]. Hyperaemia is a persistent part of the inflammatory response, lasts days and is caused by local build-up of vasoactive peptides, mast cell activity and angiogenesis [22]. It is now felt that degeneration is an active process stimulated by the act of axonal disruption and division of axon from the tissue it innervates [22]. The axonal cytoskeleton degrades within seven days in humans which is mediated by a capase-independent system of self-destruction [23]. Again, high levels of Ca^{2+} present at the site of injury activate calcium-dependent enzymes which dissolve cytoskeletal elements [22]. Even though the axon in the distal portion disappears, the structural basement membranes persist

Figure 2.2 Degeneration and regeneration of the peripheral nerve. A, Transection of the axon. B, Traumatic degeneration in the zone of injury and Wallerian degeneration distally. C, Growth-cone regeneration down the basal lamina tube. D, Schwann cells aligning to form Büngner bands. From Lee SK, Wolfe SW. Peripheral nerve injury and repair. *J Am Acad Orthop Surg.* Jul-Aug 2000;8(4):246.

and become endoneurial tubes along which multiplying Schwann cells gather and provide guidance for regenerating axons [24]. Dormant Schwann cells cannot support axonal regeneration but are able to re-myelinate regenerating axons [25] but if they are not stimulated by regenerating axons they degrade and disappear [26]. Consequently, endoneurial tubes not stimulated by a regenerating axon scar over and are resorbed. With second to fourth degree injury it has been shown that axonal disruption is incomplete. Spontaneous reinnervation is possible with these injuries because there is a level of neural tissue continuity. However the more severe the injury, the less likelihood there is

of recovery. Fifth degree injuries with total axonal disruption however, have no chance of spontaneous reinnervation and require surgical intervention.

2.3 **Peripheral Nerve Regeneration**

After a peripheral nerve injury occurs, a complex cascade of events ensues, with the ultimate goal of self-repair and reinnervation. The processes that are initiated after an injury happen at many different levels including the nerve body, the proximal stump, the distal stump and the target organ [27]. Spontaneous repair can get underway almost immediately in mild injuries (e.g. Sunderland first degree) but may take longer in more severe injuries due to an acknowledged "shock" phase [13].

The central nervous system and the peripheral nervous system respond very differently to injury. The central nervous system uses neural plasticity to overcome injury, where uninjured areas compensate for the injured areas by taking over their function whereas the peripheral nervous system tries to repair itself [28]. Repair in the peripheral nervous system occurs in three distinct ways: remyelination, distal collateral sprouting and regeneration from spared axons at the site of injury [29]. The extent of the damage incurred is one of the main determinants of the means of repair. For example, if a partial injury is sustained and many axons are spared, collateral sprouting can adequately repair the harm done. It has been shown that lateral sprouting is the main means of repair following lesions of less than 20-30 % of axons. Repair can occur over a period of up to 6 months. When a lesion involves more than 90 % of axons, the primary means of self repair is regeneration from the site of injury, with success dependent on the gap created by the injury. Motor reinnervation is often more successful than sensory reinnvervation after an injury and that despite adequate motor supply, function can be impaired by lack of proprioception [13].

On a microscopic and molecular level, a series of complicated and tightly regulated events occur straight after a peripheral nerve injury is sustained, involving neurotransmitters, neurotrophic factors and other cell signalling molecules [29-30]. The role of the Schwann cell cannot be overstated in nerve regeneration. The Schwann cell forms structural scaffolds by fabricating basement membrane which contains

extracellular matrix proteins like fibronectin and laminin and also produces cell surface adhesion molecules [31]. Schwann cells produce cell signalling molecules that activate tyrosine kinase receptors that in turn play a role in gene activation [32]. In fact, it has been shown that intracellular activity in neurones occurs within half an hour of sustaining an injury [33]. In the days after an injury, Schwann cells divide and produce dedifferentiated daughter cells which, if no axonal contact is made, downregulate their normal protein expression and change into the phenotype of a premyelinating cell [22]. These new cells produce nerve growth factor, cytokines and other neurotrophic agents that result in Schwann cell proliferation and differentiation in order to create the optimum environment for any regenerating nerve endings. Receptors for nerve growth factor on Schwann cells in endoneurial tubes in the distal nerve stump also increase in number and experiments have shown that in a transected rat sciatic nerve, there is a 50-fold increase in nerve growth factors on Schwann cells in the distal stump [34]. Neural growth factor interacts with these Schwann cell surface receptors to promote neural sprouting [35]. Macrophages also appear to work with Schwann cells in promoting neural regeneration [36]. Macrophages move into the distal stump after an injury. Macrophages upregulate IL-1 and this upregulates neural growth factor transcription, increase the density of neural growth factor receptors and also the secretion of mitogens which all contribute towards Schwann cell multiplication. Denervated Schwann cells have been shown, in experimental work, to upregulate neural cell surface molecules and the extracellular matrix molecules laminin and tenascin that are implicated in peripheral nerve regeneration [37]. Experiments have shown severed axons secrete cytokines such as IL-6 and transforming growth factor beta-1. They are secreted in large volumes and encourage axon regrowth until the axon encounters a Schwann cell [38]. When an axon is divided, signals are sent back up to the nerve cell body where different cytokines and growth factors promote regeneration. The primary function of a nerve is to transmit impulses, so when axons are severed, protein expression must switch from a transmitting role to a regenerative role. Tubulin, GAP-43, actin, and host of other potential neuro-regenerative substances are expressed as part of this shift in function [31]. The gene expression in damaged neurons has been shown to change from providing a transmission role to a regenerative role within twelve hours post injury [33]. In experiments on rat sciatic nerve, it has been shown that heat shock protein 27 mRNA is upregulated in damaged neurons in the ipsilateral dorsal root ganglion. Heat shock protein 27 is involved in actin filament dynamics as well as protection against programmed cell

death, and its role in the regenerating neuron is thought to be involved in cytoskeleton remodelling for regenerating axons as well as in preserving damaged neural cells [39-40].

When a damaged axon is regenerating, it forms a growth cone at the tip of each sprout [41-42]. Calcium plays an important role in growth cone formation [33]. It is the growth cone coming in contact with dormant Schwann cells that causes them to redifferentiate and start expressing myelin mRNAs to start the process of covering the regenerating axon in its sheath. The growth cone secretes a protease that allows it to burrow through materials blocking its path as it attempts to reinnervate its target organ. Success of reinnervation is greatly dependent on the gap between proximal and distal stump. Axons that do not reach the stump distal to the site of injury can inadvertently innervate nearby tissue or become encased in scar tissue at the site of injury. Scar tissue poses problems for regenerating axons as it can bar the path of regenerating axons causing them to divert into adjacent endoneurial tubes leading to disruption of nerve function [13]. Advancing sprouts and their associated growth cones are controlled by signal transduction [30, 43-44]. Filopodia ("thread-like feet") are projections that form from growth cones and are able to sense the environment in front of the regenerating axon and pick up on navigational cues in order to guide the axon as it regrows [45]. The growth cones are dotted with receptors that pick up signals from the environment. As the sprouting axon advances it senses these cues and can turn and branch accordingly. Four mechanisms of growth cone guidance have been described in the literature: contact mediated attraction, chemoattraction, contact mediated repulsion and chemorepulsion [46]. These four mechanisms appear to act together in synchrony, to guide the regenerating axon [47]. Filopodia lengthen when actin filaments accumulate after stimulation from navigational cues. The cues themselves are classified as either "attractive" or "repulsive" [48]. Neurotrophins modulate the response of advancing growth cones to their cues via tyrosine kinase recepetors. Collapsin-1, for example, is a molecule implicated in growth cone regression, but neurotrophins such as brain-derived neurotrophic factor, can safe-guard the growth cone against the effects of collapsing-1 [49]. The goal of sprouting axons, growth cones and their scouting filopodia is to reconnect with the distal stump. Assuming this actually occurs using the previously described mechanisms and the sprouting axon enters the distal endoneurial tube, the chances of reaching the end organ are good [13]. The filopodia also use the basal lamina of Schwann cells as a guide. In

the clinical setting, an estimate of 1mm of axonal growth per day is quoted, with regeneration more likely to be successful in younger patients with more proximal lesions [50]. Spontaneous reinnervation is more successful than reinnervation after surgery. It is also worth noting that functional recovery is dependent on factors other than axons reaching the end organ (e.g. remyelination) and that several elements are required for a nerve to work correctly. For example, a muscle not being routinely stimulated by nervous supply will scar and atrophy over a period of weeks to years [50-51]. Reinnervation seldoms results in full recovery [52] and fibrosis within muscles reduce their ability to contract. This is compounded by aberrant axonal regrowth, where axons reinnervate muscle fibres haphazardly, leading to a loss of regulated nerve impulse and resultant efficient uniform muscle contraction, ultimately leading to reduced muscle function [53].

2.4 Current Surgical Techniques in Peripheral Nerve Repair

2.4.1 Overview

Despite an explosion in knowledge in the area of peripheral nerve injury, advances in repair technique have not moved on significantly in the last 25 years [54]. Experimental research has greatly expanded our knowledge of the inner workings of injured neurons, rejuvenating axons and the microenvironment created after a peripheral nerve injury, but the translation of this wealth of data into clinical applications has not occurred at the same rate. In fact, in a survey of clinicians, 78 % of cases are treated by direct surgical repair, autografts make up 15 % of cases, alternative methods (such as nerve conduits) are used 4 % of the time with the remaining 3 % of cases receiving no repair at all [55].

The timing of nerve repair is a key determinant in positive clinical outcome. It appears that nerve response to an injury is improved if a pre-existing injury has been sustained and that experimentally, a ‘conditioning lesion’ applied 1 to 3 weeks earlier, can lead to accelerated axonal regeneration [56-58]. This observation makes perfect sense when we think about how nerve cells switch modes between “transmission” and “repair” as alluded to earlier. The conditioning lesion interval can be as short as 2 or 3 days and still

show a significant effect on regeneration [59]. Some data suggests that nerves achieve an optimal state for regeneration and the metabolic environment in a regenerating nerve peaks 2 to 3 weeks post injury [60]. However, from what we know about Wallerian degeneration and cell response to injury, a period of 2 to 3 days delay seems more than enough to improve outcome. There is still no clinical data to support this view and immediate primary repair (when possible) appears to be the optimal treatment for peripheral nerve injury.

2.4.2 Primary Anastomosis

The gold standard for peripheral nerve repair without extensive tissue loss is primary anastomosis. Advancements in this area were greatly aided by the use of microscopes and microsurgical instruments that allowed surgeons to work on such tiny, delicate structures [61-62]. It became apparent that the method of end-to-end approximation of severed axons by aligning endoneural sheaths was not satisfactory to produce adequate reinnervation as fascicular alignment was negated [63]. The same study also commented on the importance of suture material choice to complete the approximation and that a certain materials (e.g. monofilament nylon) induce a minimal inflammatory response at the anastomotic site that in turn promotes regeneration. Research has even shown that suture size has a bearing on surgical success with primary anastomosis with 9-0 nylon being the suture of choice. 8-0 nylon tends to pull on the repaired nerve ending and 10-0 just is not strong enough [64]. For many years the “de rigeur” approach was to attain a “tension free” anastomotic line [65-66] but some experimental data using primate subjects has shown that a modest amount of tension in a primary anastomosis yields better outcomes than tension free autograft [67].

Figure 2.3 A, Epineurial neurorrhaphy. B, Group fascicular neurorrhaphy. From Lee SK, Wolfe SW. Peripheral nerve injury and repair. *J Am Acad Orthop Surg.* Jul-Aug 2000;8(4):248.

The dilemma of fascicular alignment appears to be an area of contention when it comes to primary repair. Theoretically, one would imagine that direct fascicular repair would lead to better axonal regeneration and thus better functional outcome, but to perform fascicular repair, you must subject the nerve to additional manipulation and trauma which in turn leads to increased scarring and inflammatory response and reduced blood supply. This may be harmful to nerve regeneration [5]. Experimental data, based on the hypothesis that trauma induced fascicular alignment reduced regeneration, showed that outcomes with fascicular alignment were equivalent to simple endoneural alignment [68]. Advances in technique and improved tissue handling have made atraumatic fascicular alignment possible [54]. No prospective, randomised clinical study has shown one coaptation technique to be superior to another. Be that as it may, simple anastomosis of the proximal and distal ends of a severed nerve is the accepted technique for nerves not topographically divided into motor and sensory branches. These techniques do not account for axonal alignment and completely disregard the molecular level of regeneration. If a nerve has a divided function and known sensory and motor branches, it has been show that fascicular repair may be preferable [69]. As a result, fascicular mapping became a burgeoning area of research, and techniques to allow for identification of fascicles at the injury site and their target became of interest. Usually it is possible for an operating surgeon to identify fascicular groups using a microscope, making the matching up of cut ends a relatively straight forward procedure. There are,

however, ways to differentiate between motor and sensory branches perioperatively. One method involves electrostimulation of motor nerves intraopertively, first proposed by Hakstian in the 60s [70]. Experimental work in the 70s then showed that it was possible to stimulate and record the response of individual fascicles, which could be used as an intraoperative branch identification technique [71]. This is a reliable method of motor branch identification but only useful in recent nerve injury as Wallerian degeneration in the distal stump can reduce the efficacy of the stimulation [5]. Even though electrostimulation is reliable for branch identification, it has gained limited practical use by experienced nerve surgeons [54]. There are also biochemical differences between sensory and motor axons that can be exploited to aid in their identification. Acetylcholinesterase is only present in motor nerves and a method for selective staining of this molecule has been developed [72]. The same group showed that staining of acetylcholinesterase could be used intraopertively to selectively label motor nerves [73]. This technique was of limited use as the staining incubation period was too long and patients had to undergo a 2-stage procedure for identification and reconstruction. Progress was made and staining time was reduced down to 2 hours [74-75]. Similarly, carbonic anhydrase is present only in sensory axons and staining techniques specific to this molecule were also developed [76]. This technique was then expanded and applied to identify sensory nerves in the surgical setting [77-78] with an incubation time of 2 hours. Refinement of staining techniques continued to develop with one group describing a staining time of just 30 minutes for sensory fascicles and no reported adverse effect on nerve regrowth [79]. Another group has shown that acetylcholinesterase can now be stained in an hour and carbonic anhydrase in 12 minutes. These latest stains persisted for 35 days in the proximal stump and 9 days in the distal stump, meaning that this technique could be of benefit in the both primary and delayed nerve repair procedures [80].

2.4.3 Nerve Grafting

When a tension-free primary anastomosis is not possible, alternatives must be sought to bridge the gap between proximal and distal stumps [81] and this is where nerve grafting comes into play. When using a nerve graft axons have two cut interfaces to traverse as opposed to just the one present in a primary anastomosis. Considering the effort and processes involved in nerve regeneration, as discussed earlier, the introduction of a second interface simply cannot be overestimated. It is also worth noting the tissue deficit incurred by a nerve injury, in practice, does not necessarily reflect the final degree of loss as optimal surgical technique dictates that nerve stumps should be debrided both proximally and distally until normal nerve tissue is encountered.

A host a various reconstructive techniques can be employed to bridge the nerve gap [16, 69], each one is dependent on the clinical scenario being encountered. The general rule in medicine is that it is preferable to replace "like with like" and this is also true with nerve grafting, insofar that the autologous nerve graft is the gold-standard material of choice. An autograft is a nerve harvested from another site in the same patient. The reasons for using autograft are numerous. As the material is taken from the patient themselves, there is no immune response against the material, unlike the foreign body reaction seen when alien tissue is inserted into the body.

When an autologous graft is used, one is, in essence, implanting a graft that contains all the building blocks that a regenerating axon theoretically needs to regrow. A fresh graft consists of a basal lamina scaffold (which contain essential molecules like laminin and fibronectin [82-83]), viable Schwann cells and all the neurotrophic factors a growing nerve needs to thrive. Autologous grafts without Schwann cells have been shown to be inferior to those with viable cells capable of producing nerve regrowth factors [84-85].

Several macroscopic factors determine the suitability of donor tissue. The sural nerve (found in the lower limb) is the most commonly used donor nerve as it is purely sensory in nature (meaning that the adverse effects of its removal are trivial) and is quite plentiful (up to 14cm of sural nerve can be harvested from a single site [86]). Other commonly used sites are: the medial and lateral cutaneous nerves of the forearm, dorsal cutaneous branch of the ulnar nerve, superficial and deep peroneal nerves, intercostal nerves, and

the posterior and lateral cutaneous nerves of the thigh [16, 87]. It has been shown that thin grafts do better than thick grafts as Schwann cells can be more easily be nourished by diffusion until neovascularisation takes place [54].

Figure 2.4 Sural nerve graft harvest. From Evans GR. Peripheral nerve injury: a review and approach to tissue engineered constructs. *Anat Rec.* Aug 1 2001;263(4):401.

Experimental work suggests that it might be beneficial to modify an autologous graft prior to its interposition [88]. For example, several studies have shown that crushing or cutting nerve grafts causing "predegeneration" can promote neural outgrowth [59, 89-90]. In fact one group has shown that manipulating a nerve graft in this way can significantly reduce the latency period before a nerve starts regrowing [59]. Non-invasive methods can also be used to encourage the rejuvenating neural axon, with hyperbaric oxygen therapy [91-92] and vibration exposure proving to be two areas of promise.

It has proven difficult to replicate experimental results in the clinical setting. Modern nerve reconstruction techniques are based on work from the 70s by Millesi [93-94] and very little has changed in the methods since then.

A modification of Millesi's method is the use of vascularised nerve grafts. These can be used as an alternative to the traditional autograft if the recipient bed site is not very

vascular or the nerve gap is large. Many groups have published works describing vascularised nerve grafts harvested from donor ulnar and sural nerves [95-100] but the method is essentially the same i.e. a single, double or triple strand of nerve tissue supplied by the same vessel. No data has so far been produced to prove vascularised are superior to non-vascularised grafts but it is proposed that they are more desirable for use where large gaps, poor vascularity and large skin defects exist.

Another issue arises when there is a discrepancy between the diameter of the injured nerve and the diameter of the donor nerve. This problem can be overcome by suturing several grafts in parallel, using the fascicles as guides and employing the primary neurorrhaphy technique. Harvested grafts should also be 10-20 % longer than the gap as tissue fibrosis will lead to shortening of the graft [5]. Autograft also forms a very sturdy bond with the injured stumps, with a complete recovery in tensile strength in the repaired nerve achieved by 4 weeks [101].

It is worth noting that the autograft is not without its disadvantages. The human body only has a finite supply of potential donor nerve and the success rate is still inferior to primary anastomosis. Not only that, but the need for a donor site means an increase in morbidity (e.g. scarring, sensory loss) and potential adverse effects for the patient.

Another form of autologous nerve grafting involves the method of nerve transfer. This is a means of converting a proximal nerve injury into a distal one by transferring nearby redundant nerve to a distal denervated nerve close to the target [3]. The concept of nerve transfer has been around for decades [102-103] but it has recently come back into favour. Nerve transfers are being used with many investigators reporting good outcomes in a host of different anatomical sites [104-107]. The use of nerve transfers for proximal upper limb and brachial plexus injury is now well established and a reliable means of repair. When one attempts a primary repair or autograft interposition, one is trying to restore nerve function by attempting to restore the anatomy and nerve continuity. In contrast, with a nerve transfer, one is merely bypassing the injured nerve and is trying to regain partial recovery of function by hijacking a functioning nerve and using it to give a nerve supply to the target organ. Their use is considered justified where use of grafts or primary repair may give an unreliable outcome [3].

The technique of end-to-side anastomosis is also worth considering. This can be used when the proximal end of the transected nerve is not available to use in the repair. The concept for this method is over a hundred years old [108]. A distal nerve stump is sutured in an "end-to-side" fashion to a healthy, adjacent nerve trunk upon which an axotomy has been performed. It has long been known that a distal stump exerts a strong, attractive influence on regenerating axons [109] and it is this concept that the end-to-side technique relies upon. It is thought that the neurotropic effects of the distal stump are strong enough to induce collateral axonal sprouting from the intact, healthy nerve into which it is sutured. The concept of end-to-side anastomosis appeared to have fallen by the wayside in academic circles until it was resurrected and restudied by Viterbo et al in 1992 [110]. After this landmark study by Viterbo, there was a veritable explosion in knowledge and research in the area of end-to-side anastomosis [111-121]. Some studies have shown absolutely no ingrowth of nerves [122-123], whereas other have shown ingrowth of axons into the distal segment with some groups indicating a predominance of sensory fibre ingrowth with minimal motor innervation [118-119] and others showing a marked ingrowth of motor fibres [120-121]. It has, however, been postulated that these motor fibres are originating from viable axons in the distal segment. The latest research has indicated that the axotomy is the crucial part of end-to-side anastomosis. Collateral sprouting can occur in the absence of axotomy [124] but it has been shown that only sensory nerves are involved in this process [125]. For motor axon collateral sprouting it appears that donor nerve axotomy is necessary [126] whereas sensory axon collateral sprouting is independent of axotomy [127]. This method is not practiced widely but is generally used in reconstruction of noncritical sensory deficits [3].

Nerve allografting is an area of intense interest in medical research. Grafts are usually harvested from cadaveric subjects. These grafts are reserved only for very severe or segmental nerve injuries. Antigenicity and rejection are the main concerns with allografts, and these obstacles are overcome by treating the graft in numerous ways to reduce antigenicity and induce temporary immunosuppression of the host. Treatment methods to reduce allograft antigenicity include lyophilisation [128-132], cold preservation[133], irradiation[134-135] and freeze-thawing[136]. Allografts need both host and donor Schwann cells to function. As illustrated earlier, Schwann cells provide support for remyelinating axons and when used in this context they also act as facultative antigen presenting cells [3]. It is because Schwann cells are a source of major

histocompatibility complex II that they must be retained during any treatment process resulting in the need for host immunosuppression [137-143]. Immunosuppression in nerve allografting is only temporary whereas solid organ transplantation requires lifelong host immunosupression. This is explained by the replacements of native Schwann cells in the allograft by recipient Schwann cells after 24 months. By then the host's immune system considers the allograft to be similar to native tissue. It has also been shown that Tacrolimus (a commonly used immunosuppressant) has neuroregenerative properties that promote nerve regrowth [144-145]. Immunosuppression is a burgeoning area of research and as medical advancements occur in this area it pushes back the boundaries of what is achievable with surgery. Surgical techniques are well established and can achieve excellent results but it is only by understanding and modulating the body's own physiological responses that we can hope to improve results with allografting.

2.5 A Biomaterials Approach to Peripheral Nerve Repair

2.5.1 Overview

There are a plethora of surgical techniques available when a peripheral nerve injury is sustained but it is not always either possible or preferable to perform peripheral nerve repair using standard techniques. Sometimes the tissue loss can be too great or the nerve gap too large for a standard nerve graft repair. Autograft can only bridge a gap of up to 5cm [4]. Gaps over 5 cm require allografting and require prolonged immunosupression therapy that can be associated with many significant systemic side effects.

In other scenarios, such as a polytrauma, autogenous grafting is difficult due to a lack of available donor material. Even though autogenous nerve grafting is still the gold standard for nerve repair, let us not forget that it is an imperfect method and has its recognised side-effects e.g. donor site morbidity, neuroma formation etc [3]. Even with an uncomplicated repair using autogenous nerve grafting, one has to surgically harvest nerve from a donor site which in itself causes morbidity and has potential complications. An issue also arises when nerves of different type are used to repair injuries. When

harvesting donor tissue, we mainly target sensory nerves as this causes minimal functional deficit in the target tissue (e.g. sensory loss). The vast majority of peripheral nerve repairs are performed on motor nerves in order to preserve or regain function of a target tissue. It has been shown in studies that poor functional outcome in nerve repair may in fact be due to the physiological mismatch between donor sensory tissues being used in a recipient motor injury [146-147]. On a microscopic level, it has been shown that there is an axonal size mismatch between sensory (0.2 to 15μm) and motor (3-20μm) neuron diameters [148] and this may in fact limit regeneration potential [149]. When nerve regrowth occurs in the presence of an autograft, there is a healing delay as it requires time for the regenerating axon to remove degenerated axons and non-viable myelin from the donor tissue [150].

It is clear to see that even though autogenous grafting is currently the best treatment modality for nerve injuries with neuronal loss it has significant limitations. Biomaterial researchers endeavour to make up for any limitation with this technique by trying to discover a material that has all the benefits of an autogenous nerve graft but none of the morbidity. The "ideal" grafting material does not ellicit an immune response and promotes neuronal regrowth without causing neuroma formation. It should be easy to implant and relatively easy to make. By using synthetic material one avoids the need for having a second operative site generated through donor tissue harvesting. In essence, the "ideal" grafting material should address all the failings of autogenous grafting.

2.5.2 Nerve Guidance Conduits

Nerve guidance conduits (NGCs) are the simplest form of synthetic nerve implant. They are hollow, usually cylindrical tubes used to bridge nerve gaps. They are surgically implanted with the proximal and distal nerve stumps inserted into either end of the tube. Nerve guidance conduits were first described in 1881, with the first successful in vivo trial occurring in 1882 when a resorbable decalcified bone tube (originally intended for use in wound drainage) was used to bridge a 3cm gap in a canine subject [151].

Even though the materials involved have advanced over time, the core concept behind the use of a conduit has not. By using a hollow tube one creates a microenvironment for regenerating axons that physically sequesters the cut ends of the nerve (as well as the subsequent regenerating processes) and isolates them from the rest of the body. When a nerve is transected, axoplasm is secreted by the nerve ends and the fibroblasts and Schwann cells secrete neurotrophic factors [31]. It is thought that these growth factors are trapped by the conduit, between the severed nerve ends and reach high concentrations in this restricted space. However, the ideal conduit material should also allow diffusion of key factors into the microenvironment as well as allowing waste products out. Materials that are permeable up to a molecular weight limit of 50 kDa have been shown to be adequate for nutrient/waste diffusion [152-154]. The physical barrier provided by the conduit reduces collateral axonal sprouting as well as impairing myofibroblast infiltration of the site. The conduit itself also provides structural support to the axons [149]. Conduits localise Schwann cell migration and foster the formation of a fibrin matrix that is an important structural component allowing Schwann cells, macrophages and fibroblasts to perform their roles [1, 16, 155-157]. All of these processes reduce scarring and aid in guiding regenerating axons towards their target tissue [54]. Clinically, the use of nerve guidance conduits has shown some success [158-159] but functional outcomes are not as good as autograft [160].

Materials used in the production of commercially available NGCs include poly-glycolic acid (PGA), poly-lactide capro-lactone (PLCL), mixtures of the two or either animal- or plant-derived collagen [158-159, 161]. The ideal material is biodegradable, negating the need for a second operation to remove a non-absorbable implant that may cause nerve

compression [162]. The NGC should have no antigenicity so as not to ellicit a host immune response [163].

NGCs are limited for use in non-critical, small diameter, sensory nerves of 3 cm or less [164]. It appears that the volume of the space between the severed nerve ends is an important factor for regenerating axons as it determines the concentration of the released neurotrophic factors and concentration of factors impacts on regeneration potential [155]. Small diameter nerves respond better because the neurotrophic factors have a smaller non-vascularised area to diffuse into and shorter nerve gaps respond better because Schwann cells have a shorter distance to cross [3].

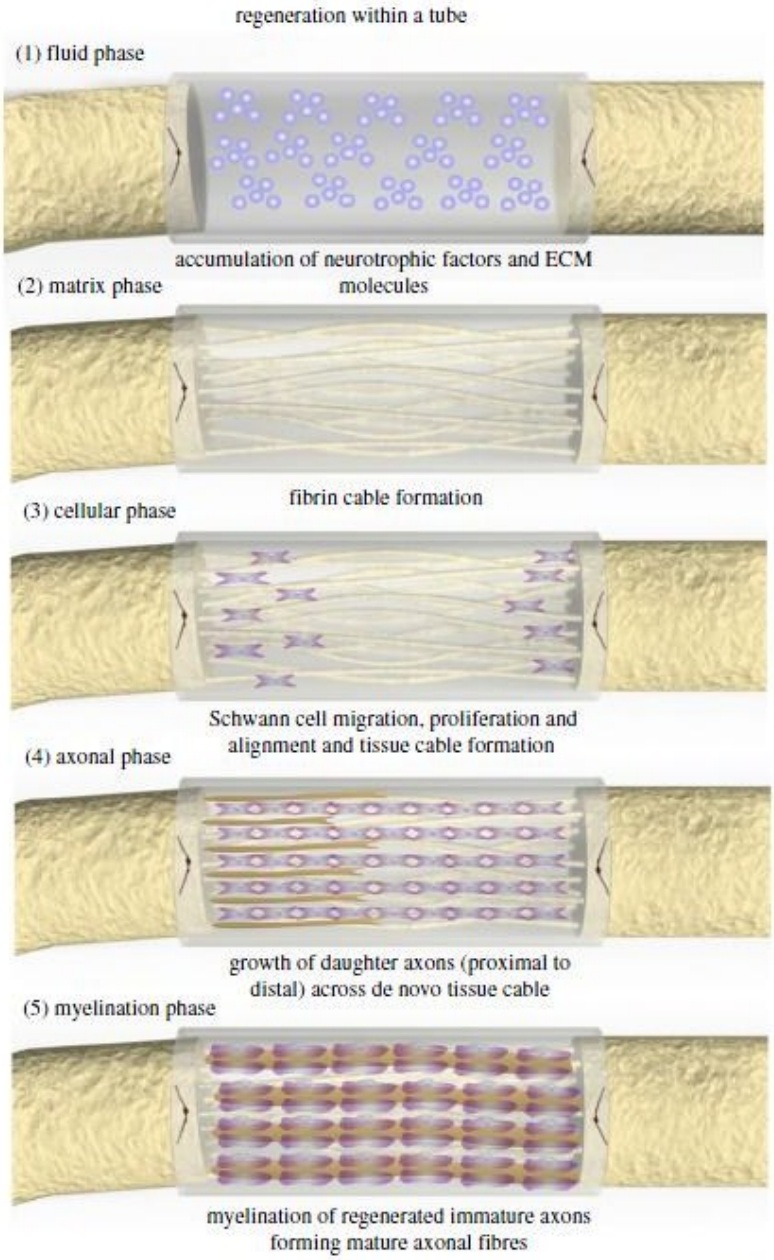

Figure 2.5 Regenerative sequence in a hollow NGC showing the different phases of the regenerative process. From Daly W, Yao L, Zeugolis D, Windebank A, Pandit A. A biomaterials approach to peripheral nerve regeneration: bridging the peripheral nerve gap and enhancing functional recovery. *J R Soc Interface.* Feb 7 2012;9(67):202-221.

Research has shown that the formation of an acellular "fibrin cable" during the "matrix phase" of neural regeneration is a key step in successful reinnervation [156, 165-166]. This cable is formed from ECM precursor molecules secreted into the nerve injury site during the initial stages of regeneration [156, 165, 167]. The "fibrin cable" forms the physical scaffold along which migrating Schwann cells, endothelial cells and fibroblasts migrate during the latter stages of nerve regeneration [156, 167]. The migrating SCs eventually align and form a SC cable. This is biological tissue complete with glial bands of Büngner that guide axonal sprouts towards their target during the "axonal phase" of reinnervation. Studies have shown that this process can occur in NGCs with a nerve gap of up to 4cm in humans and 1.5cm in rat sciatic nerve models [168-171].

It has been shown that NGCs perform better than end to end repair in small calibre, sensory nerve injuries with less than a 3 cm gap [164] and that in some cases, NGCs perform better than autograft in gaps of less than 1cm [4, 157]. Unfortunately, due to the nature of hollow NGCs, cross-innervation can occur as regenerating fascicles are not directed specifically at a target and specificity can be lost [155, 157, 172-173]. In fact, it has been shown that NGCs used in isolation are associated with a poor functional outcome across all nerve gaps [171, 174].

Physical modifications of the NGC itself are also possible and this is an area that has been researched extensively. Altering the surface topography of conduit luminal walls may make them more effective in achieving their goals. The two main avenues of investigation in this area are the creation of aligned microchannels in lumen walls and the fabrication of lumen walls using aligned electrospun micro- /nano-fibres. One study looking at the use of microchannels noted that channels promote direct nerve regeneration and can also be seeded with SCs that align, migrate and form structures reminiscent of native bands of Büngner during regeneration [175]. The size of the physical modifications is a key determining factor in the success of a model in neuronal regeneration. It has been shown that features that approximate the diameter of the

advancing neurite promote better guidance than at other diameters [175]. A study utilising conduits with micro-patterned channels on their internal lumens showed no difference when used in nerve gaps of 10 mm when compared to controls with no microchannels but they did show a significant improvement in functional recovery and nerve regeneration when used in the setting of a critical 15 mm nerve gap as compared to controls [176]. Another centre created hollow collagen/chitosan conduits using a method involving unidirectional freezing and freeze drying that purposefully left longitudinal microchannels along the conduits' inner surface that were of 25-55 μm in diameter. The collagen/chitosan structure conferred an optimal level of porosity to the model while remaining strong enough to function as an adequate support structure for the progressing axons. Using an in vivo model, at 12 weeks, these grafts fared as well as autograft in terms of regeneration and functional recovery depending solely on their topographical properties and without the aid of molecular or cellular guidance cues [177].

Electrospun fibres not only confer a topographical advantage to NGCs (as has already been alluded to), but NGCs made up of electrospun fibres also possess inherent structural properties that make them potentially superior to conduits made of a continuous material. NGCs made up of fibres are structurally quite flexible, making them suitable for use in recipient. They are also quite porous, allowing a necessary degree of diffusion between the injury site and the surrounding environment [178]. The fibres themselves also have a high surface area to volume ratio that is quite advantageous when trying to promote neuronal regeneration as this encourages protein absorption as well as fostering Schwann cell migration [179]. In a paper by Chew at al [179], the group studied continuous NGCs versus NGCs made up of electrospun fibres and found that electrospun conduits fared better than their continuous counterparts when measuring functional recovery and that their regenerative potential increased even more with the inclusion of growth factors. The most interesting part of this study however was the observation that not only did regeneration occur at the periphery of the conduit, adjacent to the topographically advantageous electrospun NGC wall, but also at the centre of the conduit, away from the fibrous wall. The group attributed this to possible migration of fibres from the wall towards the centre thus providing a pro-regenerative effect on processes distal to the wall. This, in the opinion of the investigators, potentially shows that wall topography is not enough to provide full thickness regeneration within

a hollow NGC and that some form of intraluminal guidance is necessary for successful axon re-growth. Another group, using a bi-layered conduit design consisting of an outer layer of non-aligned electrospun fibres with an inner core of nanofibres (diameter in the range of 250 to 1000 nm), bridged a 15 mm critical gap in an animal model and showed functional recovery comparable to autograft [178]. The researchers proposed that the inner fibre core aided Schwann cell migration while the outer layer conferred a structural advantage as well as a necessary porosity required for adequate molecule diffusion across the injury site. These studies underpin the suspicion that a simple NGC with one or two modifications will be inadequate for purpose and will never supersede auto-graft as the gold-standard.

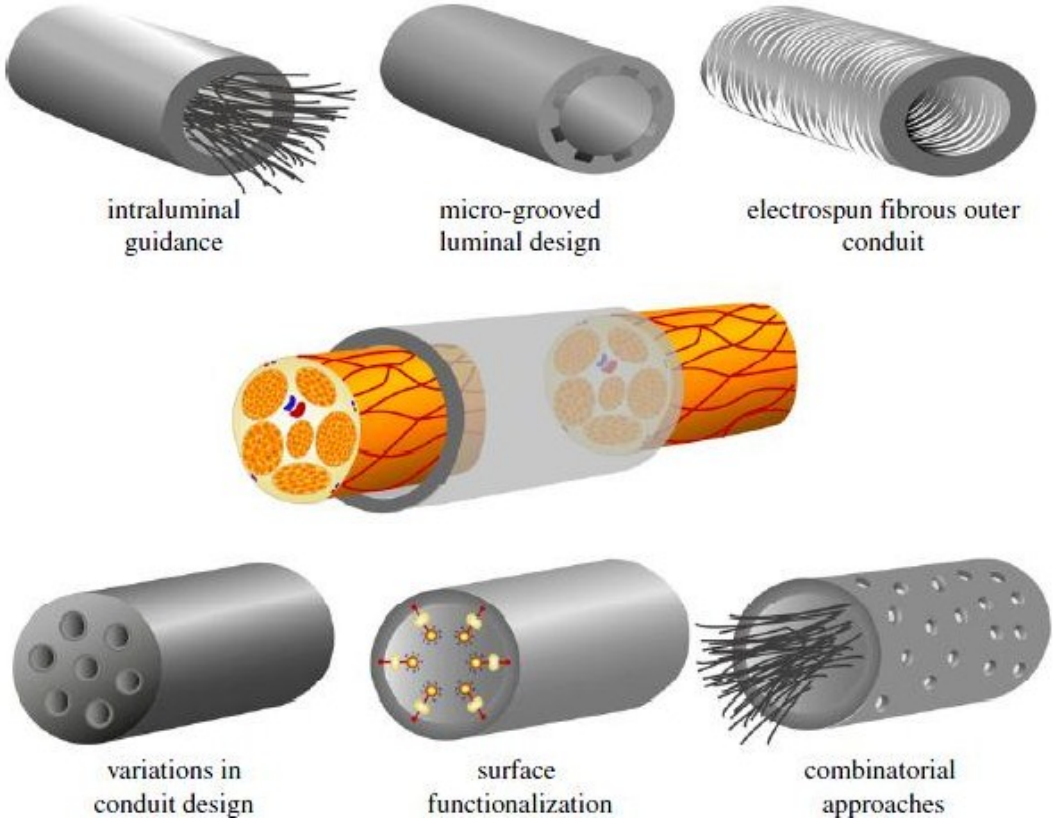

Figure 2.6 This schematic shows the various strategies employed in NGC design. Top row (from L to R): intraluminal guidance using fibres, intraluminal guidance using micro-channels, conduit wall modification using electrospun fibres. Centre: schematic showing a hollw NGC in situ and bridging a nerve gap. Bottom row: (L to R): a multo-channel conduit, surface functionalisation of the NGC lumen, a conduit showin a combined approach. From Daly W, Yao L, Zeugolis D, Windebank A, Pandit A. A biomaterials approach to peripheral nerve regeneration: bridging the peripheral nerve gap and enhancing functional recovery. *J R Soc Interface.* Feb 7 2012;9(67):206.

Modification of the NGC wall is an interesting approach to NGC design but other groups are “re-inventing the wheel”, so to speak, and are coming up with totally new conduit

designs. One avenue of investigation is the use of a multichannel conduit. Initially, solid conduits made of PLGA were synthesised with longitudinal channels running through the conduit that mimicked native neural architecture [180]. This group used a foam-processing technique with low-pressure injection moulding to fabricate conduits with longitudinally aligned channels of diameters of between 60 to 550 μm. The focus of their study was to increase surface area within the conduit to
promote seeded Schwann cell adhesion and thus increase the overall regenerative capacity of the graft. They successfully bridged a 7 mm nerve gap in a rat sciatic model using a 5-channel conduit. This study showed favourable neural regeneration when compared to autograft and the group highlighted the ability to tailor the activity of their material by the selective addition of Schwann cells and neurotrophic factors at will to different sections of the conduit dependent on the requirement [180]. Further work in the area led groups to hypothesise that multichannel conduits direct neuronal regeneration more accurately by providing a physical barrier that prevents axonal dispersion [181-182]. It was shown that multichannel and single channel conduits bridged a 10 mm critical nerve gap at the 12-week mark. However using a retrograde nerve tracing technique, it was shown that there was a marked reduction in axonal dispersion seen in the multichannel conduit when compared to single channel controls. Unfortunately, this observation was only seen in some of the specimens as the material used to make the conduits was structurally unstable leading to collapse of microchannels and thus skewed results. The lead-on study from this modified the conduit fabrication process by using collagen instead of PLGA thus improving stability and preventing microchannel collapse. This study showed successful bridging of a 10 mm critical gap (like its preceding study) and because channel collapse was no longer an issue, it clearly and unequivocally illustrated reduced axonal dispersion in a comparison with controls [182]. The authors then went on to postulate that further favourable modification of their multichannel design could include other physical or molecular cues leading to an even greater reduction in dispersion and improved regenerative efficiency.

To reiterate, the immediate goal of any peripheral nerve repair is to redirect a severed axon in such a way that eventually it reconnects with its target tissue. NGCs provide an excellent starting point for the development of an implant that allows efficient and targeted nerve regeneration. Autograft is still the gold standard grafting material and it is plain to see that autograft material, i.e. endogenous nerve, is far more complicated

and contains many more components than a hollow tube. NGCs create a gross physical space for regenerating axons, but for effective regeneration to occur, consideration must be given to the microscopic and molecular interactions of normal nerve injury and repair [164].

2.5.3 Intraluminal Physical Guidance

NGCs are an excellent starting point when considering the best options for an implantable nerve graft, but it is clear that hollow conduits alone are not the solution to the challenges faced when trying to provide regenerating nerves with the best chance of reconnecting with their appropriate target tissues. The autograft comes fully loaded with Schwann cells, basal lamina, endoneurial, perineurial and epineurial architecture [164] and also unknown phenotypic factors that promote selective reinnervation [183] as has been shown, autograft has its own limiting problems and even though it is the "gold standard" it is by no means perfect.

In an effort to promote neural regeneration within a NGC, researchers have explored the strategy of using intraluminal physical cues in the form of conduit luminal scaffolds the purpose of which is to augment "fibrin cable" formation or make its formation redundant during neuronal regeneration [171, 184]. Essentially these scaffolds mimic native ECM [178] by allowing SCs to migrate along pre-formed physical paths. They can also act directly on regenerating axons, shepherding them down specific channels in an effort to help them reach their target tissue.

The concept of using bundles of fibres within a NGC has been studied extensively. These structures (similar in arrangement to fibre optic cable) supposedly mimic "fibrin cables" as they are physical strands that bridge a nerve gap. A nerve gap of 8cm in canine subjects was bridged successfully using bundles of laminin-coated collagen fibres inserted into a polyglycolic acid NGC using histological and nerve conduction measurements [185]. It is worth noting that others have researched the area of using collagen filament bundles without an investing sheath and shown that gaps of 20 mm and 30 mm can be bridged successfully. They showed that there was an increase in the number of myelinated axons present in test groups [186-187]. Packing fibres into hollow NGCs is better than NGCs alone [186-187], and with the obvious advantages of a packed structure that is easier to handle and increased versatility in an enclosed compartment for potential modification, research into NGCs with intraluminal fibres will continue to be an area of immense academic interest.

The spatial arrangement and "packing density" [188] of intraluminal guidance structures is a critical determining factor for the degree of subsequent neural regeneration after a nerve injury treated with a filled NGC [174, 184, 189]. One particular study using poly-L-lactide (PLLA) microfilaments showed that using high density (15-35 % of cross-sectional area) implants impedes nerve regeneration whereas lower density (3.75-7.5 % of cross sectional area) implants display better regenerative properties and achieve nerve gap bridging. These "packing densities" were most favourable as lower densities caused settling of microfilaments in the base of the conduit. The same study also showed that the spatial relationship of the fibres within the tube had a bearing on neural regeneration. For example, when the fibres were bundled tightly in the centre of the conduit, regeneration failed completely [188]. The extreme end of this concept was explored by another group who filled the NGC with a dense collagen sponge that completely blocked neural regeneration [189]. The effect of the intraluminal filament concept was shown to be augmented in the presence of different types of NGC. Permeable NGCs made of poly-lactic acid (PLA) filled with PLLA microfilaments showed better regenerative abilities than PLLA microfilament packed NGCs made of impermeable silicone in an *in vivo* model [190]. Other tested intraluminal guidance cues with varying degrees of success include: collagen sponges [191], collagen gels [192], keratin hydrogels [193], fibrous films [174] and filaments of made from various materials including collagen fibres coated with laminin/mimetic peptide [194] and PLLA [188]. Also, it worth noting that there can be a tendency for bundles of fibres to move within the conduit, sometimes slipping down to the floor of the tube thus negating their topographical benefit. This is not an issue when the NGC wall is composed of electrospun fibres because the guidance is coming from the full circumference of the wall and not mobile structures placed within the conduit lumen itself [179, 188].

Research groups have also taken a keen interest in combining elements of different scale in an effort to improve neural regeneration, specifically adding nano-scale guidance cues to micrometre-scale intraluminal guidance structures [149]. As an alternative to the microfilament model, one group examined the use of aligned polymeric fibrous films in bridging a nerve gap. They used aligned electrospun films composed of fibres of poly(acrylonitrile-co-methylacrylate) or PAN-MA [184]. This group managed to bridge a nerve gap of 17 mm with the fibres themselves having a diameter of between 400 and

600 nm. It is worth nothing that the aligned films displayed a much better regenerative capacity than the unaligned control films, thus showing that nano-scale differences can translate into better outcomes. Intraluminal films have a high surface area/volume ratio. Due to the way in which they are processed they possess a compact, aligned topography that provides a physical cue to axons. Their low packing density has been shown to be advantageous in the area of nerve regeneration [174]. The precise positioning of films within the NGC lumen avoids logistical issues seen in the micro-scale filament model such as filament overlap or accumulation of fibres on the floor of the conduit, but positioning of the film also has its problems. For example, it was the positioning of a single film along the midline of a conduit that showed the best results [174] with the addition of further films only curbing axonal growth and in fact causing mismatching of supportive regenerative cells, with SCs from the proximal severed end forming a bridge within a certain zone in the conduit and SCs from the distal end forming a bridge in a different zone within the conduit, with neither bridge meeting. The "nano-scale" concept was applied to the aforementioned micro-scale filament packed NGC model by using aligned electrospun nanofibres made of PLGA with a diameter of 200 to 600 nm to make up the micro-metre scaled microfilaments [178]. The group used these nanofibre based microfilaments in conjunction with surface functionalisation and growth factor delivery in a model that bridged a 15 mm nerve gap in 12 weeks. By further modifying the model, the same group employed the use of a bi-layered conduit and showed that this implant was as good as autograft in bridging a large critical nerve gap [178].

2.5.4 Intraluminal Molecular and Cellular Guidance

When it comes to replacing lost organic tissue, the general rule is to replace "like with like". Even though this seems like a very simple statement, it rings true in many clinical scenarios. This statement certainly applies to our current topic of nerve grafting and the fact that autograft is currently the gold standard therapy for nerve injury with neural tissue loss. It therefore makes sense that a synthetic material hoping to supersede autograft could benefit from mimicking native tissue to a greater or lesser degree. To achieve this goal it is clear that addressing only structural aspects in a prototype graft material will not fulfil this brief. Many groups have conducted research into the

biochemical and cellular cues that may be incorporated into scaffold design to encourage neural regeneration.

Neurotrophic factors are proteins responsible for the promotion and normal development of healthy young neurons and also for the maintenance and regulation of mature neurons. They are also important in the injured neuron as they are involved in axonal regrowth, Schwann cell upregulation and neuroprotection using signalling cascades [195]. Neurotrophic factors are loosely divided into three groups based on their signalling pathways: neurotrophins (e.g. nerve growth factor or NGF), glial-cell-line-derived neurotrophic ligands (e.g. glial-cell-line derived neurotrophic factor or GDNF) and neuropoeitic cytokines (e.g. ciliary neurotrophic factor or CNTF) [196].

One study bridged a critical nerve gap using ethylene vinyl acetate conduits loaded with either neural growth factor or glial-cell-line derived neurotrophic factor [197]. On histological analysis, the latter group had 4 times as many myelinated axons as the former. Another study, however, argued that multiple neurotrophic factors can display a synergistic effect when used in a nerve scaffold [198]. This study showed that by using both NGF and GDNF in a device, results were better than using each substance alone. It was postulated that the improved regeneration was due to the fact that NGF and GDNF promote regeneration in two different ways and have different targets within the nervous system. NGF acts on the TrkA receptor which is associated with sensory neurons [198] and GDNF interacts with GFRA2 and GDNF family receptor alpha 1 implicated in motor neuron function [199].

2.5.5 Biomaterial Veneers

Autograft is the current gold standard material for use in peripheral nerve repair with tissue loss. It would be remiss to think that a simple material could possibly replace endogenous nerve and previous sections have touched on this theme. Researchers are constantly searching for any method that can proffer an advantage to a material. While some groups invent whole new approaches to nerve conduit design, others are experimenting in the use of chemicals, molecules and other means to decorate the exterior of existing materials to promote successful neural regeneration.

Many approaches have been pursued in order to create the ideal neural grafting material by increasing the material's amenability to cell migration, adhesion and proliferation. Methods being employed to achieve this include protein coating, chemical treatments, surface physical modification and protein mimetic adsorption [200]. Even apparently suitable biomaterials have properties that one must overcome to render them more attractive for use as a neural graft substrate. For example, many of the current leading experimental conduit designs use biodegradable materials such as polycaprolactone, collagen, chitosan etc. These are intrinsically hydrophilic/hydrophobic impeding their ability to promote neural regeneration as ideally, regenerating axons prefer a more stable uncharged, material [200].

Logically, proteins found in endogenous extra-cellular matrix have been the subject of much study, with collagen, fibronectin and laminin being the popular choices for investigation [178, 201-202]. Laminin is a complex, trimeric glycoprotein that is intimately associated with Schwann cell activity. In biological systems, laminin is part of Schwann cell basal lamina. Experimentally, laminin has been shown to be an important molecule implicated in many levels of Schwann cell activity and neural regrowth [178, 191, 203]. Laminin has also been shown to have an effect on Schwann cell integrins - transmembrane receptors implicated in the process of neural myelination [178]. Laminin has been studied in detail when used as a decoration for neural conduits and other related structures [176, 191, 203]. Other ECM proteins such as collagen and fibronectin have been shown to promote Schwann cell activity and encourage neural regeneration but they are inferior to laminin in this regard [178, 201-202]. Many studies have used laminin in conjunction with collagen, fibronectin and other materials in the hope of benefiting from the pro-regenerative properties of each material and consistently, the results have shown that laminin coatings are better than naked materials alone [185, 191, 204]. In fact, one study using tissue engineered scaffolds loaded with laminin 1 (LN-1) and nerve growth factor (NGF) showed that when used to bridge a 10 mm rat sciatic nerve gap, the implants fared as well as autograft in terms of gross nerve morphology, regeneration success rate, total number and density of myelinated axons and, most importantly, functional outcome [201].

2.6 **Polysialic Acid and Glycomimetics**

Glycans (or polysaccharides) are compounds made up of a series of glycosidically linked monosaccharides. Glycan diversity is cell-type specific and depends on the type, number and linkages of its monosaccharide constituents [205]. The monosaccharide units include: glucose, galactose, *N*-acetylglucosamine, fucose, sialic acid, mannose (Man), *N*-acetylgalactosamine, glucuronic acid and xylose. Not only are there a number of different monosaccharide subunits but each monosaccharide can have different conformations and various glycosidic linkages can exist between the monosaccharides at different hydroxyl groups. Some biochemists have referred to glycoconjugates as the "third language of life" [206], with the first language being the one of nucleic acids, the second being that of proteins and the fourth probably being the language of lipids.

Sialic acids are electronegatively charged monosaccharides that are found in higher animals and some microorganisms [207-208]. These monosaccharides contribute to the immense structural diversity of complex carbohydrates and are components of some of the lipids and proteins found on cell membranes and secreted macromolecules [209]. Sialic acids tend to be located towards the terminal ends of these molecules in a prominent position, implying their important role in cellular processes. Numerous different kinds of sialic acids (of which there are approximately fifty) are synthesised by biological systems, adding another level of interest and complexity to these important molecules [208, 210]. Sialic acids are frequently found in the deuterostome branch of the animal kingdom and are involved in both regulatory and protective roles in cell biology [206]. It is because of their appearance in the deuterostome superphylum of animals that has led some researchers to postulate that these molecules played a pivotal role in the evolution of higher species. There is practically no mammalian biological process that occurs without one of the sialic acid monosaccharides being involved, and therefore malfunction of their synthesis or errors in their degradation can have dire consequences and ultimately lead to the development of disease. Defects in the assembly or processing of *N*-glycans can result in a variety of congenital disorders. These include psychomotor and mental retardation and other neurological conditions such as epilepsy,

ataxia, microcephaly, cerebellar and cerebral atrophy, abnormal eye movements and decreased nerve conduction velocity [211].

The discovery of the glycan polysialic acid (PSA) in the vertebrate central nervous system, and its relationship to the immunoglobulin (Ig) superfamily neural cell adhesion molecule (NCAM) heralded an explosion in research and understanding in the study of how proteins and sugars interact in the nervous system [212].

Figure 2.7 Structural formula of α-2,8-polysialic acid. This diagram shows the linear arrangement of the sialic acid residues with the interconnecting α-2,8 linkages. There can be up to 200 residues in each polymer. From Berski S, van Bergeijk J, Schwarzer D, et al. Synthesis and biological evaluation of a polysialic acid-based hydrogel as enzymatically degradable scaffold material for tissue engineering. *Biomacromolecules.* Sep 2008;9(9):2353-2359.

Figure 2.8 Diagram showing the relationship of PSA to NCAM and the cell membrane. From El Maarouf A, Petridis AK, Rutishauser U. Use of polysialic acid in repair of the central nervous system. *Proceedings of the National Academy of Sciences.* November 7, 2006 2006;103(45):16989-16994.

PSA is a linear homopolymer that can contain up to 200 sialic acid residues in α-2,8 linkage (Fig 2.7). NCAM is a glycoprotein expressed on the surface of many cell types

(including neurons). It has an extracellular domain with Ig-like subsites which are involved in homophilic binding and fibronectin domains involved in cell signalling and neurite outgrowth. Homophilic binding refers to NCAM binding to other NCAM glycoproteins on the same cell and adjacent cells. Homophilic binding induces neurite outgrowth via the fibroblast growth factor receptor and acts on the p59Fyn signalling pathway. The exact mechanism of NCAM and its PSA moiety are poorly understood. Originally it was thought that PSA inhibited NCAM function because PSA is negatively charged and had an "anti-adhesive" role {Rutishauser, 1989 #427}. The current hypothesis is that NCAM function is modulated by PSA as it inhibits *cis*-interactions of NCAM in the plane of the plasma membrane. This prevents clustering of NCAM and the formation of stable, signal transducing groups of NCAM on the cell surface {Walsh, 1997 #428}. The lack of clustering makes more NCAM available for *trans*-interactions (e.g. with proteoglycans and L1) which would promote neuronal growth. It is known that PSA is expressed in large quantities during development. It was thought at one point that PSA-NCAM was an embryonic form of NCAM [205]. Its abundant expression is closely correlated with axon pathfinding and targeting and with certain aspects of muscle formation [213]. Studies have shown that by using the enzyme endosialidase-N to cleave PSA, one alters neuronal and glial migration, sprouting of axons as well as fasciculation and branching of axons [214-215]. In fact, as has been alluded to earlier, PSA was initially thought to be of paramount importance in neural development, but as research has continued it is now known that PSA levels are maintained in the adult nervous system and play a role in neural plasticity by interacting with secreted signalling molecules [214]. PSA also plays an important role in neural regeneration after an injury. Research has shown that in an *in vitro* model of sectioned neural tissue, removal of the polysialic acid moieties of NCAM significantly delays the sprouting reaction. These results support the idea that up-regulation of highly sialylated forms of NCAM are of functional importance in neurite sprouting and synapse regeneration in this in vitro model [216]. Studies show that PSA expression increases after various types of injury, and is linked to sprouting in the central nervous system and axonal regeneration in the peripheral nervous system [213]. PSA levels are linked to neural developmental activity. It has been shown that when developmental processes cease, PSA levels drop, concurrent with stable cellular activity. PSA levels remain elevated if axon-target actions are prolonged but if these processes are pharmacologically altered and accelerated towards their end-point, PSA expression

subsequently drops [205]. In rodent animal studies looking at the highly plastic hippocampus, it has been observed that PSA is expressed by immature neurons in the dentate gyrus. It was also seen that PSA is lost as neurogenic stem cells differentiate, mature and integrate into the neuronal network of the dentate gyrus and that this process is activity-related [217]. Using a mouse model, researchers have shown that animals placed in an enriched environment, where new synapses need to be formed or old ones altered, not only achieve a higher behavioural performance, but that at a molecular level, have a higher percentage of PSA-NCAM positive neuroblasts and have a fivefold increase in adult hippocampal neurogenesis [218]. Other studies have looked at PSA-NCAM function in the rostral migratory stream (RMS). Dying olfactory nerves are constantly replaced throughout life and this is facilitated by the rostral migratory system as neuroblasts migrate from the subventricular zone towards the olfactory bulb by tangential migration and move from the rostral tip of the migratory stream by detaching from each other to initiate radial migration to their target areas in the olfactory bulb [205]. By using endosialidase-N to remove PSA, neuroblast migration from the RMS is effected and the olfactory bulb in subjects atrophies [219-220]. Experimentally it has been shown that after spinal cord demyelination in the central nervous system, oligodendrocyte precursors, reactive astrocytes and SCs secrete PSA which suggests that it plays a role in glial plasticity and axonal growth after injury [221]. With regards to peripheral processes and PSA-NCAM, it has been experimentally shown that after injury, glycoconjugates of the node of Ranvier undergo a rearrangement and that proteins with a terminal galactose are replaced by sialoglycoproteins [222]. Also, in denervation injury, research has indicated that there is a surge (12- to 15-fold increase) in NCAM and a 30- to 50-fold increase in NCAM RNA in denervated skeletal muscle [223]. The same study also showed that the NCAM and RNA in denervated skeletal muscle are similar to the same NCAM and RNA found in embryonic skeletal muscle. This implies that similar mechanisms underpin both neural development and neural regeneration. Another study looked at how PSA-NCAM affects preferential motor reinnervation (PMR) [224] by examining the selectivity of regenerating motor axons and how PSA-NCAM influenced their ability to reach their targets [225]. This study found that different motor pools differentially express PSA after injury and motorneuron pools that did not upregulate PSA expression did not selectively reinnervate muscle.

PSA has repeatedly been shown to be a key molecule in the nervous system but it is also quite an elusive substance and poses several difficulties for researchers. Glycans, including PSA, are known for being structurally complex as well as difficult to synthesis and analyse [205, 226]. In a bid to circumvent these problems associated with PSA, scientists have sought out other compounds that act like PSA. Colominic acid is a capsular polysaccharide found in E. coli K1 and is a PSA analogue [227]. However, its use is not without problems and limits its *in vivo* applications. Firstly, the process of harvesting colominic acid does not yield a uniform product as there can be variability in the lengths of the produced polysaccharide chains. It has also been observed that the degradation and metabolic clearance rates of colominic acid are quite high *in vivo*. Unfortunately the exogenous origins of the product, means it can also act as an antigen and evoke a host immune response [227].

Researchers have turned their attention to pharmacological alternatives to find a PSA analogue. The area of peptide synthesis has proven to be of particular interest to groups wanting to study PSA. Synthetic peptides can be highly specific, minimally toxic, easy to make and excellent at penetrating biological systems [226]. Using monoclonal antibodies specific for PSA (e.g. antibody 735 [228]) researchers can analyse entire libraries of peptides and see what peptide sequences bind antibody and thus mimic natural PSA. It is worth nothing that peptides conformationally mimic natural ligands but have entirely different structures to the ligand they are mimicking. In other words a mimetic has a different molecular weight, a different chemical structure but is recognised biologically as the substance it is mimicking and thus exerts the same effect as the substance it is mimicking. Several groups have successfully synthesised and identified peptides that appear to mimic PSA in experimental conditions in both *in vitro* and *in vivo* models. One group managed to synthesise a cyclic peptide (which they called 'PR-21'). PR-21 had the sequence H-CSSVTAWTTGCG-NH2. PR-21 was noted to promote neural growth using mouse dorsal root ganglion cells and exert a promotional effect when implanted into chicken retinas and mouse brains [229]. The same group proceeded to show that PR-21 exerted both functional and histological regenerative properties when used in the mouse spinal cord injury model [226]. In the *in vivo* model there was increased serotonergic axon density at and caudal to injured spinal cord segment as well as decreased reactive gliosis. It is thought that PR-21 exerts an inhibitory effect on glial scar formation and

upregulates NCAM in astrocytes both of which encourage regeneration. Some members of the same group have also worked with a peptide with the sequence H-NTHTDPYIYPID-OH, which showed similar positive results when tested on a mouse peripheral nerve injury model measuring functional and histological parameters [230]. They showed, in this instance, that PSA mimetic enhanced remyelination in axons distal to the injured peripheral nerve and it also improved Schwann cell process elongation and Schwann cell proliferation in an *in vitro* model. They also showed that this increased regenerative activity did not occur in Schwann cells deficient in NCAM thus illustrating the importance of the PSA-NCAM relationship. They postulated that the effects of the mimetic peptide are due to PSA interactions with PSA-NCAM on Schwann cells or the disruption of inhibitory PSA-NCAM/receptor interactions resulting in activation of NCAM signalling pathways.

3 Objectives and Goals

The initial goal of this project was to fabricate an implantable collagen based nerve graft loaded with PSA mimetic peptide based on the premise that PSA mimetic peptide is a safe substance that can be successfully immobilised on a collagen scaffold. To achieve this, a suitable collagen scaffold was designed, fabricated and investigated. We then investigated and synthesised a pure PSA mimetic peptide before developing a *de novo* method for immobilising the PSA mimetic peptide on the collagen scaffold.

The next step was to show that a PSA mimetic peptide loaded onto a collagen scaffold improves the neuroregenerative properties of the scaffold in an animal model. This was based on the principle that a PSA mimetic peptide would impart a biochemical cue to a regenerating axon. This should improve the efficacy of a synthetic nerve graft. This involved implanting a PSA mimetic loaded collagen based nerve graft into an animal subject, using the rat sciatic nerve model. The success of the graft was measured by comparing nerve regeneration in the intervention group with suitable controls.

4 Materials and Methods

4.1 Collagen Work

4.1.1 Collagen Extraction

The atellocollagen used in all the different elements of the final nerve conduit was extracted from bovine Achilles tendon in the laboratory. Tissue was mechanically disrupted and suspended in 0.5 M acetic acid at 4 ºC for 48 to 72 hours. Pepsin was then added to the solution in 1:100 (w/w) ratio to weight of tissue and left overnight stirring at 4 ºC. In order to precipitate the collagen 0.9 M NaCl was added and again left overnight stirring at 4 ºC. This solution was then centrifuged at 8000 rpm for 20 minutes at 4 ºC. The precipitate was collected after decanting of the supernatant. The precipitate was suspended in 0.5 M acetic acid suspension stage for a further 24 hours. The NaCl precipitation stage was repeated as above to increase the purity of the end sample. The precipitated collagen was resuspended in a lower volume of 0.5 M acetic acid to concentrate the solution. Lastly, the solution was dialysed against 0.1 mM acetic acid for 5 to 6 days. Concentration and purity of collagen was confirmed using Sircol assay and SDS-PAGE analysis respectively.

4.1.2 Collagen Fibre Extrusion

The fabrication of collagen fibres and subsequent cross-linking was performed in the manner as reported by Zeugolis *et al* [231-232]. A 5 mL syringe (BD Scientific, UK) was filled with 5 mg/mL bovine type I atellocollagen and extruded at a rate of 0.3 mL/min using a syringe driver (KD-Scientific 200, KD-Scientific Inc., Massachusetts, USA). The collagen solution was extruded through silicone tubing of 0.03 mm inner diameter (Polymer Technologies Ltd., Warwickshire, UK) into fibre formation buffer (118 mM phosphate buffer and 20 % polyethylene glycol, M_w 8000 at pH 7.50 and temperature of 37 ºC). This method ensures that all collagen fibres are of a standard diameter. The fibres spent five minutes in the formation buffer and then were transferred

into the fibre incubation buffer bath (6.0 mM phosphate buffer and 75 mM sodium chloride at pH 7.10 and temperature 37 ºC) for five additional minutes.

After the allotted time in the incubation buffer, the fibres underwent cross-linking for 24 hours using N-(3-dimethylaminopropyl)-N-ethylcarbodiimide (EDC) and N-hydroxysuccinimide (NHS) at a ratio of 30 mM : 10 mM respectively in 50 mM 2-(N-morpholino)ethanesulfonic acid (MES) buffer. EDC is a zero-length cross-linking agent that couples carboxyl groups on amino acids in collagen to amine groups. NHS stabilises the reactive intermediate ester, preventing unwanted hydrolysis and increases the overall efficiency of the reaction. Cross-linking imparts structural stability to collagen implants. After a 24 hour incubation in cross-linking solution, the fibres were washed three times with sterile distilled water and allowed to air-dry, suspended and subject to the tension of their own weight. Similarly, non-crosslinked fibres were prepared in much the same way, except after the allotted time in the fibre incubation buffer they forewent the cross-linking step and were instead rinsed with sterile distilled water for 60 seconds and allowed air-dry under the tension of their own weight for a full 24 hours. Representative collagen fibre diameters were measured using an Olympus® IX-81® inverted microscope (Mason Technology, Dublin, Ireland). Cross-linking was confirmed via the ninhydrin assay.

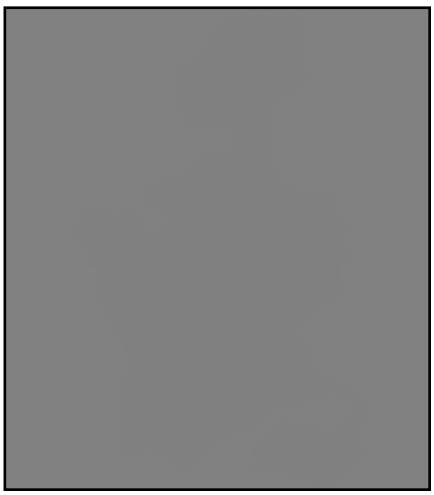

4.1 Image of Olympus® IX-81® inverted microscope. From online Olympus catalogue, accessed 10/9/2012, < http://www.olympusamerica.com/seg_section/images/product/detail_full/1022_secondary_lg.jpg>

4.1.3 Collagen Conduit Fabrication

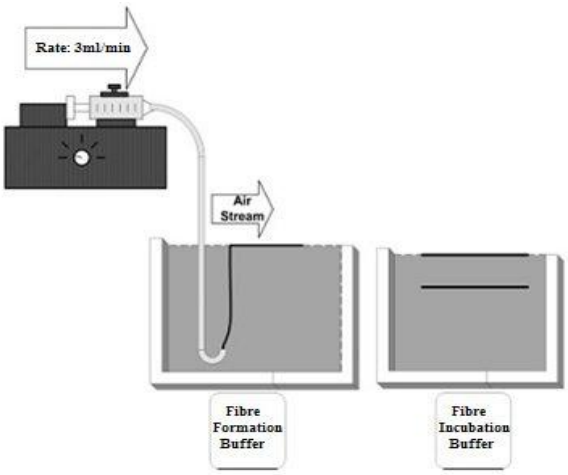

Figure 4.2 A schematic showing the set-up of the fibre extrusion method

Hollow collagen nerve guidance conduits were fabricated using a method described by Yao *et al* [233]. Type I bovine atellocollagen at a concentration of 12 mg/mL was formed over a 1.5 mm diameter machined, stainless steel, cylindrical rod, held in place between two clamps. The collagen was air dried and self assembled on the surface of the constantly rotated forming rod. The result was the creation of a uniform coating of collagen on the forming rod which was allowed to dry at ambient temperature. At this stage, the newly formed conduits were immersed in a bath of 30 mM : 10 mM EDC-NHS cross-linking solution for a full 24 hours before being rinsed in a 0.1 M wash of PBS. The conduits were then manually taken off the steel rod. The final conduits had an inner diameter of 1.5 mm (the same diameter as the forming rod), and outer diameter of 1.7 mm and a length trimmed to 12 mm.

4.1.4 Collagen Hydrogel Fabrication

A collagen hydrogel formed part of the final nerve conduit and was used for the *in vivo* testing part of the project. The final gel was synthesised by mixing 90 µL of 10X PBS with 910 µL of collagen solution (3.5 mg/mL suspended in 0.1 M acetic acid). This was

then mixed gently before the addition of 15 µL of 2 M NaOH. The pH was then adjusted to pH 7 before being placed in a water bath at 37 ºC for 40 minutes. This recipe resulted in a gel with the required viscosity for our purposes. The peptide dissolved readily in all gels, so solubility was not an issue.

4.2 Peptide Work

4.2.1 General Procedures for Peptide Synthesis

4.3 Applied Biosystem ABI 433A Synthesiser. From University of Pittsburgh peptide synthesis homepage. Accessed on 10/8/12, < http://www.peptide.pitt.edu/433a.html>

Peptides were assembled using automated solid phase peptide synthesis (SPPS) using standard fluroenylmethoxycabonyl/*tert*-butyl (Fmoc/*t*Bu) protection strategy. Automated synthesis was performed on an Applied Biosystem ABI 433A Synthesiser. This process involves loading cartridges filled with molar amounts of protected amino acid substrates onto the rack of the synthesiser in the order of addition before a computer assisted automated system adds each peptide in sequence. This occurs through a complex sequence of regulated chemical reactions that involves the deprotection of each substrate and addition of the next. The peptide chain is anchored on the resin in the reaction chamber of the synthesiser. The chain grows as each amino acid substrate is automatically activated and added to the preceding amino acid group on the resin. The

ABI 433A has feedback monitoring control which is based on the measurement of the UV absorbance of the reagents, solutions and solvents used in the synthesis cycle. The peptide at the end of the chain assembly stage of the preparation process is bound to the resin and the free peptide is cleaved using a standard cleavage cocktail solution. The bound resin is first washed with dichloromethane (DCM), air dried and then transferred to a 25 mL round bottom flask. Cocktail solution was then made up fresh in a separate vessel prior to use. The general cleavage cocktail recipe consisted of 80 % trifluoroacetic acid (TFA), 5 % triisopropylsilane (TIPS), 5 % ethanedithiol (EDT), 5 % thioanisole and 5 % water. TFA cleaves the final product from the resin and removes side chain protecting groups. During the reaction with TFA highly reactive carbocations are generated and these need to be sequestered to prevent them reacting with certain amino acids which are susceptible (e.g. cysteine or methionine). The other ingredients in the cocktail act as scavengers, preventing the build up of reactive intermediates. The reaction time varies between 60 and 90 minutes. There are different methods to remove the peptide from the highly acidic cleavage cocktail solution, such as evaporation. The method used in this project was to filter the solution from the resin followed by precipitation of the peptide in cold diethyl ether. This solution was then frozen for approximately ten minutes. The sample was then centrifuged at 2.8 x 10^3 rpm for five minutes. Precipitation in diethyl ether, washing and centrifuging was repeated two more times. The sample was then air-dried, dissolved in water and then plunged into liquid nitrogen and was subsequently freeze-dried for 24 hours. At this point the freeze-dried peptide was ready for purification.

4.2.2 Applied Techniques for Peptide Synthesis

Certain peptides were created by manually coupling amino acids onto resin bound peptides using existing free amines. This works on the exact same principle as the automated system. A series of chemical reactions are performed using protected amino acid substrates. The polypeptide chain propagates one amino acid at a time by chemically activating the free end of the ever growing chain of residues and adding an activated or deprotected amino acid substrate. The ratio of amino acid to coupling reagents used was based on the substitution of the resin. Twice the equivalents of N,N-

diisopropylethylamine (DIEA) as compared to Fmoc protected amino acid. The DIEA This ensures complete deprotection and activation of the relevant amino acid substrates and maximises the efficiency of the reaction. The coupling agents used were hydroxybenzotriazole/*N,N,N′,N′*-tetramethyl-O-(1H-benzotriazol-1-yl)uronium hexafluorophosphate (HOBt/HBTU). The coupling agent and amino acid were dissolved in dimethylformamide (DMF) before being washed with DCM. Complete coupling was tested using the colorimetric Kaiser test. This test is based on the raction of ninhydrin with amines. This test's reagents included ninhydrin and phenol, both in ethanol and potassium cyanide in pyridine. A small amount of the resin being tested was placed in a test tube and a drop of each reagent was added to this. The tube was heated to 110 ºC in an oil bath for three minutes. The heating step allows "hidden" amine groups to become more accessible and thus detectable. A positive test was indicative of free amines and indicates successful coupling. A positive test occurs when ninhydrin hydrolyses and reacts with the free amine on the peptide. This results in a rearrangement as the peptide as it loses its amine. This reaction produces a colour change and causes the sample to turn dark purple. In a negative test no reaction occurs and the sample remains colourless/light yellow.

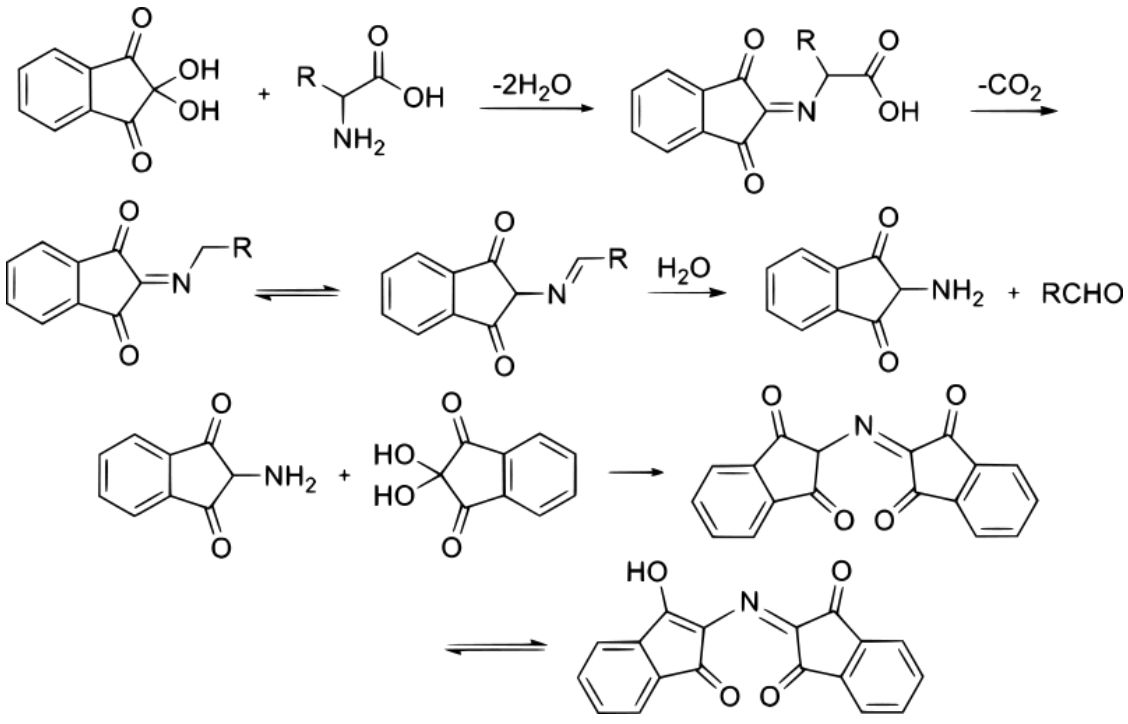

Figure 4.4 Mechanism of Kaiser test

A cyclic peptide was also produced in the course of this study. Cyclisation was performed as per Kamber et al [234]. This method uses iodine oxidation of a cycteine containing peptide which converts tritylthio groups to disulfides. These disulfide bonds are what cause the peptide to be cyclic in nature. The method involves adding DCM, methanol and water to a reaction vessel with the peptide and then dropping another solution containing iodine, DCM and methanol into this before adding sodium thiosulphate and finally extracting the product with chloroform. The separated organic layer was washed twice with water before drying over magnesium sulphate before being resuspended in water and freeze-dried.

A fluoroscein (FIT-C) tagged linear peptide was also synthesised. This was synthesised for use in immobilisation studies. Part of the challenge of this project was proving that the peptide was immoblilsed on the scaffold. It was postulated that by chemically binding a fluorescent molecule onto the peptide that it would cause fluorescence if the peptide was successfully bound to the scaffold. This was achieved by adding a beta-alanaine and cysteine amino acid unit to the N terminus of the peptide, with the beta-alanine acting as a linker for the FIT-C. The addition of these residues would give a spare reactive group for the FIT-C to attach to. The peptide was synthesised in the previously described automatic fashion, leaving a peptide attached to the resin. Instead of cleaving the peptide from the resin straight away, the fluoroscein was added to the resin bound peptide using the previously outlined manual coupling procedures. The finished, FIT-C tagged peptide was then cleaved using a slightly modified cleavage cocktail that would not disrupt the sensitive FIT-C molecule.

4.2.3 High-Performance Liquid Chromatography (HPLC) Analysis

4.5 Varian HPLC Galaxy system. From Triad Scientific online catalogue. Accessed 14/4/2011 < http://www.triadsci.com/?site=preowned&item=15571&menu=7441#prettyPhoto[itemgal_gal]/0/>

We used a Biosystems Biocad SPRINT or a Varian HPLC Galaxy workstation to perform chromatographic analysis utilising different reverse phase and size exclusion chromatography columns. Reverse phase chromatography is a form of partition chromatography. The peptide being analyses is adsorbed onto the hydrophobic surface of the analytical columns which contain a silica gel with chemically bonded phases. The peptide remains on the column substances until the concentration of the organic modifier solution elutes the molecules from the hydrophobic surface. The more soluble the solute is in water the faster it will be eluted. The specific columns we used for the reverse phase chromatography were a C-18 Gemini and a C-5 Jupiter column, Phenomenex (250 x 2.5 mm). For purification and analysis we used a flow rate of 1 mL/min or a linear gradient over 30 minutes. UV detection was performed at 214 nm because this is the wavelength at which amide bonds present in peptides are detected. Solvent A consisted of water containing 0.1 % trifluoroacetic acid (TFA) and solvent B, acetonitrile containing 0.1 % TFA.

4.2.4 HPLC Purification

Using a Perspective Biosystems Biocad SPRINT with UV detector we performed reverse phase high-performance liquid chromatography (RP-HPLC) purifications. The system was set for dual absorbance using a semi-preparative column Gemini phenomenex C-18 reversed phase chromatogram (250 x 10 mm) calibrated for a flow rate of 4 mL/min with a linear gradient programmed for a 30 minute run time from 5 to 65 % of solvent B. The solvents were prepared by being degassed using helium bubbling for 20 minutes. Monitoring of UV absorbance was at 214 nm as this is the wavelength absorbed by the amide bonds of peptide.

4.2.5 Mass Spectrometry

Mass spectrometry was performed by Matrix Assisted Laser Desorption Ionization-Time of Flight (MALDI-TOF) on a Reflex Bruker Spectrometer. The sample being analysed is uniformly mixed in a matrix. This mixture is then subjected to ultraviolet light. The matrix absorbs the light and converts it to heat energy. This causes vaporisation of the mixture containing matrix and sample. These free, charged ions are then subjected to a potential difference causing the particles to accelerate. Different ions of different mass/charge ratio travel at different speeds in the electric field. The detector then uses this to analyse the different times of ion flight and the composition of the sample being analysed can then be calculated. Two matrix styles were used, dihydroxybenzoic acid and hydroxyl cinnamic acid, dissolved in 50 % acetonitrile and 50 % water at a concentration of 10 mg/mL and 15 mg/mL respectively. 1 μL of each 1:1 solution of matrix peptide were applied on the plate

4.3 Peptide Immobilisation

4.3.1 Covalent Immobilisation of Peptide on Collagen

In order to attach peptide to inert, cross-linked collagen, a novel technique for selective collagen activation was devised. Collagen fibres were prepared in the fashion outlined previously. Collagen is mainly composed of three amino acids, namely glycine, proline and hydroxyproline. Many of the amino acid side-chains of collagen have carboxyl or amine end groups. This means that the surface of any collagen scaffold is decorated with inert carboxyls and amines. For a peptide to be bound to the surface of a collagen fibre, activation of these terminal carboxyls and amines must occur, and in this project a 3-step peptide addition protocol was devised. The first step was the amine blocking step. Standard weights and lengths of collagen fibres were prepared (approximately 15 mm in length and 0.1 mg in weight). Sulfo-NHS-acetate (SNA) was chosen for the amine blocking. It forms stable, covalent amide bonds with amine groups which prevents unwanted interaction. It was added in a ratio of 1:1 (w/w) was added to each fibre in a volume of 100 µL of 0.1M $NaHCO_3$ (pH 8.5) and incubated overnight at room temperature to allow complete reaction. The SNA was highly hygroscopic and had to be added quickly as it was discovered it loses its reactivity quickly if left exposed to atmospheric humidity. After two hours the fibre was then washed with $NaHCO_3$. The second step was the carboxyl activation step. EDC/NHS was the chosen reagent for this step. EDC/NHS activates the free carboxyl groups on the collagen by forming an O-acylisourea intermediate that is displaced by nucleophillic attack from the primary amine groups in the peptide. The "amine-blocked" fibre was incubated at room temperature for two hours and immersed in 200 µL of EDC/NHS (0.2 M EDC, 0.01M NHS, made up in MES 50 mM with pH adjusted to 5.5). This fibre was then washed with MES. The third and final step was the peptide addition step. In this step we incubated the fibre at room temp for two hours in 200 µL of peptide solution of varying concentration between 50 and 500 µg/mL (depending on the experiment being carried out).

To prove that a peptide was successfully added to a collagen fibre a TNBSA assay was performed. TNBSA solution (5 % v/v in methanol) reacts with primary amines (peptides

or amino acids) to produce a soluble coloured product which can be measured using a spectrophotometric plate reader set to read at 335 to 345 nm. Therefore, when peptide is successfully added to a collagen fibre, a drop in amine concentration is seen in the leftover peptide solution, when compared to unreacted controls.

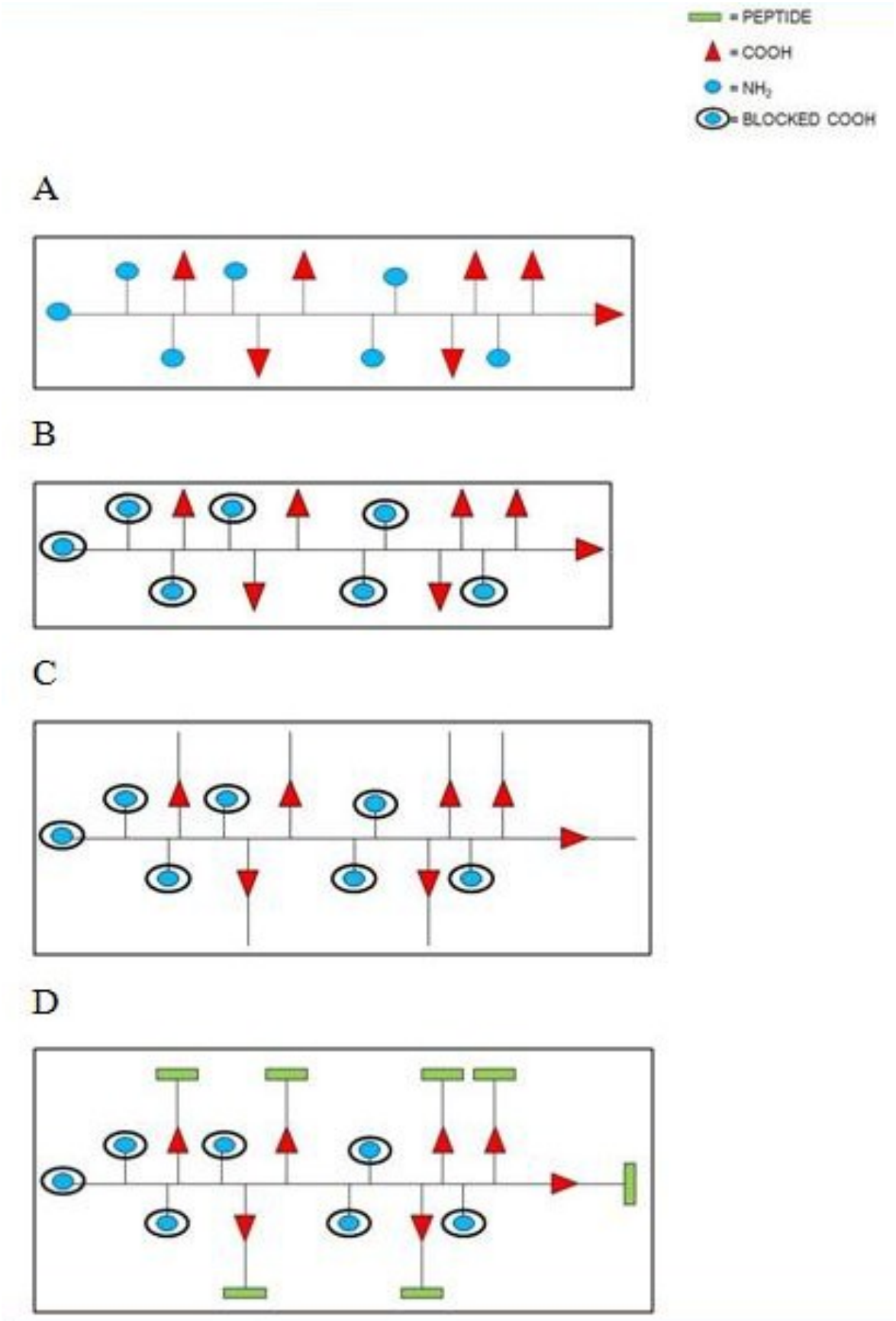

Figure 4.6 Schematic showing the stages of selective activation of collagen fibre. A, plain collagen. B, amine blocking. C, carboxyl activation. D, peptide binding

Known amounts of peptide were added to the activated collagen fibre during the final step of peptide immobilisation. 100 µL samples were taken from the reaction vessels. To these samples 125 µL of 0.01 % TNBSA and 150 µL of 0.1 M $NaHCO_3$ were added. This was then incubated for two hours at 37 ºC. The reaction is then terminated with 62.5 µL of 1 M HCl and 125 µL of 10 % SDS-PAGE. 100 µL of each of these samples was then loaded onto a 96-well plate and read on a plate reader at 335 nm. Experimental groups were compared to controls containing the same amount of peptide as that reacted with the activated collagen fibre. Results were expressed as percentage drops in peptide. Experiments were carried out examining the behaviour of peptide uptake at different time points and the relationship between the mass of the collagen fibre and the degree of peptide uptake.

In another effort to prove successful peptide immobilization on a collagen fibre, amino acid analysis was performed. The principle behind this experiment is that there are certain amino acids present in the target peptide that are not present in collagen, therefore if the peptide successfully attaches to the collagen this will show up in an amino acid analysis of a hydrolysed sample.

Hydrolysis was performed by first accurately weighing and recording the weight of the washed, modified collagen fibre being tested and placing in a glad hydrolysis tube. Concentrated HCl is added before evacuation and sealing of the hydrolysis tube. In order to prepare the sample for vapour phase hydrolysis, it was repeatedly frozen and thawed under a vacuum before the vessel is sealed. Hydrolysis was performed under this vacuumed state at 110 ºC for 24 hours.

At this point, ion exchange chromatography of the sample was performed followed by post ion column derivatisation and photometric detection using ninhydrin. In ion exchange chromatography, the analyte is immobilised on a column and subjected to increasing concentrations of similarly charged species that eventually displace the analyte from the column which is detected using visible light absorbance.

4.3.2 Physical Immobilisation of Peptide

For this part of the project, peptide was physically loaded into collagen hydrogels. This was achieved by dissolving known masses of peptide to fresh hydrogels after the last stage of gel manufacture and gently agitating the sample until the peptide was fully dissolved while carefully avoiding air bubble formation. The concentration of peptide used in the *in vivo* study was 200 μg/mL, a figure consistent with the literature[230].

4.4 Cell Work

4.4.1 Cell Culture

3T3 fibroblasts were used for cell viability studies. Cryopreserved cells were defrosted in a water bath at 37 ºC for approximately 10 minutes. A solution containing Dulbecco's modified eagle's medium (DMEM), filtered foetal bovine serum and penicillin/streptomycin was then constituted. 10 mL of this medium was placed in a Falcon tube and 1 mL of defrosted 3T3 fibroblasts was added. The concentration of fibroblasts was 2 x 10^6 per millilitre. The Falcon tube was agitated gently before being spun in a centrifuge and resuspended in fresh medium and placed in an incubator.

4.4.2 Cell Counting

Once suspended in the appropriate volume of medium, an aliquot of the cell suspension was mixed with equal volumes of trypan blue (0.4 %, w/v). Using a haemocytometer they were counted using a phase contrast microscope. To calculate the number of viable cells per millilitre, the number of viable cells in the four quadrants of the haemocytometer were counted with the resultant mean being multiplied by 2 (the dilution factor). This figure was multiplied by a factor of 10^4, which is the appropriate factor given the volume of the haemocytometer.

4.4.3 Cell Viability Study

For this project the MTT assay (3-(4,5-dimethylthiazol-2-yl)-2,5-diphenyltetrazolium bromide) was used. This is a colorimetric assay. Purple-coloured, water-insoluble formazan crystals are precipitated when the yellow-coloured, water-soluble MTT salt was reduced by the mitochondria of metabolically active cells. We seeded 3T3 fibroblast cells at an appropriate density per well on a 96-well plate the day before inoculation. Each well was treated with a corresponding concentration of test compound, at

concentrations ranging from 1 to 100 µg/well. Plates were incubated for 24 hours and 48 hours respectively. At the set time point, analysis was performed by adding 50 µL of MTT solution (5 mg/mL; made up using sterile PBS before being filter sterlilised) to each well in question. After 4 more hours of incubation, the supernatant was aspirated in such a way as to avoid disrupting the precipitated formazan crystals. These crystals were then solubilised using 200 µL DMSO. The plate is then placed on a spectrophotometric plate reader where the absorbance is read at 570 nm for 1 second. Values were expressed as a percentage against untreated controls.

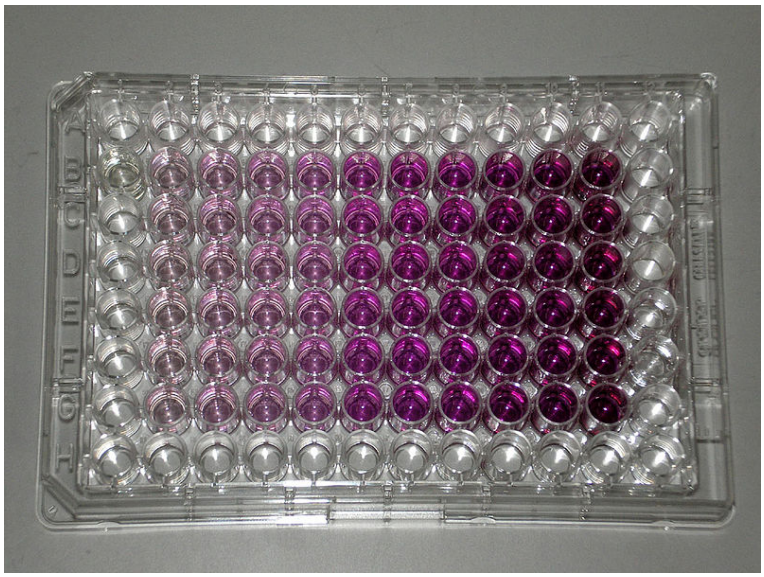

Figure 4.7 MTT assay performed on a 96-well plate. From Shinryuu, created 19 November 2010, MTT plate, accessed 10 August 2011, <http://commons.wikimedia.org/wiki/File:MTT_Plate.jpg>.

4.5 *In Vivo* Work

4.5.1 Conduit Preparation

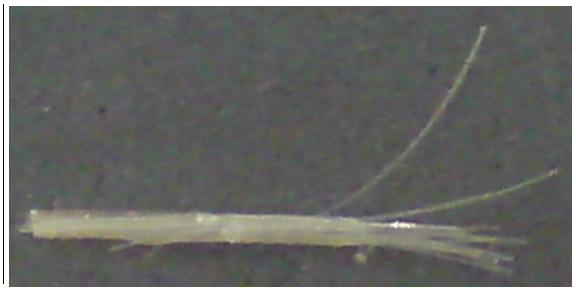

Figure 4.8 A hollow nerve guidance conduit packed with fibres

Figure 4.9 A close-up of the end of a hollow nerve guidance conduit showing the fibres *in situ*

Four different conduits were used in the *in vivo* section of the project. These four types were:

- Hollow conduit containing plain hydrogel alone
    - Plain hydrogel contains no additives
- Hollow conduit containing plain hydrogel and fibres
- Hollow conduit containing linear peptide hydrogel and fibres
    - Linear peptide hydrogel contains linear peptide at a concentration of 200 µg/mL
- Hollow conduit containing scramble peptide hydrogel and fibres
    - Scramble peptide hydrogel contains linear peptide at a concentration of 200 µg/mL

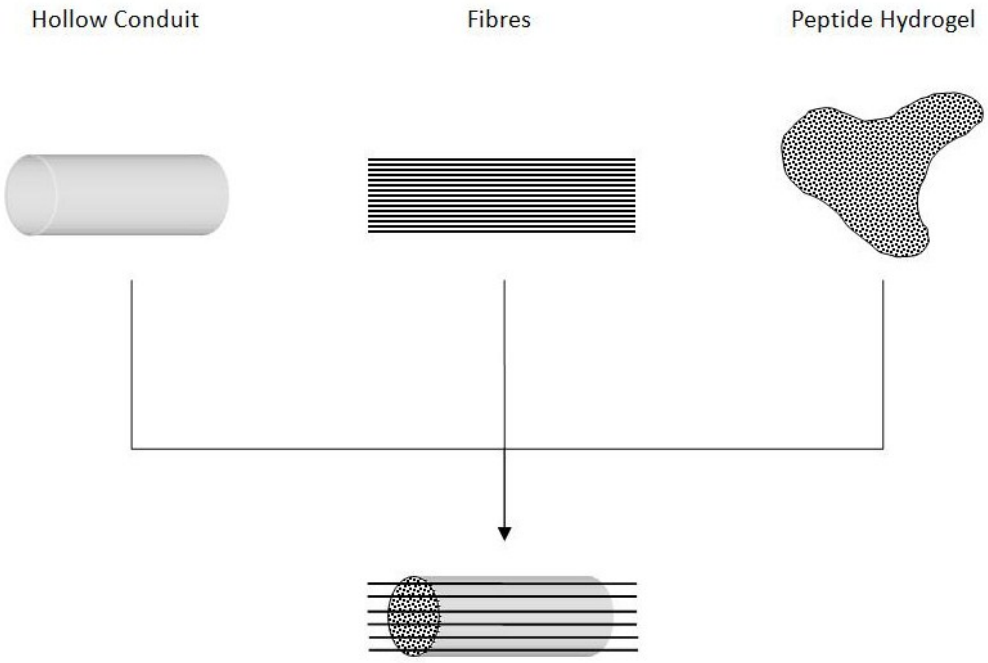

Figure 4.10 Schematic showing the composite conduit used in the experimental groups of the *in vivo* study

The data used from two more control groups (autograft and Neuragen) was sourced from a related project within the same facility whose subjects were subjected to identical procedures and conditions. The hollow conduits used in all four groups were prepared in the manner discussed previously. Prior to implantation, 18 collagen fibres were loaded into each conduit. This gives a packing density of approximately 2.2 % of the total cross-sectional area of the conduit lumen, with each fibre having a diameter of 50 μm and the conduit having an internal diameter of 1.5 mm. These fibre filled conduits are then soaked in 70 % ethanol for two hours, before being thoroughly rinsed with 0.1 % PBS to remove any residual ethanol. They were then stored under sterile conditions until use. The groups containing hydrogel underwent hydrogel loading just prior to surgery. This involved the pipetting of ten μL of a specific hydrogel into the conduit around the fibres. Thirty-two female Lewis rats, weighing between 220 and 250 g were assigned randomly to one of the four test groups (Table 4.1). Each of the four test groups was subdivided into two more groups, with each of these subgroups being subjected to nerve morphometry and simultaneous retrograde nerve testing respectively. All animal testing was conducted in accordance with both National and Institutional guidelines set out by the Cruelty to Animals Act 1876 as amended by the European Communities (Amendment of Cruelty to Animals Act, 1876) Regulations 2002 and 2005.

Table 4.1 List of treatment groups, experiment type and numbers of animals for each part of the in vivo study.

Test Group	Nerve Morphometry	Retrograde Tracing	Total
Conduit & gel	5	3	8
Conduit, gel & fibres	5	3	8
Conduit, scramble gel & fibres	5	3	8
Conduit, linear gel & fibres	5	3	8
Total	**20**	**12**	**32**

4.5.2 Surgical Procedure

General anaesthesia was administered via intraperitoneal injection of ketamine and xylazine using aseptic technique. The surgical site was prepared by shaving the fur over the rat's hind-quarter and prepped with iodine solution. A longitudinal skin incision was then made approximately 3 cm in length over the subject's hindquarter. Using microsurgical instruments and a microscope the dorsal gluteal muscle was split using blunt dissection with a forceps. The sciatic nerve was then identified and exposed along its length, from proximal appearance to the distal bifurcation. A 10 mm nerve gap was created, starting 5 mm proximal to the distal sciatic bifurcation. A 12 mm conduit was then placed in the nerve gap, and proximal and distal nerve stumps were inserted into the conduit lumen. Using a 10-0 Ethilon® non-absorbable, nylon, monofilament suture (Ethicon, J&J, Dublin, Ireland) the implant was secured using epineural suturing. The wound was closed in layers using 4-0 Vicryl Rapide™ absorbable, polyglactin, braided suture (Ethicon, J&J, Dublin, Ireland). At the conclusion of the procedure, the animals received analgesia in the form of intramuscular buprenorphine hydrochloride. The rats were observed and given respiratory support until they became fully conscious. Animals were monitored and subject to routine observations of vital parameters and signs of distress. Animals received additional analgesia if required.

4.5.3 Nerve Histology and Ultrastructural Analysis

Animals were sacrificed at the 16th post-operative week using by CO_2 asphyxiation. An incision was made along the healed scar and the sciatic nerve implant site was exposed. Fixation of the sample was performed *in situ* by pouring Trump's fixative solution (made up of 4 % formaldehyde, 1 % glutaraldehyde in 0.1 M PBS) into the wound, immersing the graft site, and leaving this for 30 minutes. Aspiration and disposal of the fixative is then performed from the wound. The graft and a cuff of sciatic nerve adjacent to either end of the graft are resected *en bloc*. The final specimen consists of three one mm sections harvested from 1 mm proximal to the graft, 1 mm from the centre of the graft and 1 mm distal to the graft, and labelled accordingly before being placed in Trump's solution in advance of sectioning. The samples from the centre of the grafts were then post-fixed in a solution of osmium tetroxide (concentration 1 %). Osmium tetroxide binds to lipid in cell membranes, coating them with a heavy metal and acts as a stain in electron microscopy. Osmium tetroxide is a good alternative to other methods of coating cells with heavy metal for electron microscopy as it does not obscure the dine detail of cell architecture. Serial dehydration was performed by immersion in a series of alcohol solutions. Embedding of samples was performed in spur resin (EMS, Fort Washington, USA). The block was then sliced into 1 μm semi-thin sections using a Leica UltraCut E™ Microtome (Rankin Biomedical Corp., MI, USA). These sections were stained with 1 % toluidine blue. Light microscopy and subsequent electron microscopy was performed on these samples. In order to examine myelin sheaths and axons under high resolution, ultrathin sections were taken from the samples and analysed using a transmission electronic microscope (TEM).

4.5.4 Morphology and Stereology

Nerve morphology and stereology were performed by examining the three different harvested graft sections (proximal, centre and distal) and examining the regenerated nerve segments therein. The centre section was analysed for axonal density, area, diameter, size and g-ratio as well as myelinated fibre diameter and myelin thickness. The g-ratio was calculated by working out the ratio of inner axonal diameter to total

axonal diameter. This figure was acceptable as a functional index of myelination and has an ideal value of between 0.6 and 0.7 [235].

The listed parameters were assessed using an upright fluourescent microscope (BX51 Upright Fluorescent Microscope®, Olympus Inc., Center Valley, USA). The obtained images were analysed using ImageJ software (NIH, Bethseda, USA). Each nerve area quantification was performed by examining the section under 100x magnification and tracing the circumference of the tissue. Revascularisation was calculated by counting the number of blood vessels visible in each section at 100x magnification. Stereological evaluation was performed at 1000x magnification in order to count axons using the area fraction method as detailed by Canan et al [236]. This method samples axons equally from the entire nerve area. Using an unbiased counting frame, individual areas of 1600 μm^2 were taken and randomly and systematically analysed one at a time. Calculation of the axon number per unit area was performed and extrapolated in an appropriate fashion to give the total axon number for the entire section. The other parameters listed above (axon size distribution, average axon and myelinated fibre diameters and myelin thickness) were counted similarly. At least 50 axonal profiles were taken per sample.

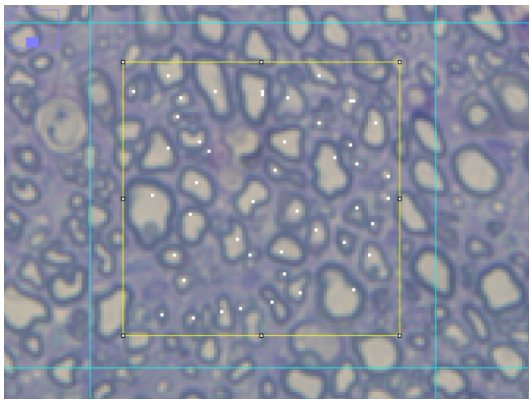

4.11 Microscopic image showing axonal counting method

4.5.5 Simultaneous Retrograde Tracing

Animals in this arm of the study underwent a second procedure at post-operative week 16. Using the same anaesthetic regime, the previous graft site was opened up. The nerve was traced distally to the bifurcation site and the tibial and peroneal branches were divided. The proximal cut ends of both nerves were then treated with retrograde nerve tracers. The tibial cut end was soaked in 5 % fast blue solution (Sigma Aldrich, Wicklow, Ireland) for 30 minutes. The peroneal cut end was simultaneously soaked in 5 % diamidino yellow solution (Sigma Aldrich, Wicklow, Ireland) for 30 minutes. The cut ends were washed with normal saline and sutured into the surrounding muscle to prevent dye from escaping. One week later, the animals underwent general anaesthetic and transcardial perfusion with 4 % paraformaldehyde and 10 % sucrose in PBS. The vertebral column, with intact spinal cord, from L1 to L6 was removed and immersed in fixative overnight. The vertebral samples were then embedded in Cryo-Gel® (Instrumedics Ltd., St. Louis, MO) and sectioned longitudinally in a saggital plane into 30 µm sections using a cryostat (Microm HM505E Cryostat®, Walldorf) at a temperature of -20 ºC. Using an upright fluorescent microscope (BX51 Upright Fluorescent Microscope®, Olympus Inc., Center Valley, USA) sections were immediately examined. Fast blue (FB) labelled neurons were identified by having blue cytoplasm and diamidino yellow (DY) labelled neurons had a yellow nucleus. If a section showed a neuron with a yellow nuceleus with blue cytoplasm, it was designated as FB/DY-double-labelled. All of the neurons were counted in each section. Due to a technical difficulty in sample harvesting, the data from this part of the project was unreliable and subsequently omitted.

4.5.6 Statistical Analysis

Graphpad^{TM} v5.1 (Graphpad Software, CA, USA) statistical software was used for all statistical analysis. The quoted graphical data is depicted as the mean ± standard error of the mean. Analyses used for data interpretation included a one-way analysis of variance (ANOVA) followed by a Tukey *post hoc* test for multiple comparisons. A p-value of <0.05 was deemed statistically significant.

5 Results

5.1 Peptide Work

5.1.1 Background

Mehanna et al describe the neuroregenerative properties of a linear PSA mimicking peptide (LP) of sequence H-NTHTDPYIYPID-OH[230] (M_w with specific reference to remyelination and functional recovery. They identified the activity of this peptide by screening a linear 12-mer phage display peptide library with a PSA recognising monoclonal antibody and verified its activity as a PSA mimetic using competition ELISA.

In the course of this project several different peptides were synthesised. The data in this section pertains to synthesis of the linear peptide and its scramble. Data regarding the other peptides can be found in the relevant section of the appendices

5.1.2 Preparation of Linear PSA Mimicking Peptide and Its Scramble

LP was assembled using automated solid phase peptide synthesis (SPPS) with a standard fluroenylmethoxycabonyl/*tert*-butyl (Fmoc/*t*Bu) protection strategy on an Applied Biosystem ABI 433A Synthesiser. The particular peptide was assembled using a special "Wang resin" which ensures that the peptide terminates with a carboxyl group, which is important when it comes to peptide immobilisation on a collagen scaffold. A standard cleavage cocktail of 300 µL TA, 300 µL TIA, 300 µL H_2O, 300 µL EDT and 4.8 mL TFA was used. However, the reaction time was reduced to 60 minutes because the peptide bond formed between apspartic acid (D) and proline (P) is notoriously weak and excessive reaction time would reduce yield. The yield of this peptide was excellent at 24.5 mg with a purity of 83.08 %.

For control purposes a scramble peptide (SP) was synthesised using the same basic method as outlined above. The scramble peptide had the same amino acid content as the

linear peptide, but the amino acids were assembled in a different order, namely H-YDIDTITPHYPN –OH. For the scramble we avoided the aspartic acid/proline peptide bond so the cleavage cocktail reaction time reverted back to the usual 2 to 2.5 hour duration. Subjecting the peptide to a prolonged period of time in the cleavage cocktail would ultimately lead to breakdown of the peptide itself, and reduce overall yield. The scramble peptide had a yield of 28.4 mg with a purity of 90.4 %.

Successful synthesis of the peptide was confirmed using MALDI-TOF mass spectrometry. Figure 5.1 shows a spike indicating a singly charged protonated species of molecular weight 1448.6, the predicted weight of the linear peptide. Figure 5.2 shows the spectra produced after fragmentation of the sample. These figures again correlate with the projected results of the analysis of a species with a molecular weight of 1448.6. The numbers at the peaks refer to "mass to charge" ratio. The formula for working out the molecular weight of a protonated sample is:

$$\text{Molecular Weight} = (\text{mass} + \text{charge})/\text{charge}$$

If we apply this to the results in figure 5.2 we see that there is a peak of a doubly charged ion at approximately 725. This is the predicted figure as per the above formula: $(1448.6 + 2)/2 = \sim 725$

The same applies to the triply charged ion which is present at ~484. This is again the predicted figure: $(1448.6 + 3)/3 = \sim 484$.

Figure 5.3 is another MALDI-TOF analysis looking at the fragmented, charged, peptide confirming the predicted molecular weight.

Figure 5.4 illustrates the fragmentation patter of the linear peptide generated during collision induced dissociation fragmentation, whereby the peptide sample is vaporised using MALDI-TOF and the particles are accelerated through a field containing an inert gas. The collision of the peptide fragments with the gas causes fragmentation of the peptide. The graph shown here shows peaks consistent with the pattern of fragmentation one would expect, given the known structure of the linear peptide.

Figure 5.5 shows the graph produced during HPLC analysis of the crude linear peptide. Each peak represents a pure product of a specific molecular weight. Each pure sample is collected individually and tested using mass spectrometry to confirm what

the molecular weight of the sample is. The target peptide is identified in this fashion and then the other collected samples are discarded. Figure 5.6 shows the graph generated when the purified peptide is passed through HPLC purification. The single peak is indicative of a pure sample. Retention time refers to the point in time at which the eluted sample is freed from the analysing column and is dependent on its solubility in the TFA/acetonitrile solution at that particular time. Figures 5.7 and 5.8 show the same process as applied to our scramble peptide. Table 5.1 shows the collated data for peptide synthesis.

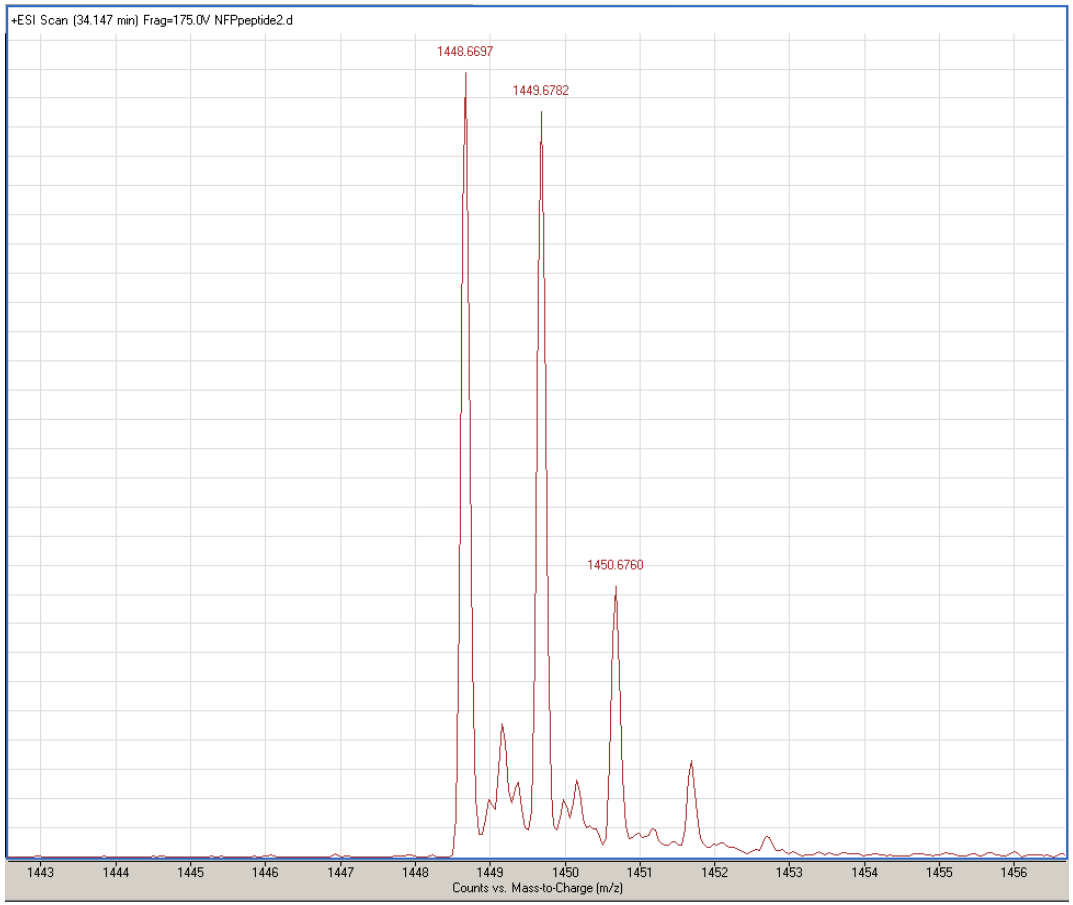

Figure 5.1 MALDI-TOF spectrum of the purified linear peptide H-NTHTDPYIYPID-OH showing a singly charged form of the protonated peptide at 1448.6, which is the predicted molecular weight of the peptide product.

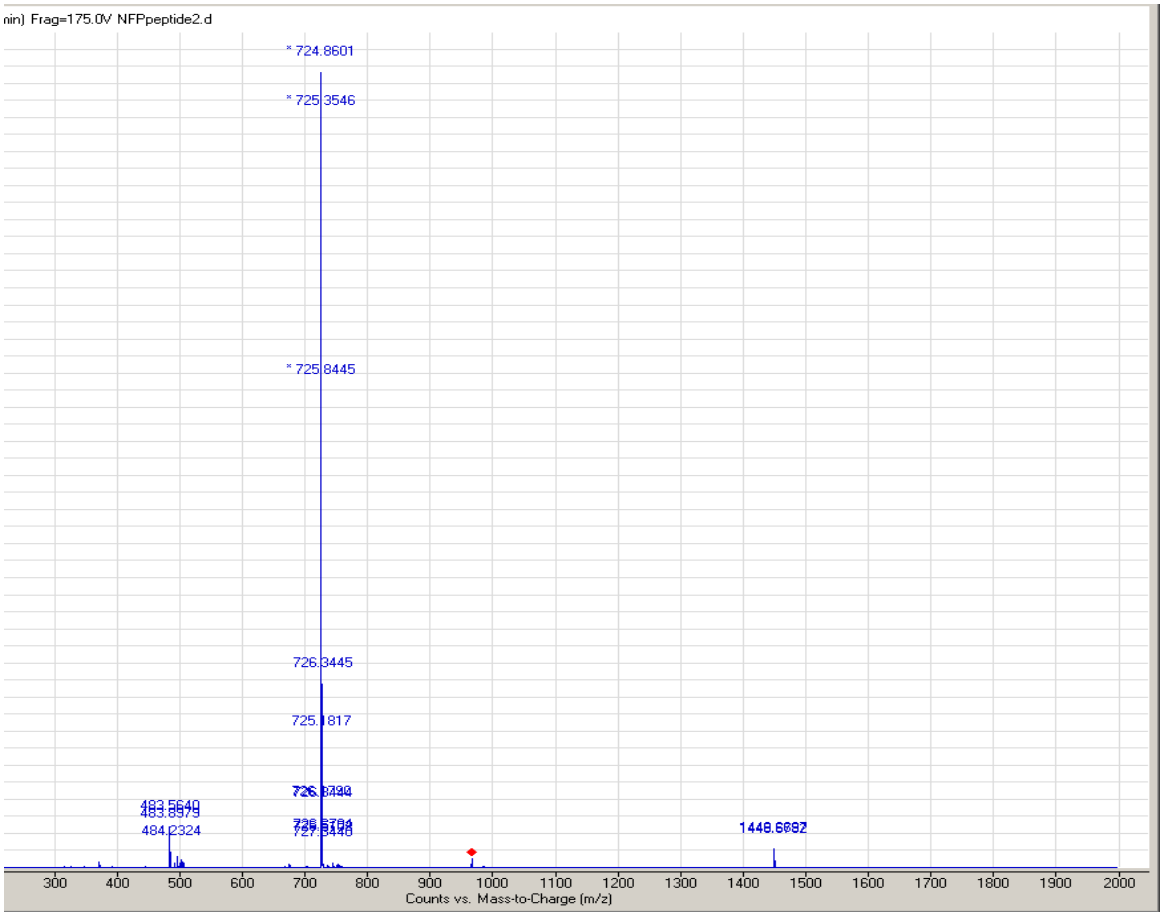

Figure 5.2 MALDI TOF spectrum of linear peptide H-NTHTDPYIYPID-OH showing a doubly charged peptide ion at 724.86 as the major ion. Triply and singly charged minor species are shown at 1448.7 and 483.5 respectively. During analysis of a peptide during MALDI-TOF the sample becomes protonated

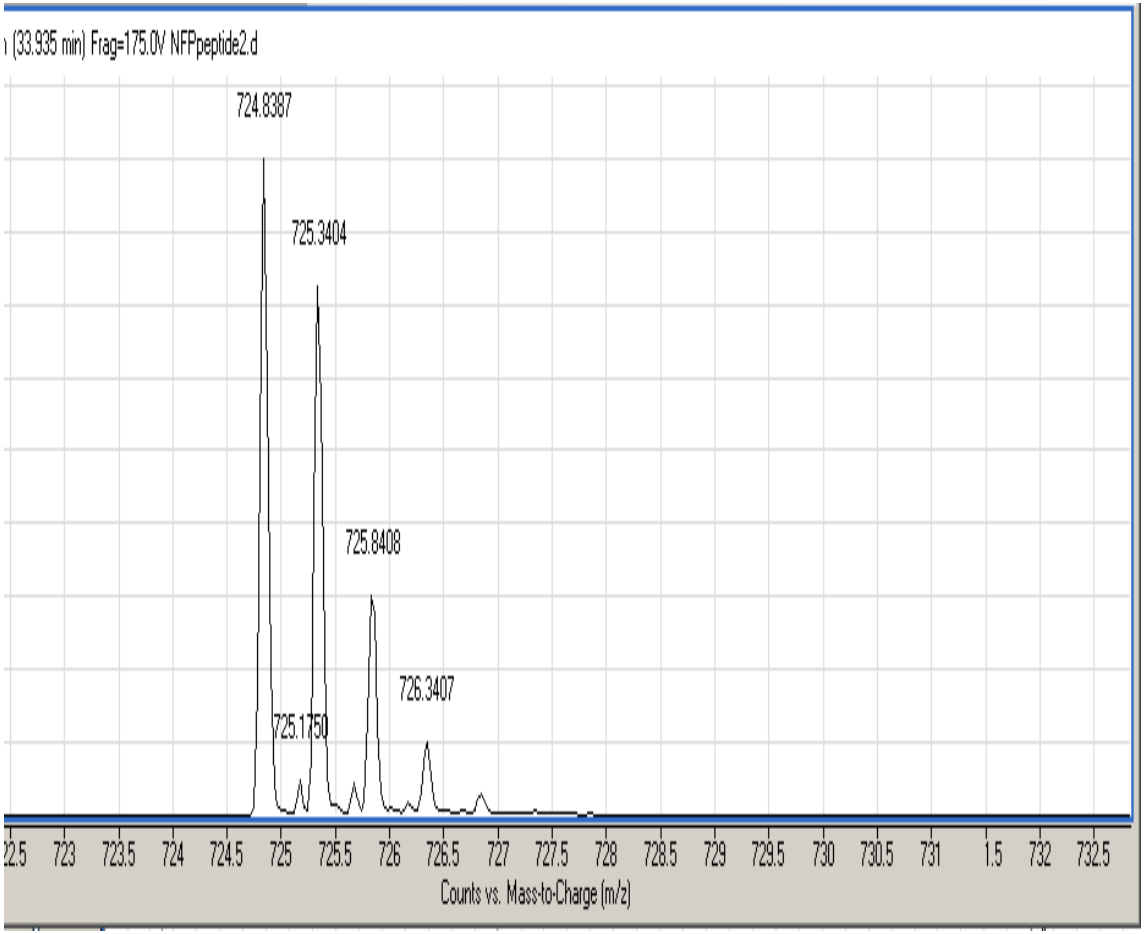

Figure 5.3 MALDI TOF spectrum of linear peptide H-NTHTDPYIYPID-OH showing mass to charge ratio and that the dominant ion is the doubly charged ion of 724.8387

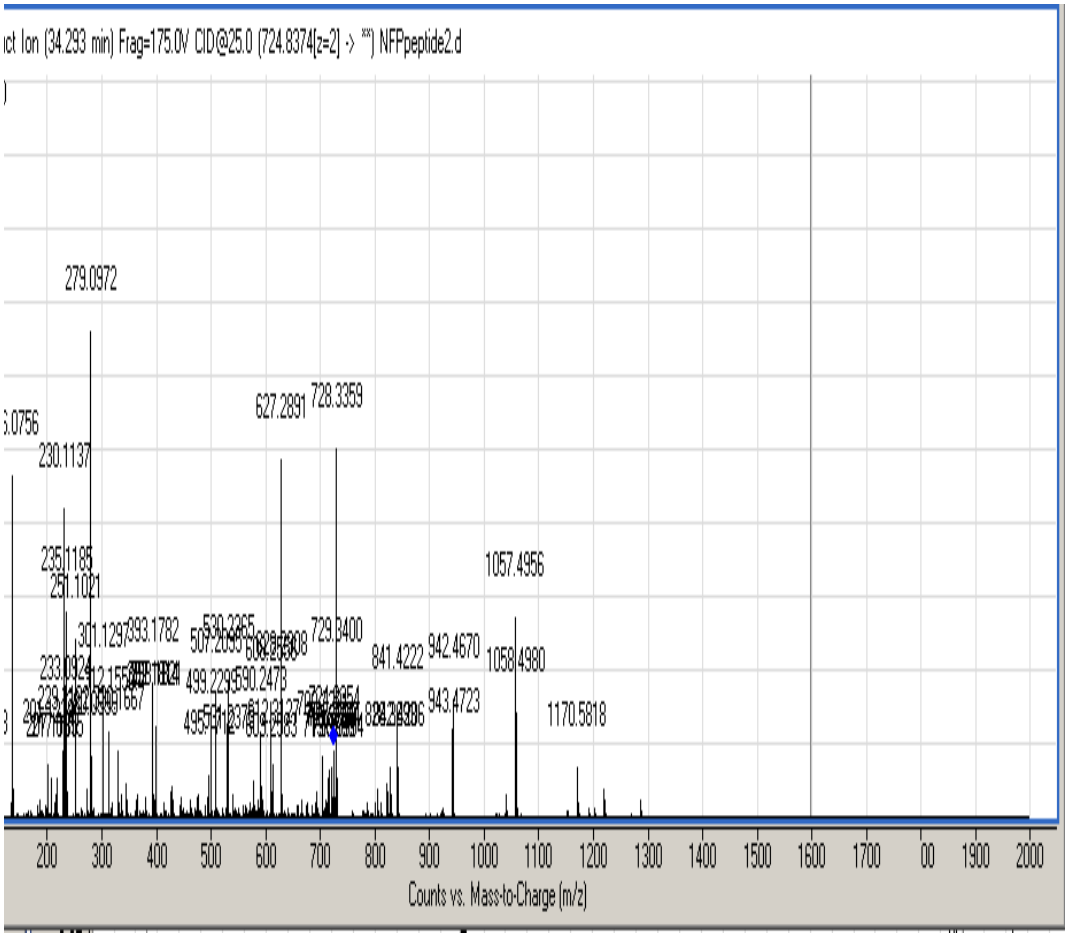

Figure 5.4 MALDI TOF spectrum of linear peptide H-NTHTDPYIYPID-OH showing the ions generated by CID ms/ms fragmentation which confirms the sequence of the peptide

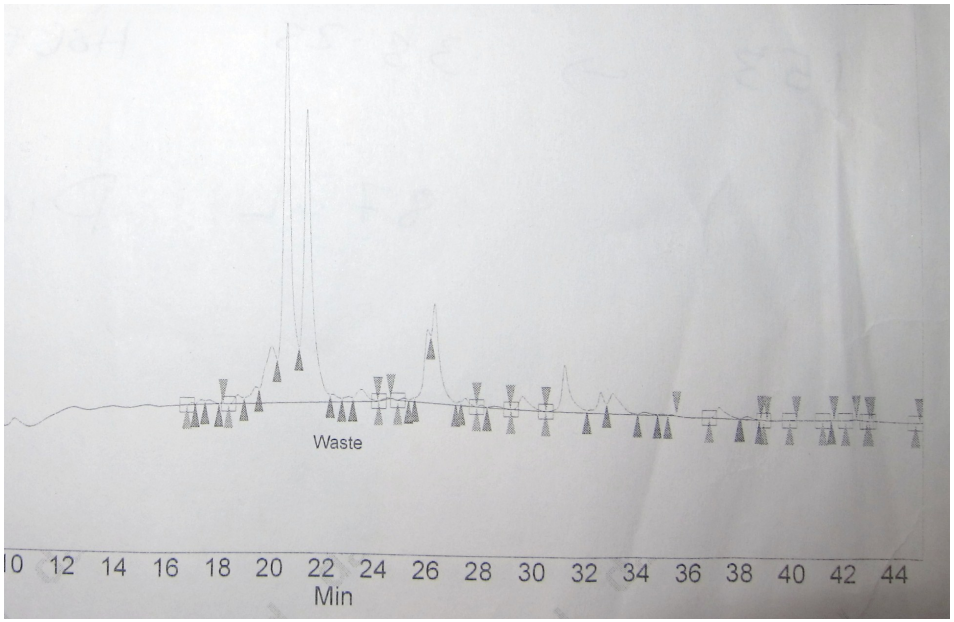

Figure 5.5 HPLC purification of crude linear peptide (H-NTHTDPYIYPID-OH)

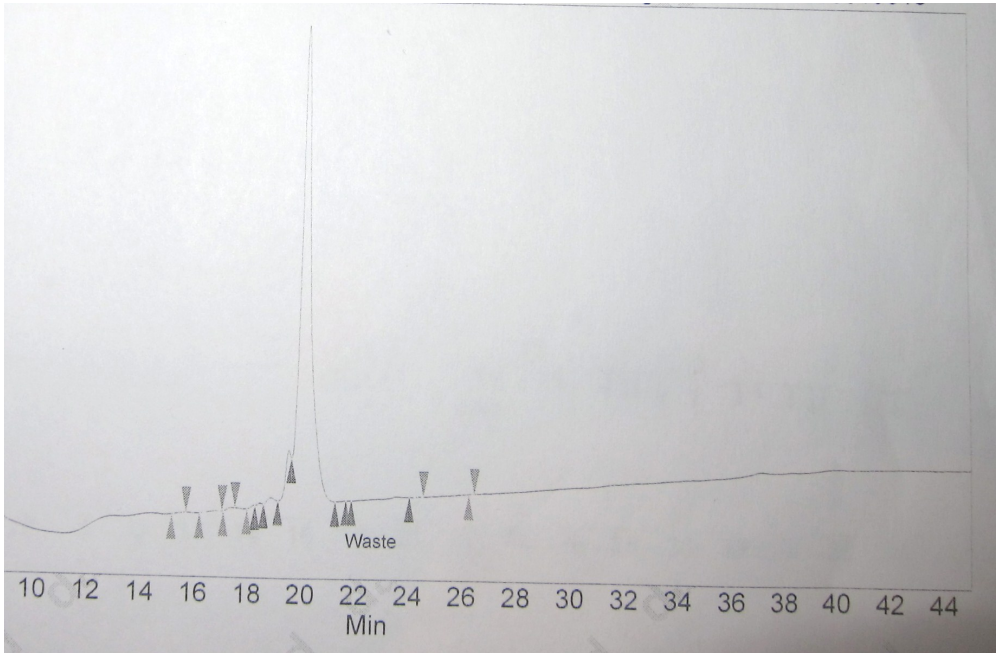

Figure 5.6 HPLC analysis showing purified linear peptide (H-NTHTDPYIYPID-OH)

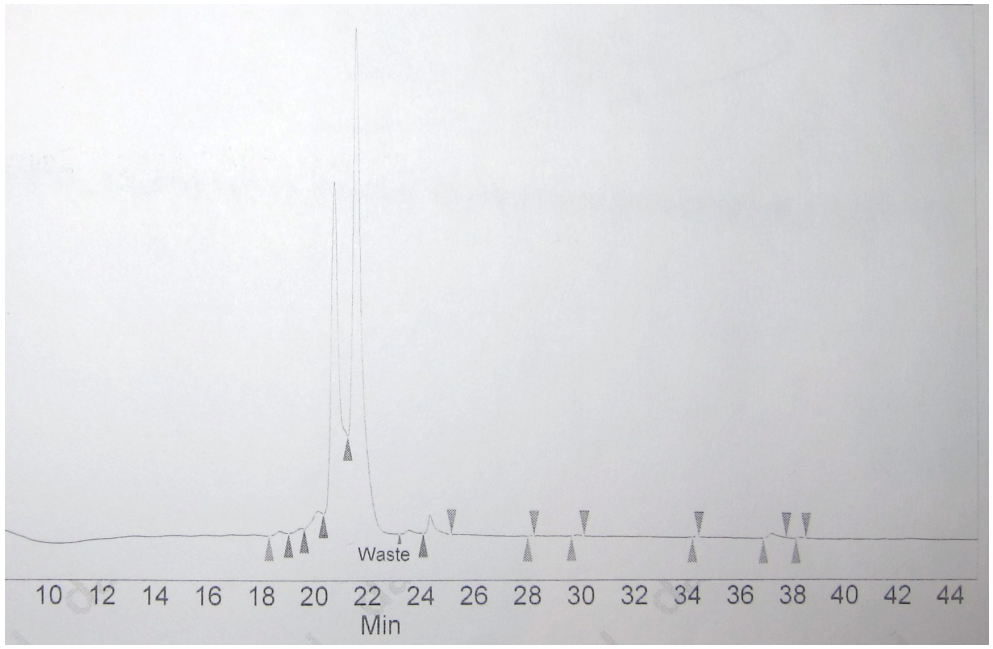

Figure 5.7 HPLC purification of crude scrambled peptide (H-YDIDTITPHYPN-OH)

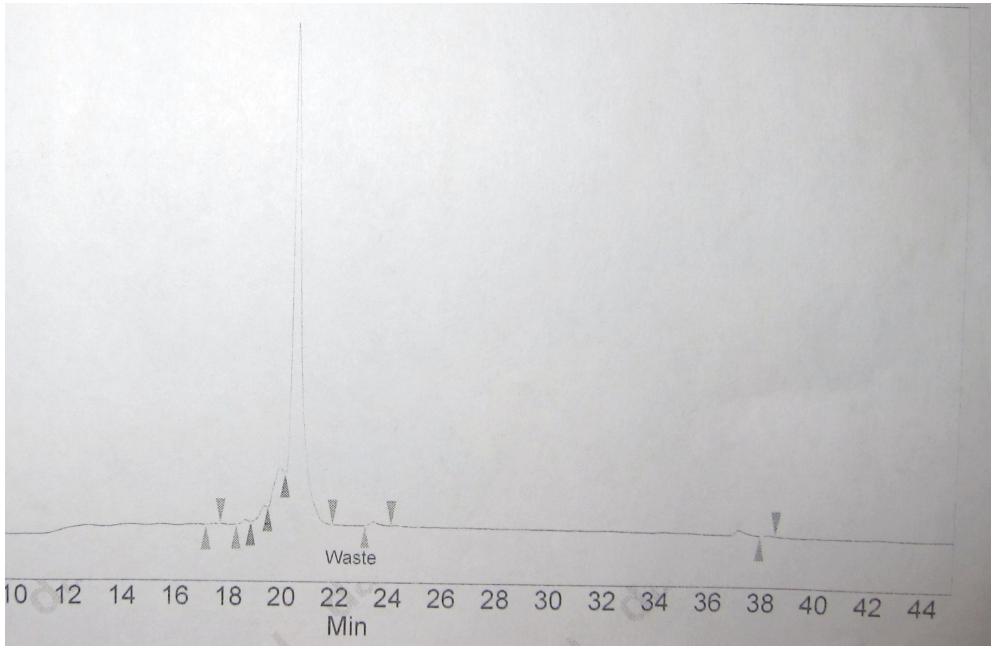

Figure 5.8 HPLC analysis showing purified scrambled peptide (H-YDIDTITPHYPN-OH)

Table 5.1 Linear and scramble peptide with mass, yield, purity and retention time

Peptide	Exact Mass (g/mol)	Found Mass (g/mol)	Crude (mg)	Pure (mg)	Yield (%)	Purity (%)	Retention Time (min)
Linear	1448.57	1448.6	89.4	24.5	27.4	83.08	20.41
Scramble	1448.57	1448.7	97.3	28.4	29.1	90.4	19.96

5.2 Cell Work

5.2.1 MTT Viability Assay

In order to ensure that the peptide was not toxic or contained any toxic impurities, a MTT colorimetric assay was performed. In this assay, purple-coloured crystals are precipitated MTT reacts with the mitochondria of metabolically active cells. In our study, 3T3 fibroblasts were seeded at a density of 40,000 cells per well in a 96-well plate in a volume of 150 µL of media per well. After 24 hours of incubation the media was removed by aspiration and replaced with media containing linear peptide at concentrations serially diluted from 100 µg/mL to 1 µg/mL. After the allotted time period (24 or 48 hours), 20 µM of MTT 5 mg/mL in 0.1 M PBS at pH 7.4 was added to the plates and left to incubate for 4 hours. Media was gently aspirated from the cells and 100 µM of DMSO was added to the wells. The plate was read on a plate reader at Abs 550nm for 1 second. The assay was repeated in triplicate and statistical analysis was carried out (ordinary ANOVA one-way and Tukey's multiple comparisons test, $p < 0.05$).

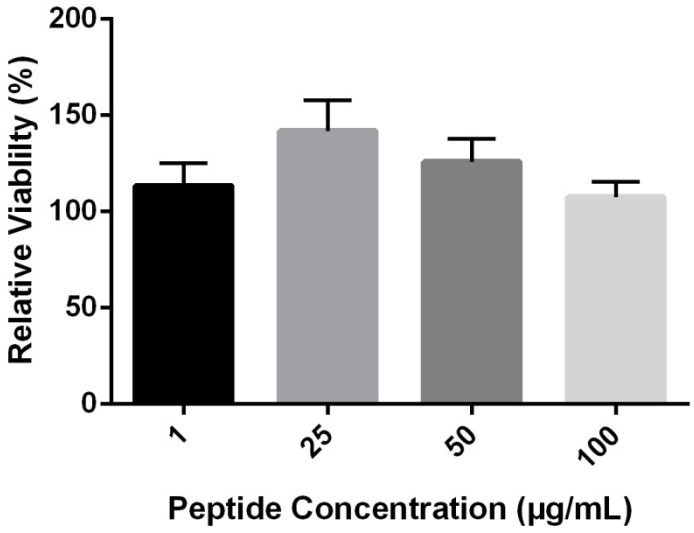

Figure 5.9 A graph shoing a MTT assay examining the effect of different concentrations of linear peptide on the viability of 3T3 cells after 24 hours of incubation. No statistical difference between the groups was shown using an ordinary ANOVA one-way analysis.

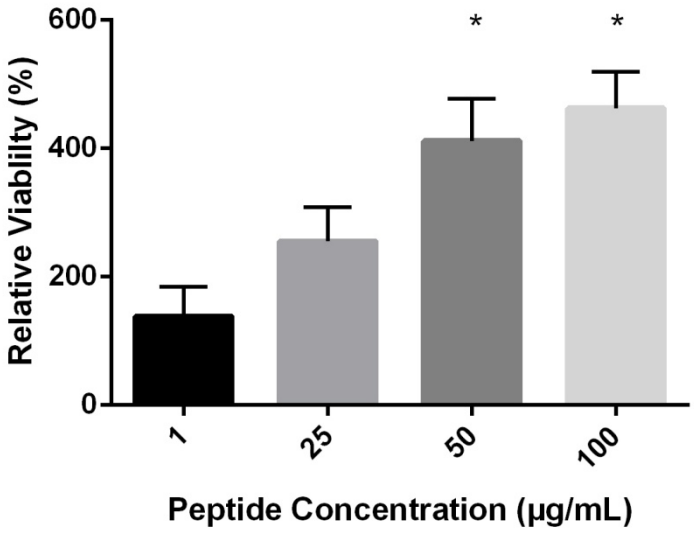

Figure 5.10 A graph shoing a MTT assay examining the effect of different concentrations of linear peptide on the viability of 3T3 cells after 48 hours of incubation. The groups denoted with * showed a static difference on analysis with an ordinary ANOVA one-way with post hoc Tukey's multiple comparisons test, $p < 0.05$

Results showed that after 24 hours the linear peptide had no statistically significant effect on cell viability. After 48 hours however a statistically significant effect was shown in cells treated with peptide of contrations 50 µg/mL and 100 µg/mL, respectively. These groups showed a mean percentage viability of 412 % and 463 % respectively, when compared to controls that were not peptide treated proving that this peptide is not only non-toxic but also induces a proliferative effect on 3T3 cells. There was another experimental group where samples were inoculated with foetal bovine serum, but this side-arm yielded unusual data and has been left out of this section.

5.3 **Peptide Immobilisation**

Several strategies were investigated in order to load our peptide onto its collagen scaffold prior to implantation. These ranged from simply dissolving the peptide in a collagen based hydrogel to chemically binding the peptide to the surface of the collagen scaffold.

In this project, a method was devised to make collagen selectively reactive. Methods exist to non-selectively activate collagen. For example, cross linking with EDC:NHS activates the carboxyls and amines natively present on collagen. This method, although simple, would not allow the efficient binding of a peptide as both the N terminus and C terminus would become reactive as well as the amines and carboxyls and amines on the collagen itself, leading to a very haphazard and unregulated reaction. A method was devised to selectively block amines using sulfo-NHS-acetate, before activating the carboxyls using EDC/NHS. This created a surface with only negatively charged carboxyl groups free of charged amines, which allowed selective and predictable binding of our peptide to the collagen surface. This method was further refined and we compared an "all-in-one" method against a "stepwise" approach. The "all-in-one" method involved adding the sulfo-NHS-acetate to a collagen fibre, washing the fibre and then adding and EDC/NHS and peptide simultaneously. The "stepwise" approach involved adding the sulfo-NHS-acetate to the fibre, washing it, then adding EDC/NHS, washing it again, and then finally incubating the fibre in the peptide solution.

Type I Collagen is mainly composed of three amino acids, namely glycine, proline and hydroxyproline (see Figure 5.15 and Table 5.2). Type I bovine collagen (that used in all experiments listed here) has an approximate molecular weight of 300 kDa. Using the amino acid sequence of Friess et al [237], there are 240 moles of carboxyls per mole of collagen. Therefore one mole of uncrosslinked collagen will react with 240 moles of amines i.e. 240 moles of peptide. This means that 1 g of collagen will require approximately 1.16 g of peptide. Most of the fibres we use are in the vicinity of 0.15 mg which means a perfect uptake of peptide equates approximately to 0.173 µg of peptide.

This selective activation of collagen was proven by two methods, namely TNBSA assay and amino acid analysis of a modified collagen fibre.

5.3.1 TNBSA

A TNBSA assay is a colorimetric assay that measures free amines in solution. It is technically quite challenging to analyse a peptide-modified collagen fibre as collagen itself is a protein and therefore made up of amino acids. The approach taken here was to activate a collagen fibre, add a known quantity of peptide and then measure the amount of peptide left behind in order to deduce the uptake.

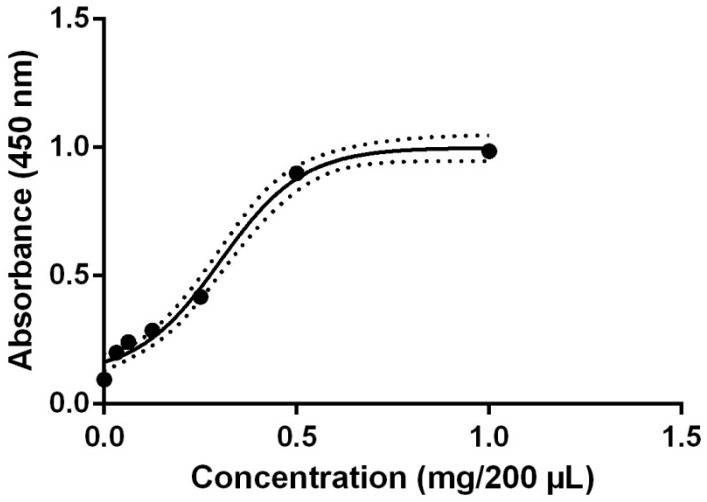

Figure 5.11A graph showing the sigmoidal curve of the relatioship between peptide concentration and TNBSA absorbance at 450 nm

Figure 5.11 above shows the correlation between peptide concentration and absorbance. It was important to establish this fact going forward with subsequent experiments that depended on accurate peptide measurements.

The next set of experiments was performed to prove the concept that the proposed method for activating collagen was due to activation alone. A study was performed comparing the method of sequential amine blocking followed by carboxyl activation versus an all in one reaction.

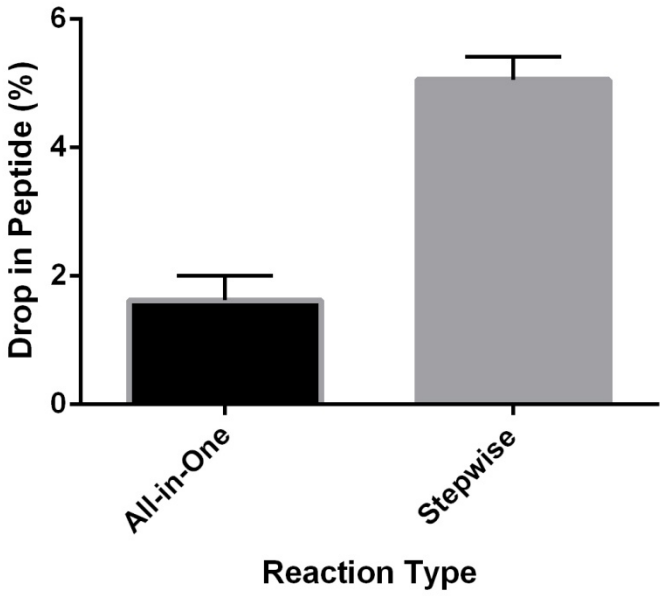

Figure 5.12 Graph comparing peptide uptake in an "all-in-on" reaction versus a step-wise reaction. A statistical difference was shown with $p < 0.05$

This study showed a significant difference ($p < 0.05$) in the two methods with a step-wise reaction method howing a higher degree of peptide binding (5.1 % vs 1.6%)

In order to prove that the peptide taken up is chemically bound to the collagen and not merely soaked into the collagen fibre, a collagen fibre of known mass was soaked in peptide solution of known concentration and the remaining peptide solution was measured against a control.

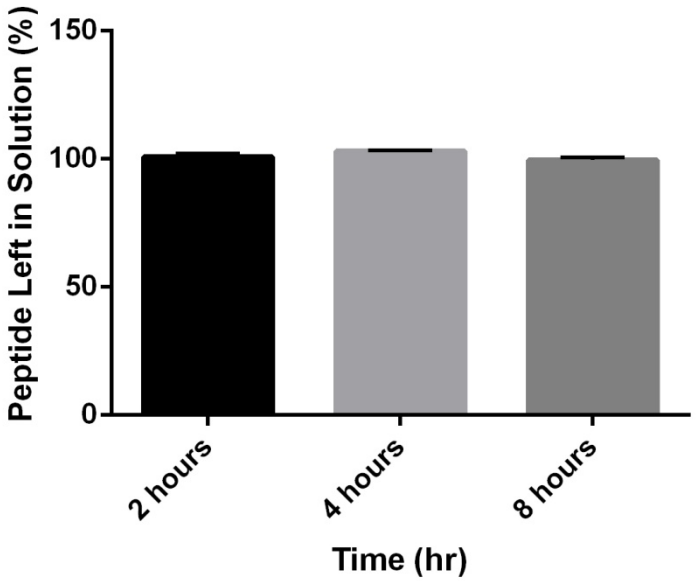

Figure 5.13 Graph showing uptake of peptide onto a collagen fibre using physical soaking alone. There was no uptake of peptide at any time point

There was no appreciable loss of peptide from solution due to physical retention of peptide alone, proving that any peptide absorbed in the stepwise reaction was done so by the activated collagen fibre.

The relationship between the mass of the collagen fibre and its ability to react with higher quantity of peptide was also studied. The reasoning behind this study was that greater masses of collagen contain greater masses of carboxyl groups. Therefore, if peptide is in fact reacting with carboxyls, there should be a relationship between the mass of the collagen fibre and the mass of peptide used up in the reaction.

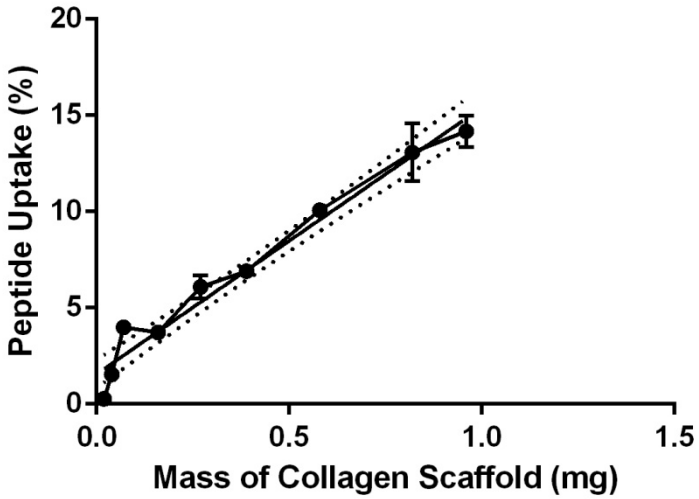

Figure 5.14 Graph showing the linear relationship of collagen scaffold mass and uptake of peptide with r^2 =0.9335

A linear relationship between collagen mass and peptide uptake was shown using a linear regression study (r^2 =0.9335). This results supports the hypothesis that peptide binds chemically to the carboxyl groups on collagen.

Several attempts were made at increasing the incubation period of the activated fibre in the peptide solution. No statistically significant data was yielded from this part of the study. It was noted however that the 2 hour time point seemed to be associated with the highest drops in peptide and this was noted in other experiments too.

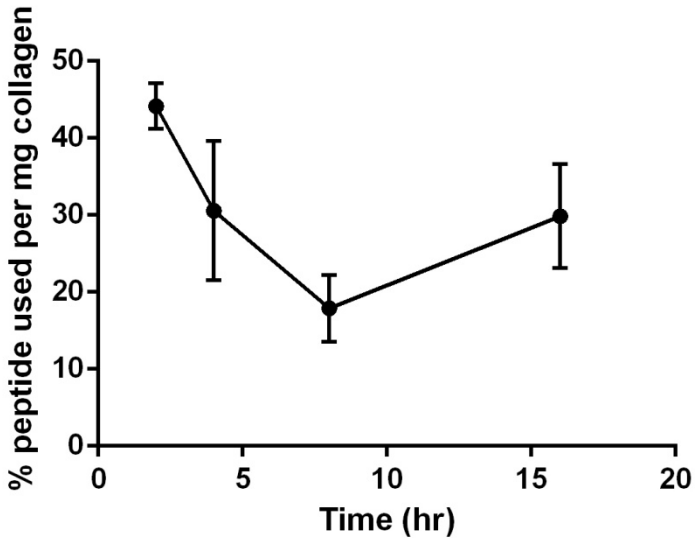

5.3.2 Amino Acid Analysis

Amino acid analysis is an invaluable modality for examining the constituents of proteins. Before a sample is ready to be analysed, it must first be hydrolysed and broken up into its amino acid units. Amino acid analysis is an intricate and time consuming process. Amino acid analyses performed in this study were performed both in our laboratory and in an off-site analytical laboratory

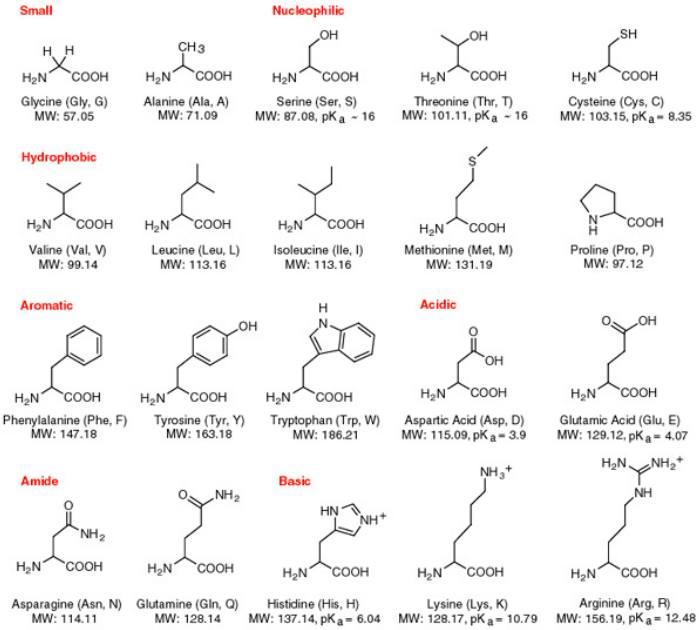

Figure 5.15 Chart of different amino acid structures accompanied by three- and one-letter code, residue molecular and side chain pK_a

Type I bovine collagen has been studied extensively and its amino acid precursors are seen in Table 5.2. The linear peptide used in this study is of the sequence NTHTDPYIYPID. This peptide is rich in threonine, isoleucine and tyrosine, amino acids which are not particularly prevalent in Type I bovine collagen, as we can see from table 5.2. If peptide was bound successfully to a collagen fibre a spike in concentrations of these four amino acids should be seen.

Peptide was added to a collagen fibre as per our newly devised protocol. This sample as well as an unmodified collagen fibre were analysed as per standard amino acid

Table 5.2 The amino acid composition of type I collagen isolated from calf-skin. From Friess W. Collagen--biomaterial for drug delivery. Eur J Pharm Biopharm. Mar 1998;45(2):113-136.

Amino acid	α1(I)-chain	α2(I)-chain
Alanine	124 (2)	111 (3)
Arginine	53 (2)	56 (1)
Asparagine	13	23
Aspartic acid	33 (3)	24 (2)
Glutamic acid	52 (2)	46 (2)
Glutamine	27(3)	24 (1)
Glycine	345 (6)	346 (6)
Histidine	3 (1)	8
Hydroxylysine	4	9
Hydroxyproline	114	99
Isoleucine	9 (1)	18
Leucine	22 (3)	33
Lysine	34 (2)	21 (1)
Methionine	7	4
Phenylalanine	13 (1)	15 (3)
Proline	127 (4)	108 (1)
Serine	37 (5)	35 (1)
Threonine	17 (1)	20
Tyrosine	5 (5)	4 (3)
Valine	17 (1)	34
Total	1056 (42)	1038 (24)

analysis protocols and the results of these analyses are displayed in Figures 5.16 and 5.17, respectively.

Only one collagen fibre and one modified collagen fibre were compared, so no statistical significance could be drawn from this study but the results clearly indicated that there were higher concentrations of the amino acids associated with the peptide in the analysis of the modified fibre compared to the control, unmodified fibre, with noticeable spikes in the concentrations of histidine, threonine, isoleucine and tyrosine. Collagen is a notoriously variable protein with high variability in both its amino acid composition and overall molecular weight making a comparative analysis difficult, but the results of this experiment, given the context of previous experiments, indicate that peptide was successfully bound to the collagen fibre.

AA	n.mole / mg	u.g / mg	m.g / mg	g / 100g
Cysteic acid	–	–	–	–
Hydroxyproline	418	47.2	0.0472	4.72
Aspartic acid	209	24.0	0.0240	2.40
Threonine	94.2	9.53	0.00953	0.953
Serine	174	15.1	0.0151	1.51
Glutamic acid	344	44.5	0.0445	4.45
Proline	553	53.7	0.0537	5.37
Glycine	1560	89.1	0.0891	8.91
Alanine	529	37.6	0.0376	3.76
Cystine	–	–	–	–
Valine	98.4	9.75	0.00975	0.975
Methionine	15.1	1.98	0.00198	0.198
Isoleucine	54.8	6.20	0.00620	0.620
Leucine	113	12.8	0.0128	1.28
Tyrosine	6.41	1.05	0.00105	0.105
Phenylalanine	53.7	7.91	0.00791	0.791
Histidine	37.4	5.13	0.00513	0.513
Tryptophan	–	–	–	–
Lysine	109	14.0	0.0140	1.40
Arginine	224	35.0	0.0350	3.50
Totals	4590	415	0.415	41.5

Figure 5.16 Amino acid analysis of an unmodified collagen fibre

AA	n.mole / mg	u.g / mg	m.g / mg	g / 100g
Cysteic acid	–	–	–	–
Hydroxyproline	581	65.8	0.0658	6.58
Aspartic acid	457	52.5	0.0525	5.25
Threonine	240	24.3	0.0243	2.43
Serine	212	18.5	0.0185	1.85
Glutamic acid	459	59.2	0.0592	5.92
Proline	858	83.3	0.0833	8.33
Glycine	2040	116	0.116	11.6
Alanine	694	49.3	0.0493	4.93
Cystine	–	–	–	–
Valine	129	12.8	0.0128	1.28
Methionine	26.5	3.48	0.00348	0.348
Isoleucine	189	21.4	0.0214	2.14
Leucine	145	16.4	0.0164	1.64
Tyrosine	127	20.8	0.0208	2.08
Phenylalanine	63.9	9.41	0.00941	0.941
Histidine	99.5	13.7	0.0137	1.37
Tryptophan	–	–	–	–
Lysine	139	17.9	0.0179	1.79
Arginine	299	46.6	0.0466	4.66
Totals	6760	632	0.632	63.2

Figure 5.17 Amino acid analysis of a modified collagen fibre

There was also a macroscopic difference seen in the collagen fibres treated with amine blocking/carboxyl activation/peptide addition. They were obviously more translucent in suspension, indicating some kind of structural change (Figure 5.18).

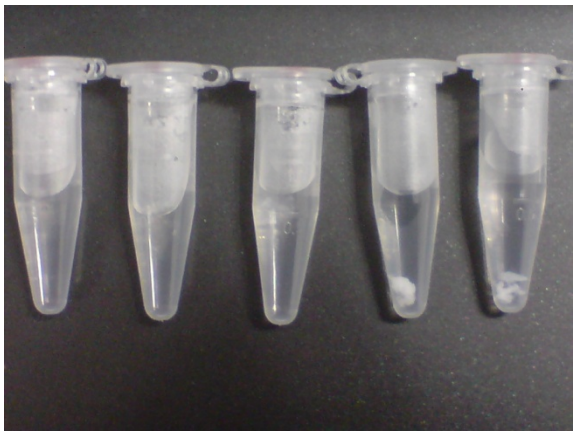

Figure 5.18 Photograph showing the macroscopic differences between fibres. The first three fibres (from left to right) were treated with peptide using the stepwise method. The last two are crosslinked fibres with no peptide addition

5.4 *In vivo* Work

5.4.1 Surgical Outcome

Composite nerve grafts were implanted successfully in all animals. Most animals had an uneventful post-operative recovery period with only 9 % of animals showing minor signs of irritation/pain that were easily treated as per accepted analgesia protocols documented in the appendices. All animals survived the extended recovery period and were uneventfully sacrificed at 16 weeks post-implantation. The graft and surrounding nerve tissue were harvested easily. No animals developed neuroma. All nerve conduits survived the post-implantation period and showed minimal signs of degradation and retained their structural integrity. All groups developed a macroscopically visible nerve tissue cable (Figure 5.22). There was a technical difficulty in processing animals from the "retrograde nerve tracing" part of the project and consequently, data for this arm of the project has not been included.

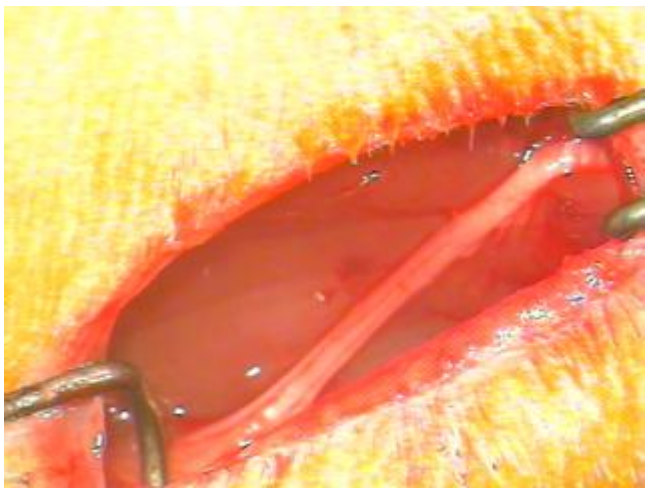

Figure 5.19 Intraoperative photo showing the exposed sciatic nerve prior to resection

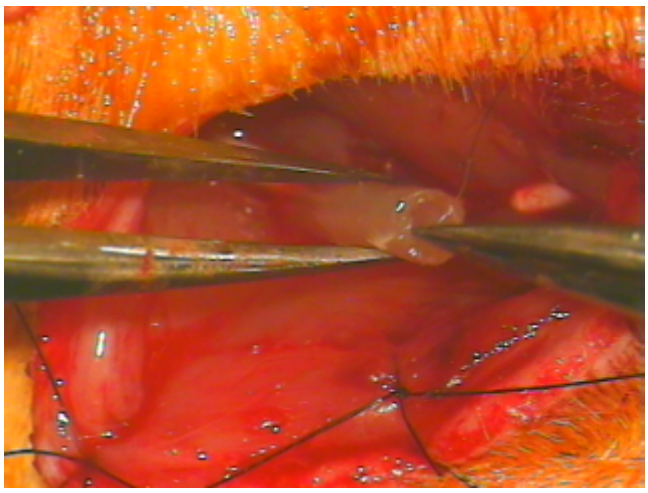

Figure 5.20 Intraopertive photo showing the cut proximal sciatic nerve and the method for suturing in the nerve conduit

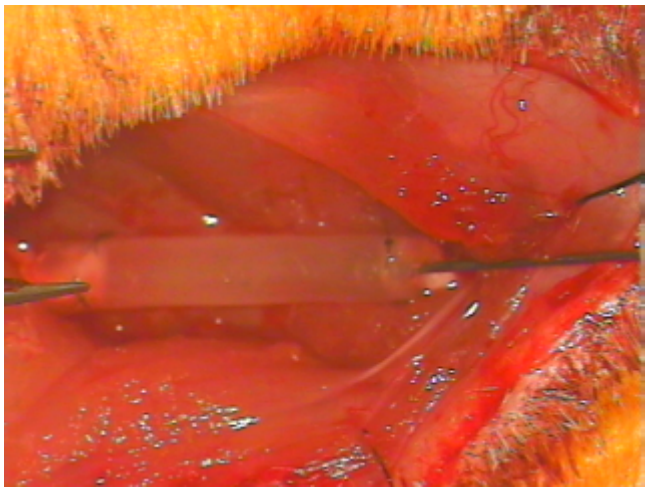

Figure 5.21 Intraoperative photo showing the sutured nerve conduit in situ (Day 0)

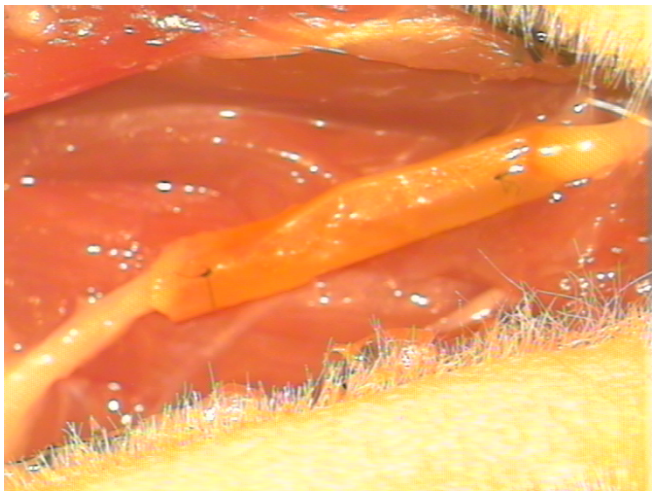

Figure 5.22 Intraoperative photo of a linear peptide containing composite graft taken just before tissue harvest at week 16. Note the structural integrity of the conduit remains intact with no obvious collapse

Figure 5.23 Explanted tissue with corresponding linear peptide containing composite nerve graft clearly demonstrating a regenerating nerve cable along its length after week 16

5.4.2 Morphological and Histological Studies of Implanted Nerve Grafts

After removal of tissue samples from the test subject, they were then prepared for sectioning. All samples for this part of the study were embedded in spur resin and each 1 µm thick section was stained with 1 % toluidine blue before visualisation with light microscopy. Magnifications of 100 x were used to accurately assess the graft tissue midpoint for accounting for nerve regeneration and quantitative analysis (Figures 5.23 – 5.26).

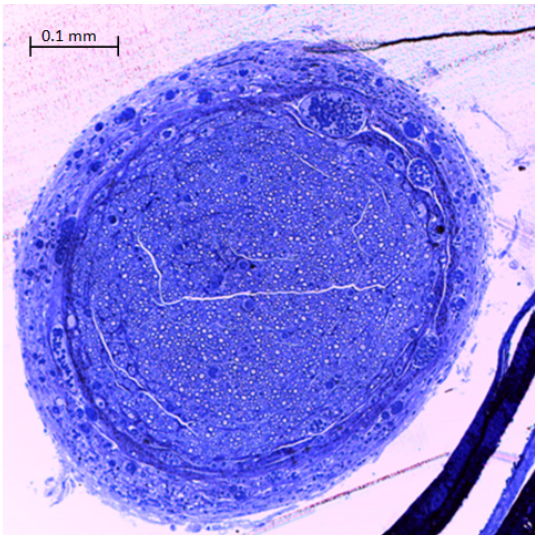

Figure 5.24 Microscopic image stained with toluidine blue showing a representative section from the "conduit and plain gel" group from tissue harvested at week 16

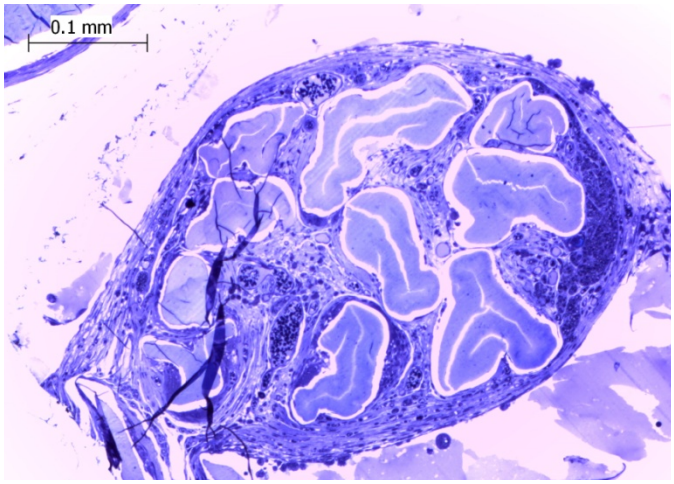

Figure 5.25 Microscopic image stained with toluidine blue showing a representative section from the "plain gel and fibre" group from tissue harvested at week 16, with intraluminal fibres clearly visible

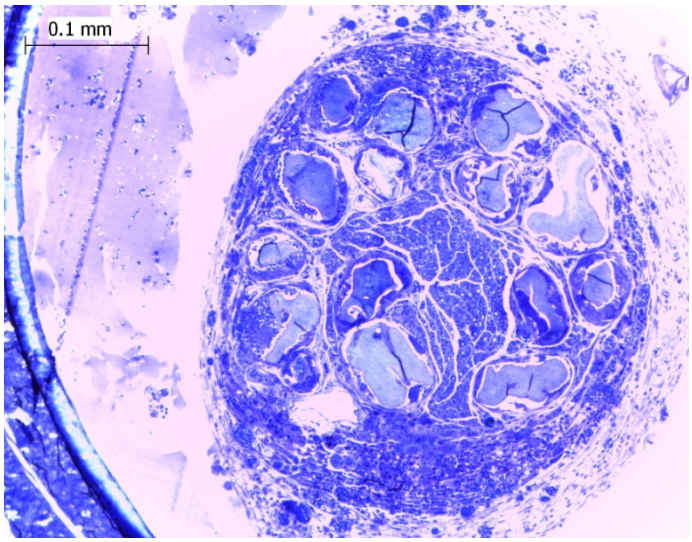

Figure 5.26 Microscopic image stained with toluidine blue showing a representative section from the "fibre and linear peptide gel" group from tissue harvested at week 16, with intraluminal fibres clearly visible

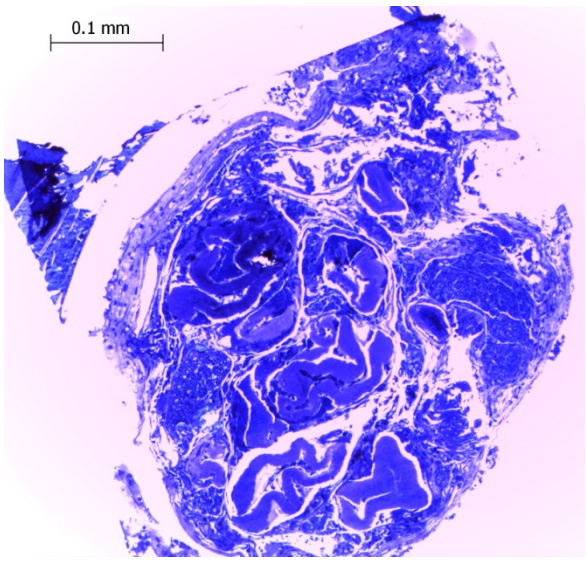

Figure 5.27 Microscopic image stained with toluidine blue showing a representative section from the "fibre and scramble peptide gel" group from tissue harvested at week 16 with intraluminal fibres clearly visible

5.4.3 Interaction Between Host Tissue and Implanted Conduits

On inspection at 100 x magnification it was noted that a nerve tissue cable was present in all experimental groups (Figures 5.23 – 5.26). It was also noted that in all groups containing fibres, the host regenerative process had incorporated the fibres and displayed no obvious tissue reaction. Axons regenerated in close proximity to the collagen fibres as is evident from the enclosed representative figures (Figures 5.27 – 5.30). Accompanying vascular regeneration was also noted in the groups which is apparent from the various included images.

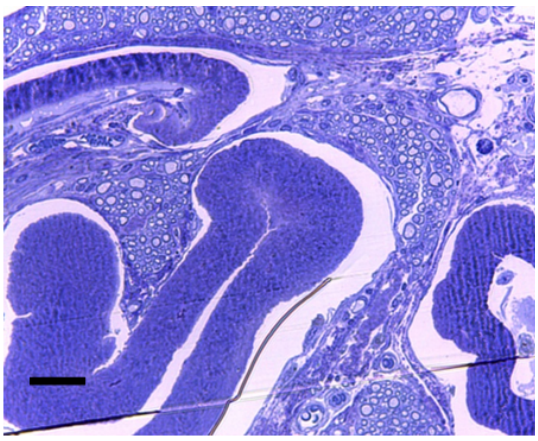

Figure 5.28 Microscopic image stained with toluidine blue showing a incorporation of fibre into host's regenerative process in a section from the "fibre and linear peptide gel group. Magnification is 400 x and scale bar represents 25 µm

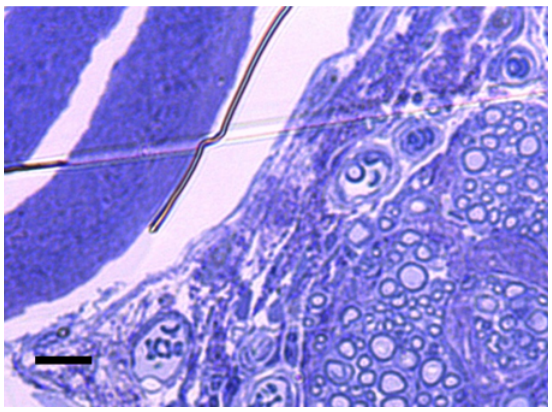

Figure 5.29 Microscopic image stained with toluidine blue showing a incorporation of fibre into host's regenerative process in a section from the "fibre and linear peptide gel group. Magnification is 1000 x and scale bar represents 10 µm

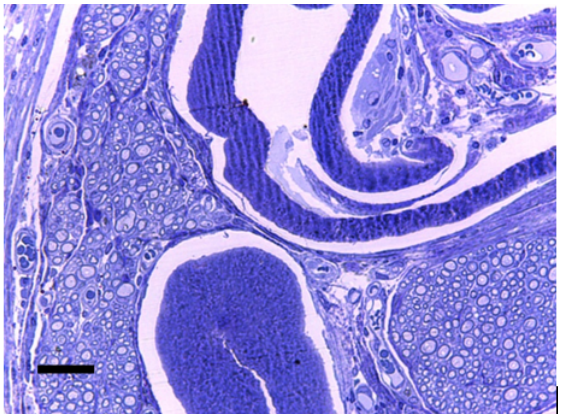

Figure 5.30 Microscopic image stained with toluidine blue showing a incorporation of fibre into host's regenerative process in a section from the "fibre and scramble peptide gel group. Magnification is 400 x and scale bar represents 25 µm

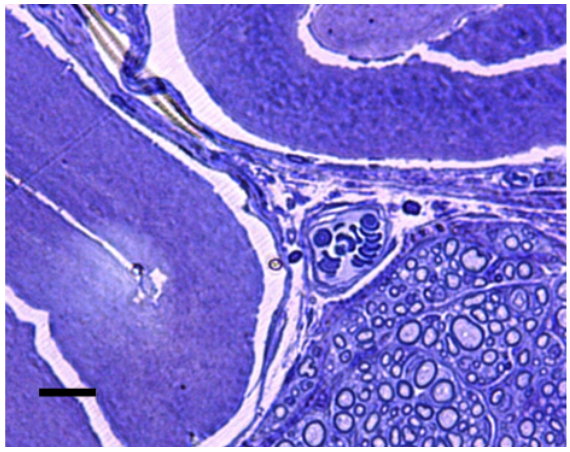

Figure 5.31 Microscopic image stained with toluidine blue showing a incorporation of fibre into host's regenerative process in a section from the "fibre and scramble peptide gel group. Magnification is 1000 x and scale bar represents 10 µm

In order to calculate the total fascicular area, J-image software first calculated the total area in the graft seen under 100 x magnification and then subtracted the area occupied by the fibres. Using 1000 x magnification and a systematic stereological approach, analysis of total myelinated fibre number, myelinated fibre density, mean fibre diameter, mean axon diameter, mean myelin thickness and g-ratio was performed.

Fascicular area is the total surface area of a fascicle. This was similar in all groups, however there was a statistical difference between the neuragen and autograft groups ($p < 0.05$) (Figure 5.34). There were lower densities of myelinated fibres in the scramble peptide, fibre gel and gel only groups ($p < 0.05$) (Figure 5.35). As for the total number of myelinated fibres, there was no statistical difference between all groups when compared to autograft with autograph showing approximately 40 % more myelinated fibres (Figure 5.36). There was no statistical difference in the mean fibre diameter across all groups, except for the gel only group whose diameter was approximately 55 % less than the autograft (Figure 5.37). The results for mean axon diameter, mean myelin thickness and resulting g-ratio showed similar patterns with the gel only group showing a statistically significant mean diameter size when compared to the autograft group (Figure 5.38 – 5.40).

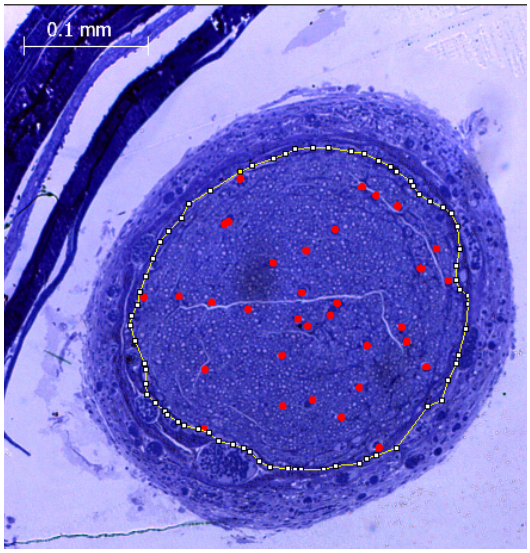

Figure 5.32 Microscopic image showing J-image software calculating axonal area

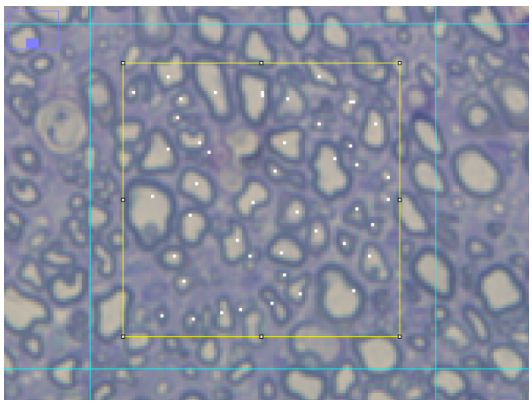

Figure 5.33 Microscopic image showing axonal counting method

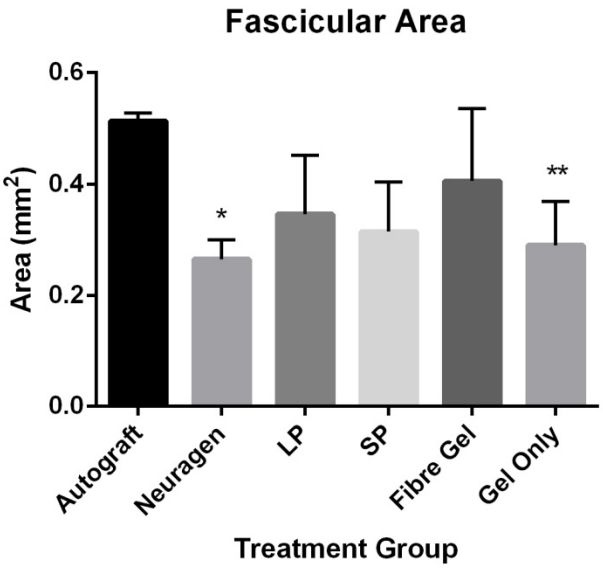

Figure 5.34 Graph comparing the fascicular area of the different treatments groups with onlt the neuragen and gel only groups showing a statisctically significant difference when compared to autograft

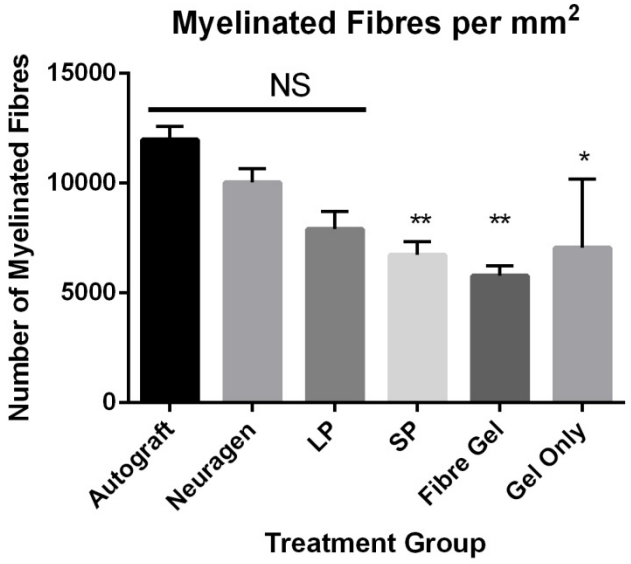

Figure 5.35 Graph comparing the differences in myelinated fibre density amongst the treatment groups. Note that there was a statistically significant difference in the scramble peptide, fibre gel and gel only groups when compared to autograft ($p < 0.05$)

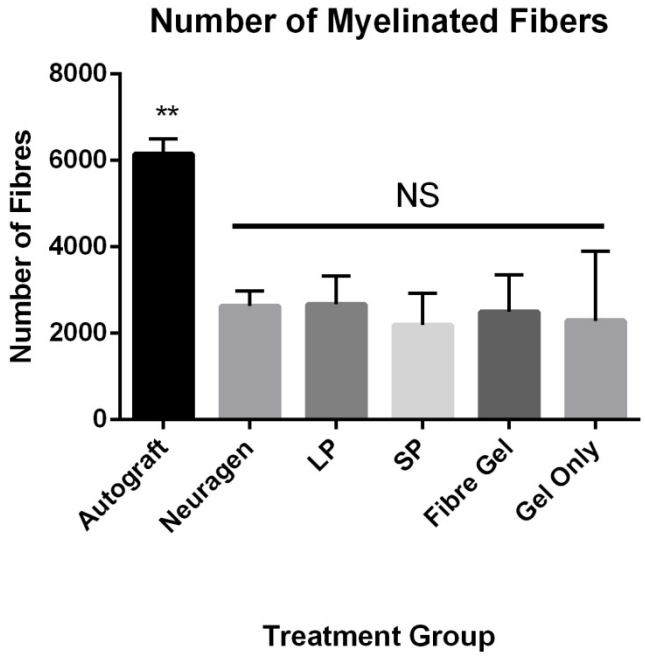

Figure 5.36 Graph comparing the differences in myelinated fibre number amongst the various treatment groups. The autograft group was the only group to show a statistically significant difference ($p < 0.05$)

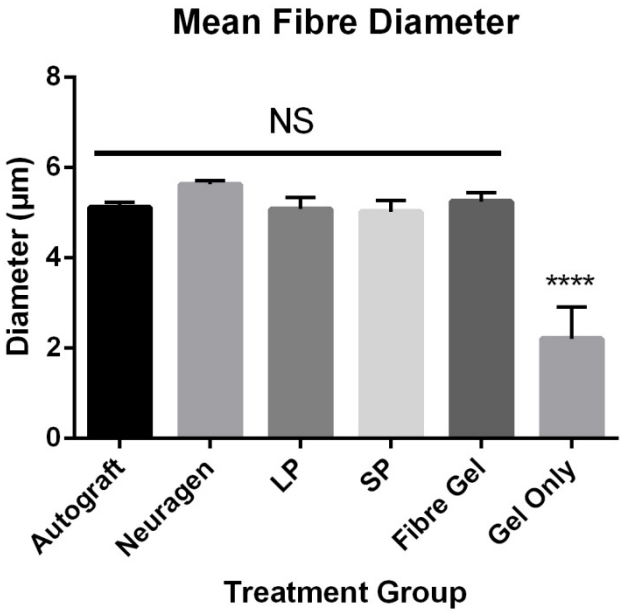

Figure 5.37 Graph showing the mean nerve fibre diameter across all the treatment groups. The gel only group was the only group to show a statistical difference when compared to autograft ($p < 0.05$)

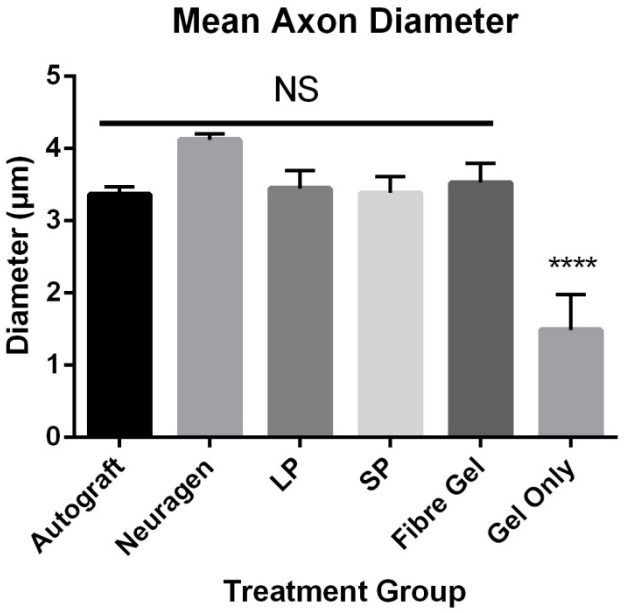

Figure 5.38 Graph showing the mean axon diameter across all the treatment groups. The gel only group was the only group to show a statistical difference when compared to autograft ($p < 0.05$)

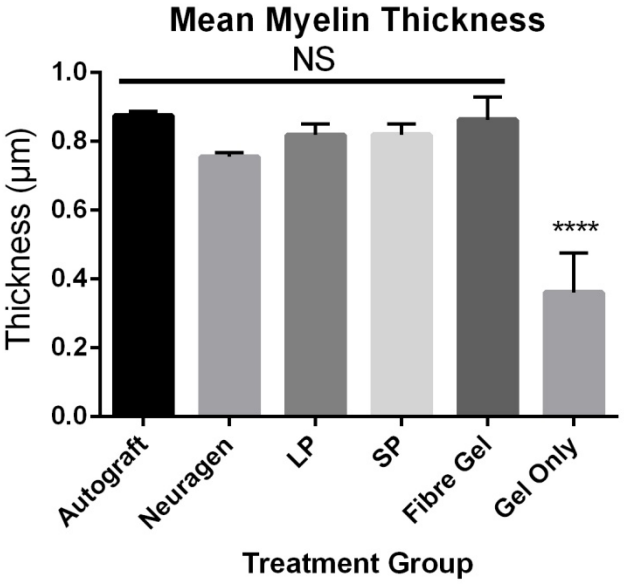

Figure 5.39 Graph showing the mean myelin thickness across all the treatment groups. The gel only group was the only group to show a statistical difference when compared to autograft ($p < 0.05$)

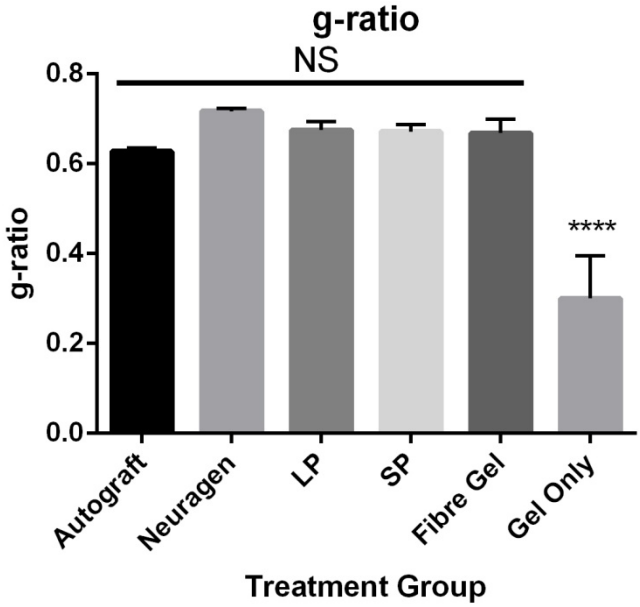

Figure 5.40Graph showing the g-ratio across all the treatment groups. The gel only group was the only group to show a statistical difference when compared to autograft ($p < 0.05$)

6 Discussion

Polysialic acid is an important molecule in the peripheral nervous system. It has been implicated in nearly every key stage in the nervous system. PSA has been shown to be secreted in vast quantities during foetal development [205] and is linked to axon path finding and targeting and associated with muscle formation [213] and in fact studies, have shown that enzymatically cleaving PSA in a neural environment alters neural development [214-215]. PSA is also apparently important in the mature, adult nervous system especially in the area of neural plasticity [214]. PSA is also of importance in the area of peripheral nerve regeneration after an injury. For example, it has been shown that removing PSA from the site of a nerve injury delays axonal sprouting in vitro [216]. Surges in NCAM (the PSA binding molecule in the nervous system) are seen in target tissue after a peripheral nerve injury[223].

Problems arise when PSA is used in the lab environment. Glycans, including PSA are structurally quite complex and are difficult to analyse and make, and can switch conformation easily [205, 226]. Naturally existing compunds similar to PSA, such as colominc acid, exist. Colominic acid has its limitations. Although similar to human PSA it is not PSA. Commercially produced colominic acid is not a uniform product. Colominc acid behaves differently to PSA *in vivo* and because it can elicit a host immune response [227]. Initially work was done looking at commercially available colominic acid and PSA. These substances were very hard to work with and the project soon shifted focus onto another way of utilising the properties of PSA without the established difficulties of working with PSA.

A PSA mimetic peptide answers a lot of the problems associated with native PSA. A mimetic peptide is a synthetic polysaccharide that has all the characteristics of a specific molecule but bears no resemblance to it structurally. Work has been done in the area of PSA peptide mimetics, and groups have shown that peptide mimetics can promote neural regeneration and even promote functional recovery in an *in vivo* model [226, 229-230].

In this project several different peptides (and modification of established peptides) were synthesised. The main focus of the project was on the linear peptide H-NTHTDPYIYPID-OH as studied by the group Mehanna et al. [230]. This group used a

scramble version of this peptide as a control in their experiments (of sequence H-TNYDITPPHDIYC-OH) as well as another control of sequence (H-DSPLVPFIDFHPC-OH). In this project the linear peptide was synthesised successfully, as shown by HPLC and MALDI-TOF analysis, but a different control peptide was chosen. For reproducibility purposes a scramble peptide was chosen as opposed to a peptide with different amino acid constituents as per Mehanna et al. A scramble peptide of sequence H-YDIDTITPHYPN-OH was chosen given the stability of the peptide bonds in this sequence. This peptide was synthesised successfully. The yield was sufficient in both quantity and purity for the purposes of the project.

Synthesis was also attempted of the cyclic PSA mimetic peptide PR-21 quoted by Torregrossa et al [229]. The initial product was of a poor yield. The production of a cyclic peptide involves a "cyclisation" step. Cyclisation is a very difficult process. The method used in this project was described by Kamber et al [234]. When attempted, this step all but obliterated the peptide leaving only a thin residue behind that was insufficient for the purposes of this project. Given the success and ease at which the linear peptide was synthesised, the decision was made at this point to halt the production of PR-21 and divert all efforts and resources into the synthesis of the linear peptide, and its scramble.

One of the main goals of this project was to immobilise the peptide on a collagen scaffold and also develop methods were to prove/quantify peptide immobilisation. One such strategy involved the synthesis of a fluoroscein linked peptide. It was reasoned that a fluoroscein tagged peptide, if successfully attached to a collagen fibre, would make the fibre become luminescent. The fluoroscein tagged peptide was successfully synthesised and with a sufficient yield. However linking this peptide to the collagen fibre proved elusive and immobilisation studies moved in a different direction and this product was not used. A variation of the linear peptide was also synthesised with a terminal cysteine residue. While exploring the use of different crosslinkers it was postulated that perhaps a cysteine residue could be used as a linking amino acid. However as the project evolved, it was decided not to proceed with testing this peptide further as it was felt that it was structurally too dissimilar to the active linear peptide and that it might not behave accordingly in subsequent experiments. An attempt at quantifying peptide immobilisation by using a fluorescent antibody reaction was also

executed, but at this stage of the experiment the peptide addition protocol had not yet been developed and results were inconsistent.

Peptide production is a highly specialised, costly and time consuming process. The peptides used in this study took approximately four months to manufacture and had to be performed off-site in another facility and a whole new skill-set had to be learned. In future studies, the time and cost-element should be factored into the project planning from the outset in order to facilitate timely and efficient testing. A major disadvantage of peptide synthesis is the relatively low-yields produced. The vast majority of projects in the literature focus on *in vitro* peptide studies, and consequently only small amounts of peptide are required. Upscaling to *in vivo* studies requires exponentially more peptide and therefore a lot more preparation goes into that phase of the project, leaving less time for peptide testing. The low yields also limit the number of experiments that can be done. Experiments have to be well planned as wasting peptide is totally unacceptable given its value.

Before proceeding to animal testing *in vitro* analysis of the linear peptide was performed in order to ensure low toxicity. There are many hazardous chemicals used in the synthesis of peptides. and it was decided that a formal dose/toxicity study was carried out using 3T3 cells in a MTT cell viability assay. The results of this were encouraging. The mimetic peptide was not only safe, but showed an increase in cell proliferation with increasing concentrations of peptide. These findings were in line with observations made with native PSA in *in vitro* cell culture experiments as seen in the literature [238]. The effect that linear peptide has on Schwann cells has been well documented [230]. In future projects it would be preferable to perform cell studies on a linear peptide modified fibre using Schwann cells, to see if the chemical immobilisation of the linear peptide imparts a neuroregenerative advantage.

The Mehanna paper included an *in vivo* study which looked at how PSA mimetic peptide affected the functional outcome in an animal model. In this study the peptide was suspended in a hydrogel before loading the gel into a non-absorbable polyethylene nerve conduit tube. This conduit was then implanted in the host. It has been established that hollow conduits provide an excellent microenvironment for regenerating axons as well as a physical support [149]. However, while hollow conduits are acceptable as a basic nerve grafting material, research also shows that there are a host of alternative and

superior intraluminal guidance strategies to augment neural regeneration (see chap 2.5.3). A practical nerve conduit should provide adequate physical guidance. NGCs themselves can be modified or structured in a way to provide physical guidance to regenerating axons. The list of strategies for NGC customisation include: multichannel conduits, electrospun fibre walls and microchanneled walls. The empty lumen of a NGC is also an important consideration when designing a nerve graft. Intraluminal guidance is a key modification of the hollow NGC. There are a myriad of options when considering strategies for intraluminal physical cues, which include: fibres, gels, sponges, films and filaments. These intraluminal guidance cues are all based on the unifying concept of recreating the infrastructure of ECM in the regenerating nerve injury site [178] and forming a scaffold for components like SCs to migrate along and augment the healing process. Logically speaking if a physical structure is introduced across a nerve injury, you have created a physical guide for regeneration, and the body does not have to start bridging a nerve gap from scratch. Physical cues exert a local effect on the advancing growth cone by direct contact and how this influences cell signalling is not fully understood just yet [166]. In the Mehanna study no such intraluminal guidance cue was included for the *in vivo* studies. In this project it was hypothesised that a physical guidance cue would impart an added advantage to a PSA mimetic containing nerve grafts. This was relatively easy to accomplish. Hollow nerve conduits were packed with fibres and a peptide containing hydrogel was pumped into the lumen, just before implantation. The conduits themselves were easy to handle and implantation was achieved using basic microsurgical techniques and a microscope. The drawbacks of this method were that even though the dry fibres could be loaded into a conduit in advance of testing, the peptide hydrogel had to be pumped just prior to surgery. Future studies could look at optimising the gel and perpas increasing its viscosity in order to facilitate mass production of finished composite grafts well in advance of any testing.

In their study, the Mehanna group used a polyethylene conduit for carrying their peptide gel. This material choice has several disadvantages. Firstly, polyethylene is non-absorbable and has to be removed from the host at a later date, once the enclosed nerve has healed. For research purposes this is not a major disadvantage but non-absorbable grafts are impractical in real life use and absorbable scaffolds are far more desirable in clinical practice as this negates the need for a second operation and reduces overall morbidity for the patient. The choice of bio degradable materials for nerve conduits (and

intraluminal physical cues) is extensive and includes: collagen, laminin, PLGA, PLLA, keratin and PAN-MA. This study uses collagen as the base material for much of the final nerve graft. Collagen is highly suitable for the purposes of this study for several reasons. Collagen is a ubiquitous structural protein that makes up approximately 30 % of the proteins in the body. Collagen is also present in neural tissue [237] with types I and II collagen found in the inner endoneurium and collagen fibres providing structural support to the outer perineurium [239].Collagen is a very versatile substance that can be made into many different physical forms: gels, sponges, conduits, fibres, discs, films, foams, sheets etc. In this study collagen was chosen as the material of choice for the NGC, the gel suspension and the intraluminal fibres. Correctly treated collagen is acellular and therefore hypoallergenic, initiating little or no host inflammatory response with little or no antigenicity. It is also chemically quite inert. It was felt that by choosing collagen as the sole ingredient in all the major structural parts of the composite graft, a certain universality would be achieved and even though the overall design is quite complex, the material choice could be kept as simple and as uncomplicated as possible. The degradation rate of collagen implants can be controlled by adjusting the degree of crosslinking that occurs during component manufacture. Polyethylene is a foreign body and initiates an antigenic host immune response. Polyethylene does not allow free diffusion of molecules across its wall. This is necessary to allow outward diffusion of waste products and inward diffusion of essential molecules out of and into the injury site, respectively. The short-term goal of this project was to develop a practical, implantable, biodegradable nerve conduit that rivalled autograft in terms of regenerative capabilities; however the long-term goal is that the work in this project could be translated into clinical practice and used in human subjects. It is for this reason also that polyethylene is an unsuitable material choice as this material is well short of ideal given its total lack of biodegradability.

From a macroscopic and practical point of view, the composite graft used in this study was ideal for purpose. It was easy to handle and was a perfect fit for the cut rat sciatic nerve. It was easily sutured into place using basic surgical technique. At 16 weeks both the NGC and intraluminal fibres in the composite grafts were clearly visible in all specimens thus illustrating the sturdiness of the composite graft. This allows the nerve to regenerate in an enclosed and protected environment for a prolonged period of time. Analysis of the 16 week old grafts showed they were starting to display minimal signs

of biodegradability, which is ideal given the fact that the intent is to leave these conduits in situ and not remove them with a second procedure. Very few animals showed any sign of irritability or pain. None of the surgical sites showed signs of infection or inflammation. This highlights the benefit of using collagen as an implant material due to its low allergenicity. The fact that no animal developed a wound infection shows that good, sterile, surgical technique was used. These surgical outcomes show that a peptide loaded composite collagen nerve graft is a suitable graft for use in living subjects and could perhaps be used in human subjects in some form. In the Mehanna study, the animal was sacrificed at day 6 for analysis of nerve regrowth. The animals observed for functional recovery were measured at 1, 4, 8 and 12 weeks post procedure. Our study wanted to find out the long term benefits of a PSA mimetic peptide on the structure of regenerating axons on a cellular level. Mehanna pointed out that PSA is a molecule that plays a part in the acute phase of injury as peptidase activity limits the life of the initial PSA surge seen post injury. Mehanna postulated that the exaggerated stimulus that exogenous PSA imparts on a freshly severed axon and the regenerating Schwann Cells "primes" the nerve and "that early cellular and molecular responses to injury are modulated so that the subsequent regeneration process is favourably influenced over weeks". This was another reason our study looked at nerve regrowth 16 weeks post injury and focused on the long term effects of using a PSA mimetic peptide. Although it is very interesting to look at early recovery after a traumatic nerve injury, what matters most is the long term outcome in the patient. Also, for analysing the long term biodegradability of the nerve graft, a more distant time point was needed to assess the structural integrity of the graft.

Unfortunately, one of collagen's main advantages when used as an implant is also a major draw-back: its inertness. Inertness in a structural protein is beneficial because it means the protein is resistant to being broken up by chemical means and retains its integrity. However, this also means that modifying collagen in order to make it a more advantageous implant can be difficult. One of the main objectives of this study was to chemically modify a collagen fibre and add a neuroregenerative synthetic peptide to the surface of the collagen fibre in a controlled fashion. It is widely known that EDC/NHS crosslinks collagen by activating carboxyl groups and this in turn allows carboxyl containing amino acids residues such as aspartic acid and glutamic acid to reach with corresponding amine containing amino acid residues to create chemical bonds. A

problem arises when trying to add a peptide to collagen using EDC/NHS because in this scenario crosslinking occurs between peptide and collagen, collagen and collagen and peptide and peptide, leading to chemical pandemonium. After an extensive literature search it was discovered that it was possible to block amines using SNA. By pre-treating an un-crosslinked collagen fibre with SNA before adding EDC/NHS in a stepwise fashion, we were successfully able to add our peptide to the collagen fibre. A major difficulty arose with the use of SNA however. The substance is listed as being hygroscopic. There are different degrees to which a substance can be hygroscopic and other hygroscopic reagents were used to great effect in this project with similar precautions taken. However with each successive procedure the potency of the SNA rapidly decreased. Initially it was not apparent that the abnormal results were due to the nature of SNA but rather it was thought that there was an error in experimental protocol. After several failed experiments it was realised that these bad results were due to the high degree of SNA hygroscopy and that fresh SNA had to be used for all experimental procedures henceforth.

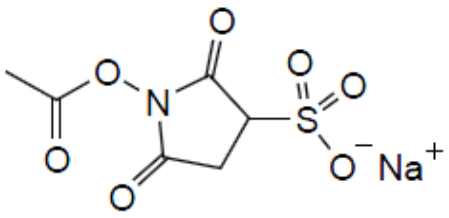

Figure 6.1 Structure of sulfo-NHS acetate

Difficulties were encountered when it came to proving that peptide was chemically attached to the fibre. As was stated previously, efforts at tagging the peptide proved fruitless. FTIR analysis was attempted to show peptide addition but the signal of peptides are indistinct from collagen using this kind of analysis. TNBSA assays proved to be an effective method for quantifying amines. A series of experiments showing the relationship of amine reduction in supernatant after stepwise peptide addition proved to be a productive area of research. Initial experiments compared the “all-in-one” reaction to the “stepwise” reaction (i.e. SNA amine blocking followed by EDC/NHS carboxyl activation then peptide addition) and the results strongly favoured the “stepwise” approach. In the course of these experiments it was shown that the peptide reacted in a

predictable manner with TNBSA and that there was a fixed relationship between peptide concentration and absorbance. It was also shown that peptide was not taken up by fibres in a physical manner in the absence of collagen fibre activation and that peptide was not physically taken up by a collagen fibre after various timepoints. It was shown that there was a relationship between the mass of an activated fibre and the degree of peptide uptake. It was also shown that reaction time did not make a difference to peptide uptake, however patterns suggest two hours was a reasonable reaction time with time points beyond this showing no benefit with regards to peptide uptake.

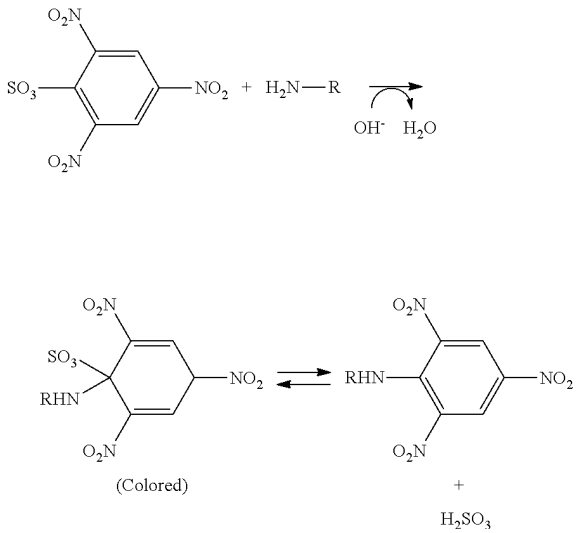

Figure 6.2 Reaction of TNBSA with amine containing compounds yielding a coloured product

In order to prove that peptide was successfully immobilised on a collagen fibre and amino acid analysis was performed on both a peptide modified collagen fibre and a plain collagen fibre as a control. Amino acid analysis involves hydrolysing proteins and breaking them up into their constituent amino acids. The product of hydrolysis is then analysed using a technique such as chromatography to quantify the amounts of each amino acid present in the sample. The hypothesis behind the amino acid analysis experiment in this project was relatively simple. There are certain amino acids present in the linear peptide are not present in large amounts in collagen (i.e. tyrosine, histidine, isoleucine and threonine). Therefore if the peptide is successfully added to collagen, we should see an increase in these key peptides on amino acid analysis. The results of this section of the project were very promising with spikes seen in the concentration of the

four amino acids listed above. Difficulties arose in establishing exactly how much peptide was added using this analytical technique. Collagen is not a very uniform substance. It does not have a constant molecular weight and the quoted molecular weight of 300 kDa is only an average. The amino acid composition of collagen is also variable with varying amounts of different amino acids present in different samples from the same source. This lack of standardisation of collagen poses a challenge for any amino acid analysis. Due to logistical reasons, only one control and one peptide modified fibre were analysed. Given the positive result seen in this project, repeat samples should be analysed to corroborate this pilot data.

Before the development of the method for stepwise activation of collagen using SNA, we investigated other possible cross linking methods. One such method involved using 4-(4,6-Dimethoxy-1,3,5-triazin-2-yl)-4-methylmorpholinium chloride (DMTMM). DMTMM is a triazinyl ester, commonly used in peptide synthesis[240] and is an effective agent for ester coupling and amide bond formation[241]. DMTMM reactions are simple, "one-pot" reactions that result in amide bond formation and the production of an insoluble hydroxytriazine by-product that is removed easily by filtration[242]. Again, in the course of this project, good results were being obtained with the "stepwise" reaction so this crosslinking method was not pursued further.

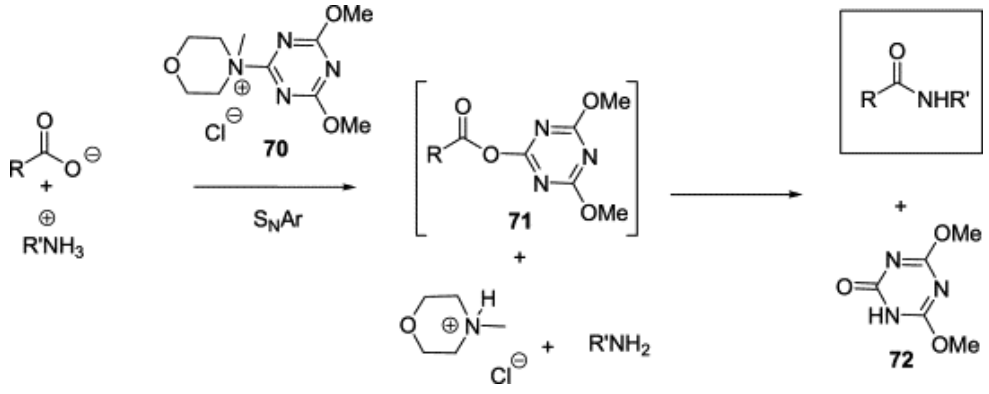

Figure 6.3 Schematic illustrating "one-pot" reaction of DMTMM

The stepwise amine blocking of a solid collagen scaffold followed by the controlled activation of its carboxyl groups is an entirely novel technique. The implications of this new method for future research and development could be massive. By perfecting this

technique, it will become possible to add any positively charged molecule to an otherwise inert collagen fibre in a controlled manner. This means that any scaffold that contains collagen can be veneered with any peptide, transmitter, cell signalling molecule as long as it is charged. Conceivably, with the addition of funtionalising molecules such as multi-armed star-PEG, the ability to modify the collagen fibre could increase exponentially. Unfortunately, by the time this breakthrough occurred, *in vivo* testing of the composite graft had already commenced and due to time constraints it was not possible to test the modified collagen fibre *in vivo*. This new way of modifying collagen could prove to be a very fruitful area of academic research and future studies in this area could yield some excellent results.

The Mehanna study examined how a PSA mimetic peptic hydrogel influenced peripheral nerve regeneration by loading the gel into a non-absorbable hollow NGC and implanting this into an animal. As mentioned earlier, the hollow NGC creates a microenvironment for nerve regeneration but it does not provide any topographical or physical guidance cues. In this project we provided intraluminal physical guidance cues in the form of bundles of collagen fibres in the hope that the physical guidance cues and the chemical guidance cue of the PSA mimetic would act synergistically to promote neural regeneration.

Our study made use of the rat sciatic nerve model. Macroscopically, all of the test subjects had developed a nerve cable that crossed the neural defect, that is to say, all groups had 100 % success rate for bridging a nerve gap of 10 mm. On examination of the mid-graft nerve sections stained with 1 % toluidine blue it was noted that the host response had progressed around the nerve fibres in all groups containing nerve fibres, with incorporation of all grafts evident at 400 x magnification. Overall the data was quite positive. It is interesting to note that there was no statistical difference in the total fascicular area of the regenerated nerve at the graft mid-point when comparing conduits with fibres present to autograft. A proportion of the area at the mid-section is taken up by the unabsorbed fibres. This area was subtracted from the total area of the fibre groups and still no statistical difference was noted between fibre containing groups and autograft controls. The linear peptide performed well when compared to the gold-standard of autograft in certain nerve morphometry studies. There was no statistical difference between the myelinated nerve fibre density of the linear peptide group and autograft (means 7903.4 and 11976.9 fibres per mm^2 respectively). There was however

a statistical difference between the scramble peptide group and autograft when analysing the total myelinated nerve fibre density (means 6727.4 and 11976.9 fibres per mm^2 respectively) which shows that the linear peptide performed as good as autograft and significantly outperformed the scramble peptide, when compared to autograft, in this modality. There was no significant difference between the linear peptide and the other interventions when measuring the total number of myelinated fibres, as compared to autograft (the mean of the LP group was 2668.6 compared to 6149.14 fibres in the autograft group). There was no significant difference between all groups (excluding the gel only group) when the mean fibre diameter was measured. There was also no significant difference shown the measurement of mean axon diameter across all groups (except the gel only group). There was no significant difference in the measurement of myelin thickness across all groups (except gel only). And lastly, similar results were seen the the g-ratio measurement with the gel only group being the only group to show a significantly poorer result.

It is clear from the nerve morphometry results that presence or absence of intraluminal collagen fibres was the main determinant in promoting successful nerve regeneration, with all groups containing intraluminal collagen fibres significantly outperforming the only group without intraluminal fibres in five out of the seven criteria measured. The linear peptide did significantly outperform the scramble peptide in one modality (nerve fibre density). Autograft was only significantly better than all groups when the total number of myelinated fibres were measured.

Going forward and looking at future studies, it would be recommended that the use of higher concentrations of peptide should be explored. The concentration of peptide used in this project was 200 µg/mL, as per Mehanna et al {Mehanna, 2009 #407}. Perhaps if a higher dose of peptide was used this might help promote neural regeneration better. Also, future studies should look at the functional outcome, as well as the histological and morphological outcomes when testing composite nerve grafts. Given that other papers look at earlier time points, perhaps a shorter study analysing composite nerve grafts should be commenced. It is also proposed that peptide modified collagen fibres, once optimised, should be considered for *in vivo* testing as this could prove to be a very promising area of research going forward and may prove to be the key to finding a new gold-standard synthetic nerve graft.

7 Conclusion

PSA mimetic peptides have been proven to promote neural regeneration in animal models. Physical guidance cues have been proven to promote successful nerve regeneration in animal models. This study combined both physical and guidance cues in the form of a composite nerve graft and *in vivo* testing showed that this graft was as good as autograft in several different areas of nerve morphometry testing. Further research into this area could eventually yield a composite nerve graft that surpasses autograft and becomes the new gold-standard.

Collagen is quite an inert substance. During the course of this project a method was devised to selectively activate certain side groups in collagen and peptide was successfully bound to these groups. Patenting of this process should be strongly considered as this is an entirely new method for collagen activation, hitherto undescribed in the literature. Further research into this area could lead to a patentable process for the selective modification of collagen scaffolds.

Bibliography

1. Evans, G.R., *Peripheral nerve injury: a review and approach to tissue engineered constructs.* Anat Rec, 2001. **263**(4): p. 396-404.
2. Rosberg, H.E., et al., *Injury to the human median and ulnar nerves in the forearm – analysis of costs for treatment and rehabilitation of 69 patients in southern sweden.* The Journal of Hand Surgery: British & European Volume, 2005. **30**(1): p. 35-39.
3. Ray, W.Z. and S.E. Mackinnon, *Management of nerve gaps: Autografts, allografts, nerve transfers, and end-to-side neurorrhaphy.* Experimental Neurology, 2010. **223**(1): p. 77-85.
4. Siemionow, M. and G. Brzezicki, *Chapter 8 Current Techniques and Concepts in Peripheral Nerve Repair*, in *International Review of Neurobiology*, G. Stefano, T. Pierluigi, and B. Bruno, Editors. 2009, Academic Press. p. 141-172.
5. Lee, S.K. and S.W. Wolfe, *Peripheral Nerve Injury and Repair.* Journal of the American Academy of Orthopaedic Surgeons, 2000. **8**(4): p. 243-252.
6. Wiberg, M. and G. Terenghi, *Will it be possible to produce peripheral nerves?* Surg Technol Int, 2003. **11**: p. 303-10.
7. *Chapter 3 - The Nerve Trunk*, in *Nerve Injury and Repair (Second Edition)*, L. Göran and M.D. Mda2 - Göran Lundborg, Editors. 2004, Churchill Livingstone: Philadelphia. p. 27-cp2.
8. Sinnatamby, C., *Chapter 1 - Introduction to regional anatomy*, in *Last's Anatomy Regional and Applied*. 2000, Churchill Livingstone.
9. Mackinnon, S.E., *Surgery of the Peripheral Nerve*. 2003: W.B. Saunders.
10. Seddon, H.J., *Peripheral Nerve Injuries.* Spec Rep Ser Med Res Counc (G B), 1954. **282**.
11. Robinson, L.R., *Traumatic injury to peripheral nerves.* Muscle & Nerve, 2000. **23**(6): p. 863-873.
12. Sunderland, S., *A classification of peripheral nerve injuries producing loss of function.* Brain, 1951. **74**(4): p. 491-516.
13. Campbell, W.W., *Evaluation and management of peripheral nerve injury.* Clin Neurophysiol, 2008. **119**(9): p. 1951-65.
14. Cooper, C., *Fundamentals of Hand Therapy: Clinical Reasoning and Treatment Guidelines for Common Diagnoses of the Upper Extremity*. 2007: Mosby Elsevier.
15. Dumitru, D., A.A. Amato, and M.J. Zwarts, *Electrodiagnostic medicine* +. 2002: Hanley & Belfus.
16. MacKinnon, S.E. and A.L. Dellon, *Surgery of the Peripheral Nerve*. 1988: Thieme Medical Pub.
17. Koeppen, A.H., *Wallerian degeneration: history and clinical significance.* J Neurol Sci, 2004. **220**(1-2): p. 115-7.
18. Waller, A., *Experiments on the Section of the Glossopharyngeal and Hypoglossal Nerves of the Frog, and Observations of the Alterations Produced Thereby in the Structure of Their Primitive Fibres.* Philosophical Transactions of the Royal Society of London, 1850. **140**: p. 423-429.
19. Turner, J.E. and K.A. Glaze, *The early stages of wallerian degeneration in the severed optic nerve of the newt (Triturus viridescens).* The Anatomical Record, 1977. **187**(3): p. 291-309.
20. Lunn, E.R., M.C. Brown, and V.H. Perry, *The pattern of axonal degeneration in the peripheral nervous system varies with different types of lesion.* Neuroscience, 1990. **35**(1): p. 157-65.

21. Yawo, H. and M. Kuno, *Calcium dependence of membrane sealing at the cut end of the cockroach giant axon.* J Neurosci, 1985. **5**(6): p. 1626-32.
22. Hall, S.M., *Mechanisms of repair after traumatic injury*, in *Peripheral Neuropathy.* 2005, Elsevier. p. 11403-11434.
23. Raff, M.C., A.V. Whitmore, and J.T. Finn, *Axonal self-destruction and neurodegeneration.* Science, 2002. **296**(5569): p. 868-71.
24. Kang, H., L. Tian, and W. Thompson, *Terminal Schwann cells guide the reinnervation of muscle after nerve injury.* J Neurocytol, 2003. **32**(5-8): p. 975-85.
25. Sulaiman, O.A. and T. Gordon, *Effects of short- and long-term Schwann cell denervation on peripheral nerve regeneration, myelination, and size.* Glia, 2000. **32**(3): p. 234-46.
26. Hall, S.M., *The biology of chronically denervated Schwann cells.* Ann N Y Acad Sci, 1999. **883**: p. 215-33.
27. Seckel, B.R., *Enhancement of peripheral nerve regeneration.* Muscle Nerve, 1990. **13**(9): p. 785-800.
28. Fenrich, K. and T. Gordon, *Canadian Association of Neuroscience review: axonal regeneration in the peripheral and central nervous systems--current issues and advances.* Can J Neurol Sci, 2004. **31**(2): p. 142-56.
29. Zochodne, D.W. and D. Levy, *Nitric oxide in damage, disease and repair of the peripheral nervous system.* Cell Mol Biol (Noisy-le-grand), 2005. **51**(3): p. 255-67.
30. Zheng, M. and D.P. Kuffler, *Guidance of regenerating motor axons in vivo by gradients of diffusible peripheral nerve-derived factors.* J Neurobiol, 2000. **42**(2): p. 212-9.
31. Fu, S.Y. and T. Gordon, *The cellular and molecular basis of peripheral nerve regeneration.* Mol Neurobiol, 1997. **14**(1-2): p. 67-116.
32. Funakoshi, H., et al., *Differential expression of mRNAs for neurotrophins and their receptors after axotomy of the sciatic nerve.* J Cell Biol, 1993. **123**(2): p. 455-65.
33. Dahlin, L., *Nerve injury and repair: from molecule to man.* Peripheral nerve surgery-practical applications in the upper extremity, 2006: p. 1.
34. Taniuchi, M., et al., *Expression of nerve growth factor receptors by Schwann cells of axotomized peripheral nerves: ultrastructural location, suppression by axonal contact, and binding properties.* J Neurosci, 1988. **8**(2): p. 664-81.
35. Liuzzi, F.J. and B. Tedeschi, *Peripheral nerve regeneration.* Neurosurg Clin N Am, 1991. **2**(1): p. 31-42.
36. Davis, J.B. and P. Stroobant, *Platelet-derived growth factors and fibroblast growth factors are mitogens for rat Schwann cells.* J Cell Biol, 1990. **110**(4): p. 1353-60.
37. Martini, R., *Expression and functional roles of neural cell surface molecules and extracellular matrix components during development and regeneration of peripheral nerves.* J Neurocytol, 1994. **23**(1): p. 1-28.
38. Creange, A., G. Barlovatz-Meimon, and R.K. Gherardi, *Cytokines and peripheral nerve disorders.* Eur Cytokine Netw, 1997. **8**(2): p. 145-51.
39. Costigan, M., et al., *Heat Shock Protein 27: Developmental Regulation and Expression after Peripheral Nerve Injury.* The Journal of Neuroscience, 1998. **18**(15): p. 5891-5900.
40. Lewis, S.E., et al., *A role for HSP27 in sensory neuron survival.* J Neurosci, 1999. **19**(20): p. 8945-53.

41. Chierzi, S., et al., *The ability of axons to regenerate their growth cones depends on axonal type and age, and is regulated by calcium, cAMP and ERK.* Eur J Neurosci, 2005. **21**(8): p. 2051-62.
42. Krystosek, A. and N.W. Seeds, *Plasminogen activator release at the neuronal growth cone.* Science, 1981. **213**(4515): p. 1532-4.
43. Gallo, G. and P. Letourneau, *Axon guidance: proteins turnover in turning growth cones.* Curr Biol, 2002. **12**(16): p. R560-2.
44. Kuffler, D.P., *Promoting and directing axon outgrowth.* Mol Neurobiol, 1994. **9**(1-3): p. 233-43.
45. Kater, S.B. and V. Rehder, *The sensory-motor role of growth cone filopodia.* Curr Opin Neurobiol, 1995. **5**(1): p. 68-74.
46. Goodman, C.S., *Mechanisms and molecules that control growth cone guidance.* Annu Rev Neurosci, 1996. **19**: p. 341-77.
47. Tessier-Lavigne, M. and C.S. Goodman, *The molecular biology of axon guidance.* Science, 1996. **274**(5290): p. 1123-33.
48. Mueller, B.K., *Growth cone guidance: first steps towards a deeper understanding.* Annu Rev Neurosci, 1999. **22**: p. 351-88.
49. Tuttle, R. and D.D. O'Leary, *Neurotrophins rapidly modulate growth cone response to the axon guidance molecule, collapsin-1.* Mol Cell Neurosci, 1998. **11**(1-2): p. 1-8.
50. Burnett, M.G. and E.L. Zager, *Pathophysiology of peripheral nerve injury: a brief review.* Neurosurgical Focus, 2004. **16**(5): p. 1-7.
51. Gutmann, E. and J. Young, *The re-innervation of muscle after various periods of atrophy.* Journal of Anatomy, 1944. **78**(Pt 1-2): p. 15.
52. Sunderland, S., *Nerves And Nerve Injuries*. 1978: Churchill Livingstone.
53. Sumner, A.J., *Aberrant reinnervation.* Muscle Nerve, 1990. **13**(9): p. 801-3.
54. Lundborg, G., *A 25-year perspective of peripheral nerve surgery: Evolving neuroscientific concepts and clinical significance.* The Journal of hand surgery, 2000. **25**(3): p. 391-414.
55. Scholz, T., et al., *Peripheral nerve injuries: an international survey of current treatments and future perspectives.* J Reconstr Microsurg, 2009. **25**(6): p. 339-44.
56. McQuarrie, I.G. and B. Grafstein, *Axon outgrowth enhanced by a previous nerve injury.* Arch Neurol, 1973. **29**(1): p. 53-5.
57. McQuarrie, I.G., B. Grafstein, and M.D. Gershon, *Axonal regeneration in the rat sciatic nerve: effect of a conditioning lesion and of dbcAMP.* Brain Res, 1977. **132**(3): p. 443-53.
58. Jacob, J.M. and S.A. Croes, *Acceleration of axonal outgrowth in motor axons from mature and old F344 rats after a conditioning lesion.* Exp Neurol, 1998. **152**(2): p. 231-7.
59. Danielsen, N., et al., *Pre-degenerated nerve grafts enhance regeneration by shortening the initial delay period.* Brain Res, 1994. **666**(2): p. 250-4.
60. Ducker, T.B., L.G. Kempe, and G.J. Hayes, *The metabolic background for peripheral nerve surgery.* J Neurosurg, 1969. **30**(3): p. 270-80.
61. Kurze, T., *Microtechniques in neurological surgery.* Clin Neurosurg, 1964. **11**: p. 128-37.
62. Smith, J.W., *Microsurgery: review of the literature and discussion of microtechniques.* Plast Reconstr Surg, 1966. **37**(3): p. 227-45.

63. Edshage, S., *Peripheral Nerve Suture. A Technique for Improved Intraneural Topography. Evaluation of Some Suture Materials.* Acta Chir Scand Suppl, 1964. **15**(331): p. SUPPL 331:1+.
64. Giddins, G.E., P.J. Wade, and A.A. Amis, *Primary nerve repair: strength of repair with different gauges of nylon suture material.* J Hand Surg Br, 1989. **14**(3): p. 301-2.
65. Millesi, H., *Microsurgery of peripheral nerves.* The Hand, 1973. **5**(2): p. 157-160.
66. Terzis, J., B. Faibisoff, and B. Williams, *The nerve gap: suture under tension vs. graft.* Plast Reconstr Surg, 1975. **56**(2): p. 166-70.
67. Hentz, V.R., et al., *The nerve gap dilemma: a comparison of nerves repaired end to end under tension with nerve grafts in a primate model.* J Hand Surg Am, 1993. **18**(3): p. 417-25.
68. Lundborg, G., et al., *Tubular versus conventional repair of median and ulnar nerves in the human forearm: early results from a prospective, randomized, clinical study.* J Hand Surg Am, 1997. **22**(1): p. 99-106.
69. Lundborg, G., *Nerve Injury and Repair*. 1988: Churchill Livingstone.
70. Hakstian, R.W., *Funicular orientation by direct stimulation. An aid to peripheral nerve repair.* J Bone Joint Surg Am, 1968. **50**(6): p. 1178-86.
71. Williams, H.B. and J.K. Terzis, *Single fascicular recordings: an intraoperative diagnostic tool for the management of peripheral nerve lesions.* Plast Reconstr Surg, 1976. **57**(5): p. 562-9.
72. Gruber, H. and W. Zenker, *Acetylcholinesterase: histochemical differentiation between motor and sensory nerve fibres.* Brain Res, 1973. **51**: p. 207-14.
73. Gruber, H., *Identification of motor and sensory funiculi in cut nerves and their selective reunion.* Br J Plast Surg, 1976. **29**(1): p. 70-3.
74. Szabolcs, M.J., et al., *Axon typing of rat muscle nerves using a double staining procedure for cholinesterase and carbonic anhydrase.* J Histochem Cytochem, 1991. **39**(12): p. 1617-25.
75. Deutinger, M., et al., *Clinical and electroneurographic evaluation of sensory/motor-differentiated nerve repair in the hand.* J Neurosurg, 1993. **78**(5): p. 709-13.
76. Hansson, H.J., *Histochemical demonstration of carbonic anhydrase activity.* Histochemie, 1967. **11**(2): p. 112-128.
77. Riley, D.A. and D.H. Lang, *Carbonic anhydrase activity of human peripheral nerves: a possible histochemical aid to nerve repair.* J Hand Surg Am, 1984. **9A**(1): p. 112-20.
78. Carson, K.A. and J.K. Terzis, *Carbonic anhydrase histochemistry. A potential diagnostic method for peripheral nerve repair.* Clin Plast Surg, 1985. **12**(2): p. 227-32.
79. Gu, X.S., et al., *Rapid immunostaining of live nerve for identification of sensory and motor fasciculi.* Chin Med J (Engl), 1992. **105**(11): p. 949-52.
80. Sanger, J.R., et al., *Effects of axotomy on the cholinesterase and carbonic anhydrase activities of axons in the proximal and distal stumps of rabbit sciatic nerves: a temporal study.* Plast Reconstr Surg, 1991. **87**(4): p. 726-38; discussion 739-40.
81. Lundborg, G., *Nerve Repair: Current Concept and Future Prospectives: Guest Editorial.* The British Journal of Hand Therapy, 1999. **4**(1): p. 5-7.

82. Bailey, S.B., et al., *The influence of fibronectin and laminin during Schwann cell migration and peripheral nerve regeneration through silicon chambers.* J Neurocytol, 1993. **22**(3): p. 176-84.
83. Wang, G.Y., et al., *Behavior of axons, Schwann cells and perineurial cells in nerve regeneration within transplanted nerve grafts: effects of anti-laminin and anti-fibronectin antisera.* Brain Res, 1992. **583**(1-2): p. 216-26.
84. Gulati, A.K., *Evaluation of acellular and cellular nerve grafts in repair of rat peripheral nerve.* J Neurosurg, 1988. **68**(1): p. 117-23.
85. Hall, S.M., *The effect of inhibiting Schwann cell mitosis on the re-innervation of acellular autografts in the peripheral nervous system of the mouse.* Neuropathol Appl Neurobiol, 1986. **12**(4): p. 401-14.
86. Riedl, O., et al., *Sural nerve harvesting beyond the popliteal region allows a significant gain of donor nerve graft length.* Plast Reconstr Surg, 2008. **122**(3): p. 798-805.
87. Norkus, T., M. Norkus, and T. Ramanauskas, *Donor, recipient and nerve grafts in brachial plexus reconstruction: anatomical and technical features for facilitating the exposure.* Surg Radiol Anat, 2005. **27**(6): p. 524-30.
88. Lundborg, G. and L.B. Dahlin, *EXPERIMENTAL NERVE GRAFTING — TOWARDS FUTURE SOLUTIONS OF A CLINICAL PROBLEM.* Hand Surgery, 1998. **03**(02): p. 165-173.
89. Kerns, J.M., et al., *The influence of predegeneration on regeneration through peripheral nerve grafts in the rat.* Exp Neurol, 1993. **122**(1): p. 28-36.
90. Gulati, A.K., *Peripheral nerve regeneration through short- and long-term degenerated nerve transplants.* Brain Res, 1996. **742**(1-2): p. 265-70.
91. Haapaniemi, T., et al., *Hyperbaric oxygen treatment enhances regeneration of the rat sciatic nerve.* Exp Neurol, 1998. **149**(2): p. 433-8.
92. Zamboni, W.A., et al., *Functional evaluation of peripheral-nerve repair and the effect of hyperbaric oxygen.* J Reconstr Microsurg, 1995. **11**(1): p. 27-9; discussion 29-30.
93. Millesi, H., G. Meissl, and A. Berger, *The Interfascicular Nerve-Grafting of the Median and Ulnar Nerves.* The Journal of Bone & Joint Surgery, 1972. **54**(4): p. 727-750.
94. Millesi, H., G. Meissl, and A. Berger, *Further experience with interfascicular grafting of the median, ulnar, and radial nerves.* J Bone Joint Surg Am, 1976. **58**(2): p. 209-18.
95. Breidenbach, W.C., *Vascularized nerve grafts. A practical approach.* Orthop Clin North Am, 1988. **19**(1): p. 81-9.
96. Doi, K., et al., *A comparison of vascularized and conventional sural nerve grafts.* J Hand Surg Am, 1992. **17**(4): p. 670-6.
97. Birch, R., et al., *Experience with the free vascularized ulnar nerve graft in repair of supraclavicular lesions of the brachial plexus.* Clin Orthop Relat Res, 1988. **237**(237): p. 96-104.
98. Merle, M. and G. Dautel, *Vascularised nerve grafts.* J Hand Surg Br, 1991. **16**(5): p. 483-8.
99. Breidenbach, W. and J.K. Terzis, *The anatomy of free vascularized nerve grafts.* Clin Plast Surg, 1984. **11**(1): p. 65-71.
100. Terzis, J.K., *Microreconstruction of nerve injuries*. 1987, Philadelphia: Saunders.
101. Sunderland, *Nerve injuries and their repair : a critical appraisal*. 1991, Edinburgh: Churchill Livingstone.

102. Kotani, T., et al., *[Postoperative results of nerve transposition in brachial plexus injury].* Seikei Geka, 1971. **22**(11): p. 963-6.
103. Tuttle, H.K., *EXposure of the brachial plexus with nerve-transplantation.* Journal of the American Medical Association, 1913. **61**(1): p. 15-17.
104. Brandt, K.E. and S.E. Mackinnon, *A technique for maximizing biceps recovery in brachial plexus reconstruction.* J Hand Surg Am, 1993. **18**(4): p. 726-33.
105. El-Gammal, T.A. and N.A. Fathi, *Outcomes of surgical treatment of brachial plexus injuries using nerve grafting and nerve transfers.* J Reconstr Microsurg, 2002. **18**(1): p. 7-15.
106. Samardzic, M., et al., *Transfer of the medial pectoral nerve: myth or reality?* Neurosurgery, 2002. **50**(6): p. 1277-82.
107. Waikakul, S., S. Wongtragul, and V. Vanadurongwan, *Restoration of elbow flexion in brachial plexus avulsion injury: comparing spinal accessory nerve transfer with intercostal nerve transfer.* J Hand Surg Am, 1999. **24**(3): p. 571-7.
108. Ballance, C.A., H.A. Ballance, and P. Stewart, *REMARKS on the OPERATIVE TREATMENT of CHRONIC FACIAL PALSY of PERIPHERAL ORIGIN.* BMJ, 1903. **1**(2209): p. 1009-1013.
109. Ramón y Cajal, S.D.J.J.E.G., *Cajal's degeneration and regeneration of the nervous system*. 1991, New York: Oxford University Press.
110. Viterbo, F., et al., *Latero-terminal neurorrhaphy without removal of the epineural sheath. Experimental study in rats.* Rev Paul Med, 1992. **110**(6): p. 267-75.
111. Noah, E.M., et al., *A new animal model to investigate axonal sprouting after end-to-side neurorrhaphy.* J Reconstr Microsurg, 1997. **13**(5): p. 317-25.
112. Viterbo, F., et al., *End-to-side neurorrhaphy with removal of the epineurial sheath: an experimental study in rats.* Plast Reconstr Surg, 1994. **94**(7): p. 1038-47.
113. Viterbo, F., et al., *Two end-to-side neurorrhaphies and nerve graft with removal of the epineural sheath: experimental study in rats.* Br J Plast Surg, 1994. **47**(2): p. 75-80.
114. Bertelli, J.A., A.R. dos Santos, and J.B. Calixto, *Is axonal sprouting able to traverse the conjunctival layers of the peripheral nerve? A behavioral, motor, and sensory study of end-to-side nerve anastomosis*. J Reconstr Microsurg, 1996. **12**(8): p. 559-63.
115. Noah, E.M., et al., *End-to-side neurorrhaphy: a histologic and morphometric study of axonal sprouting into an end-to-side nerve graft.* J Reconstr Microsurg, 1997. **13**(2): p. 99-106.
116. al-Qattan, M.M. and A. al-Thunyan, *Variables affecting axonal regeneration following end-to-side neurorrhaphy.* Br J Plast Surg, 1998. **51**(3): p. 238-42.
117. Zhao, J.Z., Z.W. Chen, and T.Y. Chen, *Nerve regeneration after terminolateral neurorrhaphy: experimental study in rats.* J Reconstr Microsurg, 1997. **13**(1): p. 31-7.
118. Tarasidis, G., et al., *End-to-side neurorrhaphy resulting in limited sensory axonal regeneration in a rat model.* Ann Otol Rhinol Laryngol, 1997. **106**(6): p. 506-12.
119. Tarasidis, G., et al., *End-to-side neurorraphy: A long-term study of neural regeneration in a rat model.* Otolaryngology - Head and Neck Surgery, 1998. **119**(4): p. 337-341.
120. Tham, S.K. and W.A. Morrison, *Motor collateral sprouting through an end-to-side nerve repair.* J Hand Surg Am, 1998. **23**(5): p. 844-51.

121. Lundborg, G., et al., *Can sensory and motor collateral sprouting be induced from intact peripheral nerve by end-to-side anastomosis?* J Hand Surg Br, 1994. **19**(3): p. 277-82.
122. Bertelli, J.A. and M.F. Ghizoni, *Nerve repair by end-to-side coaptation or fascicular transfer: a clinical study.* J Reconstr Microsurg, 2003. **19**(5): p. 313-8.
123. Bertelli, J.A. and M.F. Ghizoni, *Concepts of nerve regeneration and repair applied to brachial plexus reconstruction.* Microsurgery, 2006. **26**(4): p. 230-44.
124. Hayashi, A., et al., *Collateral sprouting occurs following end-to-side neurorrhaphy.* Plast Reconstr Surg, 2004. **114**(1): p. 129-37.
125. Hayashi, A., et al., *Axotomy or compression is required for axonal sprouting following end-to-side neurorrhaphy.* Exp Neurol, 2008. **211**(2): p. 539-50.
126. Brenner, M.J., et al., *Motor neuron regeneration through end-to-side repairs is a function of donor nerve axotomy.* Plast Reconstr Surg, 2007. **120**(1): p. 215-23.
127. Dvali, L.T. and T.M. Myckatyn, *End-to-side nerve repair: review of the literature and clinical indications.* Hand Clin, 2008. **24**(4): p. 455-60, vii.
128. Anderson, P.N. and M. Turmaine, *Peripheral nerve regeneration through grafts of living and freeze-dried CNS tissue.* Neuropathol Appl Neurobiol, 1986. **12**(4): p. 389-99.
129. Campbell, J.B., A.L. Bassett, and J. Boehler, *Frozen-Irradiated Homografts Shielded with Microfilter Sheaths in Peripheral Nerve Surgery.* J Trauma, 1963. **3**: p. 303-11.
130. Martini, A.K., *[The lyophilized homologous nerve graft for the prevention of neuroma formation (animal experiment study)].* Handchir Mikrochir Plast Chir, 1985. **17**(5): p. 266-9.
131. Singh, R. and S.A. Lange, *Experience with homologous lyophilised nerve grafts in the treatment of peripheral nerve injuries.* Acta Neurochir (Wien), 1975. **32**(1-2): p. 125-30.
132. Wilhelm, K., *[Briding of nerve defects using lyophilized homologous grafts].* Handchirurgie, 1972. **4**(1): p. 25-30.
133. Evans, P.J., et al., *Regeneration across preserved peripheral nerve grafts.* Muscle Nerve, 1995. **18**(10): p. 1128-38.
134. Hiles, R.W., *Freeze dried irradiated nerve homograft: a preliminary report.* Hand, 1972. **4**(1): p. 79-84.
135. Marmor, L., *The repair of peripheral nerves by irradiated homografts.* Clin Orthop Relat Res, 1964. **34**: p. 161-9.
136. LAWSON, G.M. and M.A. GLASBY, *A Comparison of Immediate and Delayed Nerve Repair Using Autologous Freeze-Thawed Muscle Grafts in a Large Animal Model: The simple injury.* Journal of Hand Surgery (British and European Volume), 1995. **20**(5): p. 663-700.
137. Gulati, A.K., *Immune response and neurotrophic factor interactions in peripheral nerve transplants.* Acta Haematol, 1998. **99**(3): p. 171-4.
138. Gulati, A.K. and G.P. Cole, *Nerve graft immunogenicity as a factor determining axonal regeneration in the rat.* J Neurosurg, 1990. **72**(1): p. 114-22.
139. Lassner, F., et al., *Cellular mechanisms of rejection and regeneration in peripheral nerve allografts.* Transplantation, 1989. **48**(3): p. 386-92.
140. Mackinnon, S., et al., *Nerve allograft response: a quantitative immunological study.* Neurosurgery, 1982. **10**(1): p. 61-9.

141. Pollard, J.D., R.S. Gye, and J.G. McLeod, *An assessment of immunosuppressive agents in experimental peripheral nerve transplantation.* Surg Gynecol Obstet, 1971. **132**(5): p. 839-45.
142. Trumble, T.E. and F.G. Shon, *The physiology of nerve transplantation.* Hand Clin, 2000. **16**(1): p. 105-22.
143. Yu, L.T., et al., *Expression of major histocompatibility complex antigens on inflammatory peripheral nerve lesions.* J Neuroimmunol, 1990. **30**(2-3): p. 121-8.
144. Feng, F.Y., et al., *FK506 rescues peripheral nerve allografts in acute rejection.* J Neurotrauma, 2001. **18**(2): p. 217-29.
145. Gold, B.G., K. Katoh, and T. Storm-Dickerson, *The immunosuppressant FK506 increases the rate of axonal regeneration in rat sciatic nerve.* J Neurosci, 1995. **15**(11): p. 7509-16.
146. Brenner, M.J., et al., *Repair of motor nerve gaps with sensory nerve inhibits regeneration in rats.* Laryngoscope, 2006. **116**(9): p. 1685-92.
147. Nichols, C.M., et al., *Effects of motor versus sensory nerve grafts on peripheral nerve regeneration.* Exp Neurol, 2004. **190**(2): p. 347-55.
148. Kiernan, J.A.B.M.L., *Barr's The human nervous system : an anatomical viewpoint*. 2005, Philadelphia: Lippincott Williams & Wilkins.
149. Daly, W., et al., *A biomaterials approach to peripheral nerve regeneration: bridging the peripheral nerve gap and enhancing functional recovery.* J R Soc Interface, 2012. **9**(67): p. 202-21.
150. Pollard, J.D. and L. Fitzpatrick, *An ultrastructural comparison of peripheral nerve allografts and autografts.* Acta Neuropathol, 1973. **23**(2): p. 152-65.
151. FF, I.J., R.C. Van De Graaf, and M.F. Meek, *The early history of tubulation in nerve repair.* J Hand Surg Eur Vol, 2008. **33**(5): p. 581-6.
152. Xie, J., et al., *Electrospun nanofibers for neural tissue engineering.* Nanoscale, 2010. **2**(1): p. 35-44.
153. Chang, C.-J. and S.-h. Hsu, *The effect of high outflow permeability in asymmetric poly(dl-lactic acid-co-glycolic acid) conduits for peripheral nerve regeneration.* Biomaterials, 2006. **27**(7): p. 1035-1042.
154. Evans, G.R., et al., *Bioactive poly(L-lactic acid) conduits seeded with Schwann cells for peripheral nerve regeneration.* Biomaterials, 2002. **23**(3): p. 841-8.
155. Moore, A.M., et al., *Limitations of conduits in peripheral nerve repairs.* Hand (N Y), 2009. **4**(2): p. 180-6.
156. Belkas, J.S., M.S. Shoichet, and R. Midha, *Peripheral nerve regeneration through guidance tubes.* Neurol Res, 2004. **26**(2): p. 151-60.
157. Meek, M.F. and J.H. Coert, *Clinical use of nerve conduits in peripheral-nerve repair: review of the literature.* J Reconstr Microsurg, 2002. **18**(2): p. 97-109.
158. Chiono, V., C. Tonda-Turo, and G. Ciardelli, *Chapter 9: Artificial scaffolds for peripheral nerve reconstruction.* Int Rev Neurobiol, 2009. **87**: p. 173-98.
159. Griffin, J., et al., *Design and evaluation of novel polyanhydride blends as nerve guidance conduits.* Acta Biomater, 2010. **6**(6): p. 1917-24.
160. Ribeiro-Resende, V.T., et al., *Strategies for inducing the formation of bands of Bungner in peripheral nerve regeneration.* Biomaterials, 2009. **30**(29): p. 5251-9.
161. Pabari, A., et al., *Modern surgical management of peripheral nerve gap.* J Plast Reconstr Aesthet Surg, 2010. **63**(12): p. 1941-8.
162. Schmidt, C.E. and J.B. Leach, *Neural tissue engineering: strategies for repair and regeneration.* Annu Rev Biomed Eng, 2003. **5**: p. 293-347.

163. Park, S.C., et al., *Ultrasound-stimulated peripheral nerve regeneration within asymmetrically porous PLGA/Pluronic F127 nerve guide conduit.* J Biomed Mater Res B Appl Biomater, 2010. **94**(2): p. 359-66.
164. Pfister, B.J., et al., *Biomedical engineering strategies for peripheral nerve repair: surgical applications, state of the art, and future challenges.* Crit Rev Biomed Eng, 2011. **39**(2): p. 81-124.
165. Williams, L.R., et al., *Spatial-temporal progress of peripheral nerve regeneration within a silicone chamber: parameters for a bioassay.* J Comp Neurol, 1983. **218**(4): p. 460-70.
166. Hoffman-Kim, D., J.A. Mitchel, and R.V. Bellamkonda, *Topography, cell response, and nerve regeneration.* Annu Rev Biomed Eng, 2010. **12**: p. 203-31.
167. Mukhatyar, V., et al., *Tissue Engineering Strategies Designed to Realize the Endogenous Regenerative Potential of Peripheral Nerves.* Advanced Materials, 2009. **21**(46): p. 4670-4679.
168. Jiang, X., et al., *Current applications and future perspectives of artificial nerve conduits.* Exp Neurol, 2010. **223**(1): p. 86-101.
169. Deumens, R., et al., *Repairing injured peripheral nerves: Bridging the gap.* Prog Neurobiol, 2010. **92**(3): p. 245-76.
170. Mosahebi, A., et al., *Retroviral labeling of Schwann cells: in vitro characterization and in vivo transplantation to improve peripheral nerve regeneration.* Glia, 2001. **34**(1): p. 8-17.
171. Bellamkonda, R.V., *Peripheral nerve regeneration: an opinion on channels, scaffolds and anisotropy.* Biomaterials, 2006. **27**(19): p. 3515-8.
172. Mackinnon, S.E. and A.L. Dellon, *A study of nerve regeneration across synthetic (Maxon) and biologic (collagen) nerve conduits for nerve gaps up to 5 cm in the primate.* J Reconstr Microsurg, 1990. **6**(2): p. 117-21.
173. Maeda, T., et al., *Regeneration across 'stepping-stone' nerve grafts.* Brain Res, 1993. **618**(2): p. 196-202.
174. Clements, I.P., et al., *Thin-film enhanced nerve guidance channels for peripheral nerve repair.* Biomaterials, 2009. **30**(23-24): p. 3834-46.
175. Bozkurt, A., et al., *In vitro cell alignment obtained with a Schwann cell enriched microstructured nerve guide with longitudinal guidance channels.* Biomaterials, 2009. **30**(2): p. 169-79.
176. Rutkowski, G.E., et al., *Synergistic effects of micropatterned biodegradable conduits and Schwann cells on sciatic nerve regeneration.* J Neural Eng, 2004. **1**(3): p. 151-7.
177. Hu, X., et al., *A novel scaffold with longitudinally oriented microchannels promotes peripheral nerve regeneration.* Tissue Eng Part A, 2009. **15**(11): p. 3297-308.
178. Koh, H.S., et al., *In vivo study of novel nanofibrous intra-luminal guidance channels to promote nerve regeneration.* J Neural Eng, 2010. **7**(4): p. 046003.
179. Chew, S.Y., et al., *Aligned Protein-Polymer Composite Fibers Enhance Nerve Regeneration: A Potential Tissue-Engineering Platform.* Adv Funct Mater, 2007. **17**(8): p. 1288-1296.
180. Hadlock, T., et al., *A polymer foam conduit seeded with Schwann cells promotes guided peripheral nerve regeneration.* Tissue Eng, 2000. **6**(2): p. 119-27.
181. de Ruiter, G.C., et al., *Accuracy of motor axon regeneration across autograft, single-lumen, and multichannel poly(lactic-co-glycolic acid) nerve tubes.* Neurosurgery, 2008. **63**(1): p. 144-53; discussion 153-5.

182. Yao, L., et al., *Controlling dispersion of axonal regeneration using a multichannel collagen nerve conduit.* Biomaterials, 2010. **31**(22): p. 5789-97.
183. Hoke, A., et al., *Schwann cells express motor and sensory phenotypes that regulate axon regeneration.* J Neurosci, 2006. **26**(38): p. 9646-55.
184. Kim, Y.T., et al., *The role of aligned polymer fiber-based constructs in the bridging of long peripheral nerve gaps.* Biomaterials, 2008. **29**(21): p. 3117-27.
185. Matsumoto, K., et al., *Peripheral nerve regeneration across an 80-mm gap bridged by a polyglycolic acid (PGA)-collagen tube filled with laminin-coated collagen fibers: a histological and electrophysiological evaluation of regenerated nerves.* Brain Res, 2000. **868**(2): p. 315-28.
186. Yoshii, S. and M. Oka, *Collagen filaments as a scaffold for nerve regeneration.* J Biomed Mater Res, 2001. **56**(3): p. 400-5.
187. Yoshii, S., et al., *Bridging a 30-mm nerve defect using collagen filaments.* Journal of Biomedical Materials Research Part A, 2003. **67A**(2): p. 467-474.
188. Ngo, T.-T.B., et al., *Poly(L-Lactide) microfilaments enhance peripheral nerve regeneration across extended nerve lesions.* Journal of Neuroscience Research, 2003. **72**(2): p. 227-238.
189. Stang, F., et al., *Structural parameters of collagen nerve grafts influence peripheral nerve regeneration.* Biomaterials, 2005. **26**(16): p. 3083-91.
190. Cai, J., et al., *Permeable guidance channels containing microfilament scaffolds enhance axon growth and maturation.* J Biomed Mater Res A, 2005. **75**(2): p. 374-86.
191. Toba, T., et al., *Regeneration of canine peroneal nerve with the use of a polyglycolic acid-collagen tube filled with laminin-soaked collagen sponge: a comparative study of collagen sponge and collagen fibers as filling materials for nerve conduits.* J Biomed Mater Res, 2001. **58**(6): p. 622-30.
192. Lee, D.Y., et al., *Nerve regeneration with the use of a poly(l-lactide-co-glycolic acid)-coated collagen tube filled with collagen gel.* J Craniomaxillofac Surg, 2006. **34**(1): p. 50-6.
193. Sierpinski, P., et al., *The use of keratin biomaterials derived from human hair for the promotion of rapid regeneration of peripheral nerves.* Biomaterials, 2008. **29**(1): p. 118-28.
194. Itoh, S., et al., *Synthetic collagen fibers coated with a synthetic peptide containing the YIGSR sequence of laminin to promote peripheral nerve regeneration in vivo.* J Mater Sci Mater Med, 1999. **10**(3): p. 129-34.
195. Madduri, S. and B. Gander, *Schwann cell delivery of neurotrophic factors for peripheral nerve regeneration.* J Peripher Nerv Syst, 2010. **15**(2): p. 93-103.
196. Deister, C. and C.E. Schmidt, *Optimizing neurotrophic factor combinations for neurite outgrowth.* J Neural Eng, 2006. **3**(2): p. 172-9.
197. Fine, E.G., et al., *GDNF and NGF released by synthetic guidance channels support sciatic nerve regeneration across a long gap.* Eur J Neurosci, 2002. **15**(4): p. 589-601.
198. Madduri, S., et al., *Effect of controlled co-delivery of synergistic neurotrophic factors on early nerve regeneration in rats.* Biomaterials, 2010. **31**(32): p. 8402-9.
199. Lin, L.F., et al., *GDNF: a glial cell line-derived neurotrophic factor for midbrain dopaminergic neurons.* Science, 1993. **260**(5111): p. 1130-2.
200. Chung, H.J. and T.G. Park, *Surface engineered and drug releasing pre-fabricated scaffolds for tissue engineering.* Adv Drug Deliv Rev, 2007. **59**(4-5): p. 249-62.

201. Yu, X. and R.V. Bellamkonda, *Tissue-engineered scaffolds are effective alternatives to autografts for bridging peripheral nerve gaps.* Tissue Eng, 2003. **9**(3): p. 421-30.
202. Armstrong, S.J., et al., *ECM molecules mediate both Schwann cell proliferation and activation to enhance neurite outgrowth.* Tissue Eng, 2007. **13**(12): p. 2863-70.
203. Itoh, S., et al., *A study of induction of nerve regeneration using bioabsorbable tubes.* J Reconstr Microsurg, 2001. **17**(2): p. 115-23.
204. Rangappa, N., et al., *Laminin-coated poly(L-lactide) filaments induce robust neurite growth while providing directional orientation.* J Biomed Mater Res, 2000. **51**(4): p. 625-34.
205. Kleene, R. and M. Schachner, *Glycans and neural cell interactions.* Nat Rev Neurosci, 2004. **5**(3): p. 195-208.
206. Schauer, R., *Sialic acids: fascinating sugars in higher animals and man.* Zoology (Jena), 2004. **107**(1): p. 49-64.
207. Varki, A., *Diversity in the sialic acids.* Glycobiology, 1992. **2**(1): p. 25-40.
208. Schauer, R. and J.P. Kamerling, *Chemistry, biochemistry and biology of sialic acids.* New comprehensive biochemistry., 1995. **29/B**: p. 243.
209. Varki, A., *The essentials of glycobiology*. 1999, Cold Spring Harbor, NY: Cold Spring Harbor Laboratory Press.
210. Schauer, R., *Achievements and challenges of sialic acid research.* Glycoconjugate Journal, 2000. **17**(7-9): p. 485-499.
211. Marquardt, T. and J. Denecke, *Congenital disorders of glycosylation: review of their molecular bases, clinical presentations and specific therapies.* Eur J Pediatr, 2003. **162**(6): p. 359-79.
212. Finne, J., et al., *Occurrence of α2–8 linked polysialosyl units in a neural cell adhesion molecule.* Biochemical and Biophysical Research Communications, 1983. **112**(2): p. 482-487.
213. Rutishauser, U. and L. Landmesser, *Polysialic acid in the vertebrate nervous system: a promoter of plasticity in cell-cell interactions.* Trends Neurosci, 1996. **19**(10): p. 422-7.
214. Durbec, P. and H. Cremer, *Revisiting the function of PSA-NCAM in the nervous system.* Mol Neurobiol, 2001. **24**(1-3): p. 53-64.
215. Yamamoto, N., et al., *Inhibitory mechanism by polysialic acid for lamina-specific branch formation of thalamocortical axons.* J Neurosci, 2000. **20**(24): p. 9145-51.
216. Muller, D., et al., *A role for polysialylated neural cell adhesion molecule in lesion-induced sprouting in hippocampal organotypic cultures.* Neuroscience, 1994. **61**(3): p. 441-5.
217. Seki, T., *Microenvironmental elements supporting adult hippocampal neurogenesis.* Anat Sci Int, 2003. **78**(2): p. 69-78.
218. Kempermann, G., D. Gast, and F.H. Gage, *Neuroplasticity in old age: sustained fivefold induction of hippocampal neurogenesis by long-term environmental enrichment.* Ann Neurol, 2002. **52**(2): p. 135-43.
219. Chazal, G., et al., *Consequences of neural cell adhesion molecule deficiency on cell migration in the rostral migratory stream of the mouse.* J Neurosci, 2000. **20**(4): p. 1446-57.
220. Hu, H., *Polysialic acid regulates chain formation by migrating olfactory interneuron precursors.* J Neurosci Res, 2000. **61**(5): p. 480-92.

221. Oumesmar, B.N., et al., *Expression of the Highly Polysialylated Neural Cell Adhesion Molecule During Postnatal Myelination and Following Chemically Induced Demyelination of the Adult Mouse Spinal Cord.* European Journal of Neuroscience, 1995. **7**(3): p. 480-491.
222. Carratu, M.R., L. Steardo, and V. Cuomo, *Role of polysialic acid in peripheral myelinated axons.* Microsc Res Tech, 1996. **34**(6): p. 489-91.
223. Covault, J., et al., *Molecular forms of N-CAM and its RNA in developing and denervated skeletal muscle.* J Cell Biol, 1986. **102**(3): p. 731-9.
224. Brushart, T.M., *Preferential reinnervation of motor nerves by regenerating motor axons.* J Neurosci, 1988. **8**(3): p. 1026-31.
225. Franz, C.K., U. Rutishauser, and V.F. Rafuse, *Intrinsic neuronal properties control selective targeting of regenerating motoneurons.* Brain, 2008. **131**(Pt 6): p. 1492-505.
226. Marino, P., et al., *A polysialic acid mimetic peptide promotes functional recovery in a mouse model of spinal cord injury.* Exp Neurol, 2009. **219**(1): p. 163-74.
227. Rode, B., et al., *Large-scale production and homogenous purification of long chain polysialic acids from E. coli K1.* J Biotechnol, 2008. **135**(2): p. 202-9.
228. Frosch, M., et al., *NZB mouse system for production of monoclonal antibodies to weak bacterial antigens: isolation of an IgG antibody to the polysaccharide capsules of Escherichia coli K1 and group B meningococci.* Proceedings of the National Academy of Sciences of the United States of America, 1985. **82**(4): p. 1194-1198.
229. Torregrossa, P., et al., *Selection of poly-alpha 2,8-sialic acid mimotopes from a random phage peptide library and analysis of their bioactivity.* J Biol Chem, 2004. **279**(29): p. 30707-14.
230. Mehanna, A., et al., *Polysialic acid glycomimetics promote myelination and functional recovery after peripheral nerve injury in mice*. Vol. 132. 2009. 1449-1462.
231. Zeugolis, D.I., G.R. Paul, and G. Attenburrow, *Cross-linking of extruded collagen fibers--a biomimetic three-dimensional scaffold for tissue engineering applications.* J Biomed Mater Res A, 2009. **89**(4): p. 895-908.
232. Zeugolis, D.I., R.G. Paul, and G. Attenburrow, *Post-self-assembly experimentation on extruded collagen fibres for tissue engineering applications.* Acta Biomater, 2008. **4**(6): p. 1646-56.
233. Yao, L., et al., *Multichanneled collagen conduits for peripheral nerve regeneration: design, fabrication, and characterization.* Tissue Eng Part C Methods, 2010. **16**(6): p. 1585-96.
234. Kamber, B., et al., *The Synthesis of Cystine Peptides by Iodine Oxidation of S-Trityl-cysteine and S-Acetamidomethyl-cysteine Peptides.* Helvetica Chimica Acta, 1980. **63**(4): p. 899-915.
235. Rushton, W.A., *A theory of the effects of fibre size in medullated nerve.* J Physiol, 1951. **115**(1): p. 101-22.
236. Canan, S., et al., *An efficient stereological sampling approach for quantitative assessment of nerve regeneration.* Neuropathol Appl Neurobiol, 2008. **34**(6): p. 638-49.
237. Friess, W., *Collagen--biomaterial for drug delivery.* Eur J Pharm Biopharm, 1998. **45**(2): p. 113-36.
238. Stark, Y., et al., *A study on polysialic acid as a biomaterial for cell culture applications.* J Biomed Mater Res A, 2008. **85**(1): p. 1-13.

239. Kaplan, S., et al., *Chapter 2: Development of the peripheral nerve.* Int Rev Neurobiol, 2009. **87**: p. 9-26.
240. Falchi, A., et al., *4-(4,6-Dimethoxy[1,3,5]triazin-2-yl)-4-methyl-morpholinium Chloride (DMTMM): A Valuable Alternative to PyBOP for Solid Phase Peptide Synthesis.* Synlett, 2000. **2000**(02): p. 275-277.
241. Montalbetti, C.A.G.N. and V. Falque, *Amide bond formation and peptide coupling.* Tetrahedron, 2005. **61**(46): p. 10827-10852.
242. Taylor, E.C., T.H. Schrader, and L.D. Walensky, *Synthesis of 10-Substituted "Open-Chain" Analogues of 5,10-Dideaza-5,6,7,8-tetrahydrofolic Acid (DDATHF, Lometrexol).* Tetrahedron, 1992. **48**(1): p. 19-32.

APPENDICES

Appendices

A. Materials and Reagents

Material	Supplier
Sircol Assay	Biocolor™, Antrim, Ireland
5-0 Ethicon™ sutures	Ethicon™, Somerville, NJ, USA
6-0 Vicryl Rapide™ sutures	
10-0 Ethicon™ sutures	
Cryo-gel™	Instrumedics Ltd, St Louis, MO, USA
DMEM with D-valine	Invitrogen™, Dublin, Ireland
Siltube™ 1750	Polymer Systems Technology Ltd, Bucks, UK
Collagen type I	Self-extracted
Dimethylaminoethanol (DMAE)	Polysciences™, WA, USA
2-ethoxy ethanol	Sigma Aldrich™, Dublin, Ireland
16-G needle	
18-G needle	
23-G needle	
Acetic acid	
Acetonitrile CHROMASOLV	
Ascorbic acid	
Bovine serum albumin	
Buprenorphine hydrochloride	
Calcium chloride	
Celestine blue	
Citric acid	
Collagenase	
Diamidino yellow	
Dichloromethane	
Dihydroxybenzoic acid	
Dimethylformamide (DMF)	
Dulbeco modified eagle's media	
Diisocyanathohexcane	

Diisopropylethylamine Hydroxybenzotriazole (HOBt)	
Dimethyl sulfoxide	
3-(4,5-dimethylthiazol-2-yl)-2,5-diphenyltetrazolium bromide (MTT)	
DPX mounting media	
1-ethyl-3-(3-dimethylaminopropyl)carbodiimide (EDC)	
Eosin	
Ethanedithiol (EDT)	
Ethanol	
Ethylene glycol diglycdl ether	
Fast blue	
Fast green	
Fetal bovine serum	
Fluorescein isothiocyanate	
Formaldeyhde	
Fuchsin	
Glucose	
Glutaraldeyde	
Hank's balance salt solution	
Hydrochloric acid	
Hydroxyl cinnamic acid	
Ketamine hydrochloride	
Masson's trichrome reagents	
2-(N-morpholino)ethanesulfonic acid (MES)	
N-hydroxysuccinimide (NHS)	
N,N,N′,N′-tetramethyl-O-(1H-benzotriazol-1-yl)uronium hexafluorophosphate (HBTU)	
Phosphate buffered saline	

Piperidine	
Polyethylene glycol Mw 8000	
Polyethylene glycol diglycdyl	
Poly-L-lysine (PLL)	
Potassium permanganate	
Potassium phosphate monobasic	
Propylene oxide	
Sodium chloride	
Sodium hydroxide	
Sodium metabisulphite	
Sodium phosphate dibasic	
Sodium phosphate monobasic	
Sulphuric acid	
Thioanisole	
Tin II chloride	
Toluidine blue	
Trifluoroacetic acid (TFA)	
Triisopropylsilane (TIPS)	
Tris hydrochloride	
Triton™ X-100	
Trypsin-EDTA	
Tween 20	
Wheaton al cap, natural rubber septum	
Xylene	
Xylazine hydrochloride	
Histoclear™	Thermoscientific, Fitchburg, WI, USA
Sulfo-NHS-acetate	
2,4,6-trinitrobenzene sulfonic acid (TNBSA)	
Amino acids for synthesis	Merck Chemical, Nottingham, UK
N-Methylpyrrolidone	Applied Biosystems, Dublin, Ireland
Reaction Vessel Filters	

Disposable in-line filters	
C-18 Gemini and a C-5 Jupiter columns	Phenomenex, Cheshire, UK

B. Extraction Method for Refining Atellocollagen from Bovine Tendon

1. Mechnically disrupt bovine tendon using electrical mincer
2. Wash in 0.1 M PBS
3. Weigh minced tendon
4. Resuspend in 0.5 M acetic acid solution
5. Stir for 48 – 72 hours at 4 °C in a cold room
6. In a 1:100 (w/w) ratio, add pepsin to suspended tissue, using wet weight
7. Stir overnight at 4 °C in a cold room
8. Precipitate collagen by adding 0.9 M NaCl, leave stir overnight at 4 °C
9. Centrifuge solution in batches at 8000 rpm for 20 minutes at 4 °C
10. Decant supernatant, collect tissue pellet
11. Re-weigh wet solid collagen
12. Resuspent in 0.5 M acetic acid and leave stir overnight at 4 °C in a cold room
13. Reprecipitate collagen by adding more 0.9 M NaCl and leave stir overnight at 4 °C in a cold room
14. Recentrifuge in batches at 8000 rpm for 20 minutes at 4 °C
15. Reweigh pellet, suspend in smaller volume 0.5 M acetic acid
16. Using 0.1 mM acetic acid, dialyse collagen solution for five to six days
17. Confirm final purity and concentration of collagen using SDS PAGE and Sircol assay

C. Collagen Fibre Production (Extruson and Crosslinking)

1. Preparation of solutions:
    i. Fibre formation buffer (FFB): 20% PEG, 94 mM sodium phosphate dibasic, 24 nM sodium phosphate monobasic, pH 7.8
    ii. Fibre incubation buffer (FIB): 5.5 mM sodium phosphate dibasic, 1.5 mM potassium phosphate monobasic, 75 mM NaCl, pH 7.1
2. Pre-warm FIB and FFB to 37 °C in a water bath
3. Set up syringe driver setting rate to 0.3 mL/min
4. Fill 5 mL syringe with collagen solution and load onto driver
5. Place ice pack on syringe

6. Attach silicone tubing to needle on end of syringe and secure tip of free end of tubing in tub of FFB just under meniscus
7. Start pump and allow line to flush
8. As collagen "stream" reaches surface, apply steady air flow to surface
9. Once fibre reaches desired length, press stop on driver
10. Allow fibre rest in FFB for five minutes
11. Transfer to FIB bath for five minutes
12. At this point fibre was transferred and placed in another bath overnight of either PBS (to create plain fibres) or immersed in EDC/NHS (30 mM:10 mM) solution (to create crosslinked fibres)
13. Fibres were then washed with distilled water and allowed dry under tension of their own weight at room temperature

D. Sircol Assay

1. Using manufacturer's protocol, prepare 100 µL of reagent blanks and collagen standardsin 1.5 mL microtubes
2. Using another set of 1.5 mL tubes prepare 100 µL of desrired substrate
3. Add one mL of Sircol Reagent to each 1.5 mL tube
4. Ivert each tube and agitate on a shaker for 30 minutes
5. Centrifuge each tube for ten minutres at 12000 rpm
6. Invert each tube and drain excess
7. Carefully add 750 µL of acid-salt wash to the each pellet to remove unbound dye
8. Recentrifuge each tube for another ten minutes at 12000 rpm and decant
9. Carefully remove any residue from edge of tube using a cotton swab
10. To all samples add 250 µL of alkali reagent
11. Take 200 µL of each sample and load onto a 96-wel plate
12. Read plate absorbance at 555 nm to calculate concentration

E. Collagen Conduit Manufacture

1. Coat a 1.5 mm diameter forming rod with collagen solution (12 mg/mL)
2. Dry under a vacuum on a stand
3. Place dry conduit in an EDC/NHS crosslinking solution (30 mM: 10mM in 50 nM MES at pH 5.5) for eight hours
4. Remove and rinse with distilled water before immersing in sodium carbonate buffer
5. Lyophilise for 24 hours and remove forming rod
6. Sterilise for 2 hours in 70 % ethanol and rinse with sterile normal saline solution

F. Collagen Hydrogel Manufacture

1. In an ice bath, add 500 μL of 10 x PBS to 5 mL of collagen (5 mg/mL in 0.05 M acetic acid)
2. Add between 100 and 120 μL of 2 M NaOH ensuring a neutral pH
3. Place solution in incubator at 37 ° for ten to twenty minutes to create a gel

G. Sciatic Nerve Surgery

1. Weigh subject to ensure suitable candidate
2. Administer general anaesthetic using intraperitoneal injection of ketamine and xylazine (doses 80 mg/kg and 10 mg/kg respectively)
3. Prepare operative site over left hind leg by shaving area and sterilising with bethedine
4. Apply eye drops to subject
5. Incise skin and gently part thigh muscles using blunt forceps to locate sciatic nerve
6. Dissect nerve out
7. Find trifurcation of nerve and transect nerve 5 mm proximal to trifurcation
8. Excise a 5 mm segment of nerve proximal to your initial incision
9. Suture conduit to proximal and distal nerve stumps using 10-0 Ethicon™ sutures
10. Close wound in layers using 6-0 Vicryl Rapide™

11. Administer subcutaneous buprenorphine hydrochloride (0.1 – 0.25 mg/kg) as well as a bolus of normal saline for the post-operative recovery period
12. Subject animals to routine observations and intervene as necessary (e.g. analgesia, fluid support etc)
13. At the appropriate timepoint, sacrificing was carried out by CO_2 asphyxiation
14. For nerve morphometry analysis, fixation was performed by instilling fixative solution *in situ* over the exposed graft and nerve tissue (4 % formaldehyde, 1 % glutaraldehyde in 0.1 M PBS)

H. Spurr Resin Preparation

1. Weigh ERL4221, NSA, DER 736 in a ratio of 5:4:12.5 (w/w/w)
2. Mix and place in 60 °C oven for five minutes
3. Remove and mix again for five minutes
4. Add DMAE catalyst (and mix for several minutes before transferring to 50 mL centrifuge tubes (ratio of catalyst: 0.35 mL tp 10 g of ERL, 0.75 mL to 20 g of ERL, 1.4mL to 40 g of ERL)
5. Degas in a vacuum dessicator for another five minutes and seal tubes
6. Store at 4 °C until use and warm up prior to use

I. Embedding Samples in Spurr Resin

Step	Solution	Time	Temperature	Under Hood
1	PBS	15 mins	Room Temp	No
2	PBS	15 mins	Room Temp	No
3	1% OsO4	1 hour	Room Temp	Yes
4	DH20	10 mins	Room Temp	Yes
5	DH20	10 mins	Room Temp	Yes

6	DH20	10 mins	Room Temp	Yes
7	2% uranyl acetate	30 mins	Room Temp	Yes
8	DH20	10 mins	Room Temp	Yes
9	60 % EtOH	15 mins	Room Temp	Yes
10	70% EtOH	15 mins	Room Temp	Yes
12	95% ETOH	15 mins	Room Temp	Yes
13	100% EtOH	15 mins	Room Temp	Yes
14	100% EtOH	15 mins	Room Temp	Yes
15	100% polyproplen e oxide	15 mins	Room Temp	Yes
16	100% polyproplen e oxide	15 mins	Room Temp	Yes
17	1:1 spur and 100% propylene oxide	1 hour	Room Temp	Yes
18	2:1 spur and 100% propylene oxide	overnight	Room Temp	Yes
19	Pure spurr	4 hours	Room Temp	Yes
20	Embed in moulds			
21	Place in oven 50 -55 C	3-4 days	50 – 55 ºC	Yes

J. Stereological Assessment of Nerve Sections Using Manual Methods

1. Place stained sections on microscope stage
2. Using 4 x or 10 x magnification (as needed) image capture entire nerve sections
3. Using ImageJ software, mark out the circumference of the nerve section (to measure entire surface area) and if necessary mark out and measure the area of the intraluminal fibres, which you can subtract in order to get fibre area
4. Then count the number of fields in each section at 100 x magnification

5. Use systematic random sampling to sample fields
6. Count the number of axons contained within an unbiased axon counting frame
7. ImageJ software can measre axon diamtere, myelinated fibre diameter and myelin thickness
8. Total axon number is calculated by multiplying total axonal area by average axonal density

K. Retrograde Nerve Tracing

1. One week before the designated endpoint, the animal is put under general anaesthetic and the previous operative site is opened an material therein exposed
2. The tibial and peroneal branches of the sciatic nerve are transacted distal to the sciatic nerve
3. The proximal end of transected tibial branch is immersed in 5 % fast blue solution for 30 minutes
4. The proximal end of the transacted peroneal branch is immersed in 5 % diamidino yellow solution
5. Both cut ends are sutured into two different areas of surrounding muscular tissue to prevent leaching of dye
6. Close wound in layers using 6-0 Vicryl Rapide™ sutured
7. A week later, the animals undergo transcardial perfusion with a solution of 4 % paraformaldehyde/10 % sucrose in 0.1 M PBS
8. Isolate and harvest the vertebral column (L1 to L6) and post-fix overnight
9. Transfer samples to 10 % sucrose solution for a period of 24 hours to ensure adequate cryoprotection
10. Embed the sample in Cryo-gel™ ensuring it is arranged longitudinally
11. Take 30 µm sections using a cryostat and evaluate under a microscope
12. Tibial nerve axons will be labelled blue, peroneal nerve axons will be labelled yellow and "dual" nerve axons will be both blue and yellow

L. Haematoxylin and Eosin Staining

1. Immerse waxed sections in xylene for ten minutes to de-wax and repeat
2. Pass through alcohol for two minutes and repeat
3. Using reducing concentrations of alcohol (90 %, 70 % then 50 %), bring samples to water
4. Using running water supply, remove alcohol
5. For six minutes stain with Mayer's haematoxylin
6. Rinse under running water supply for four minutes
7. Perform examination under microscopy and differentiate using acid alcohol if necessary. (Note: if acid alcohol used, rinse under running water for four minutes)
8. For two minutes stain with eosin
9. Rinse under running water immediately
10. Use successive rising with graded alcohols to dehydrate
11. Immerse in xylene twice for 15 minutes each time
12. Use DPX mounting medium to cover sections and place coverslip
13. Allow mounting medium to solidify in an oven

M. Toluidine Blue Staining

1. Use an ultramicrotome to cut semi-thin sections
2. Once sections mounted on glass slide, dry rapidly on hotplate set to 90 °C
3. Once off hotplate cover section with 1 % toluidine blue
4. Place slide back on hotplate for approximately 10 seconds
5. Rinse slide under cool running water to remove excess dye
6. Mount and view under a microscope

N. Cell Culture – Thawing of Frozen Cells

1. Place Hank's balance salt solution (HBSS), DMEM, FBS and penicillin/streptomycin (P/S) in a water bath at 37 °C for 15 minutes
2. Stock solution of media is made up by removing 50 mL from 500 mL flask of DMEM and adding 50 ml FBS and 5 mL of P/S. Mix and label carefully be sure to writing date solution was made
3. Using inventory list, locate and remove cell line to be used from cryostorage
4. Place vial in water bath at 37 °C for one to two minutes for defrosting
5. Place vial contents and 7.5 mL of media in a 15 mL tube and centrifuge for 5 minutes at 1200 rpm
6. Decant supernatant
7. Resuspend pellet in 7.5 mL of HBSS at 37 °C
8. Re-centrifuge at 1200 rpm for five minutes
9. Decant supernatant
10. Resuspend in 5 mL of media

O. Cell Culture – Cell Counting

1. Using a 96-well plate, pipette 20 µL of cell suspension to be quantified into a well along with 20 µL of trypan blue (1 in 2 dilution factor)
2. If a particularly abundant sample, can repeat dilution to ge a factor of 1 in 4
3. Ensure haemocytometer is clean (use ethanol and non fibrous tissue) if not and place 10 µL of solution on each side of haemocytometer
4. Place on microscope stage and visualise counting grid
5. Using a counter, count cells, ignoring those on edge of grid at bottom and lower right but including those on top and upper left. Exclude non-viable cells (stained dark blue)
6. Repeat procedure for opposite side of haemocytometer using the same inclusion/exclusion criteria
7. Calculate cell number per mL by multiplying total count by dilution factor and 10^4

P. Cell Culture – Cell Seeding

1. Using established protocols, deduce the ideal concentration of cells per surface area for the culture flask you are using
2. Add correct volume of cell suspension solution to flask to achieve said concentration
3. Label flask correctly
4. Incubate at 37 °C and 5 % CO_2 for desired time point

Q. Cell Culture – Maintenance and Feeding

1. Remove flask from incubator and place in sterile fume hood
2. Invert and decant media
3. Replace with 10 mL of fresh media
4. Replace lid, invert flask
5. Ensure media covers cell containing side of flask
6. Perform cursory check of cells ensuring integrity

R. Peptide Synthesis

1. Change inline filter and ensure top and bottom filters are adequate
2. Ensure adequate amounts of reagents in relevant reservoirs
    i. 2 L NMP (minimum)
    ii. 500 mL DCM (minimum)
    iii. 250 mL piperidine (minimum)
    iv. 15.3 g HOBt + 38 g HBTU + 38 g HBTU in 200 mL DMF
    v. 70 mL DIEA + 130 mL NMP (minimum 100 mL)
3. Weigh out appropriate mass of resin dependent on scale of production (i.e. 0.1 mmol for small reactor vessel pr 0.25 mmol for large reactor vessel)
4. Weigh out 1 mmol (i.e. 10 excess) of each protected amino acid and place in correctly labelled cartridge
5. Seal each cartridge with a Wheaton seal
6. Place on Applied Biosystems 433A peptide synthesiser in order with C-terminus on far right (1st position on synthesiser)

7. Ensure waste container empty and check nitrogen pressure (should be over 60 bar)
8. Ensure correct program running on synthesiser software and begin
9. Reaction time takes approximately one hour per cartridge/amino acid

S. Peptide Immobilisation

1. Weigh fibre to be modified and place in 1 mL Epindorff tube
2. Quickly make up an appropriate volume of SNA solution (12 % w/v in Na_2HCO_3)
3. Immerse fibre in an excess of SNA solution for two hours
4. Wash with MES
5. Immerse fibre in excess of EDC/NHS solution (0.2 M : 0.01 M in MES at pH 5.5) for 2 hours
6. Wash quickly with MES pH 5.5
7. Place now activated collagen fibre in peptide solution of desired concentration for two hours
8. Wash with MES and allow air dry

T. TNBSA Assay

1. Prepare a fresh stock of 5 % TNBSA solution in Na_2HCO_3
2. Pipette 500 µL of solution to be analysed into an Epindorff tube
3. Add 250 µL of stock TNBSA
4. Incubate at 37 °C for two hours
5. Add 250 µL of SDS and 125 µL of 1 M HCl
6. Measure absorbance on plate reader at 335 nm

U. Publications

1. J Doody, D Zeugolis, G Kelly, M Devocelle, M Kilcoyne, L Joshi, J Kelly, A Pandit. A strategy for sialylation of a collagen scaffold to promote neural regeneration and modulates host inflammatory response when used as a nerve grafting biomaterial. *Ir J Med Sci.* 2010/09/01 2010;179(9):313-373
2. J Doody, W Daly, D Zeugolis, G Kelly, M Kilcoyne, M Devocelle, A Pandit, J Kelly, L Joshi. A polysialic acid mimetic peptide modified collagen fibre conduit promotes peripheral nerve regeneration. *Ir J Med Sci.* 2011/09/01 2011;180(8):233-284

V. Podium Presentations

1. J Doody, D Zeugolis, G Kelly, M Devocelle, M Kilcoyne, L Joshi, J Kelly, A Pandit.(2010); A Strategy for Sialylation of a Collagen Scaffold to Promote Neural Regeneration and Modulates Host Inflammatory Response when used as a Nerve Grafting Biomaterial. September. Plenary Session, XXXVth Sir Peter Freyer Memorial Lecture and Surgical Symposium. Galway
2. J Doody, D Zeugolis, M Monaghan, G Kelly, M Devocelle, M Kilcoyne, L Joshi, J Kelly, A Pandit (2010); Collagen Fibres Modified with Polysialic Mimetic Peptide are a Suitable Material for Use as a Synthetic Peripheral Nerve Graft. 26th November. Irish Association of Plastic Surgery Meeting, Eccles Street, Dublin
3. J Doody, W Daly, D Zeugolis, G Kelly, M Kilcoyne, M Devocelle, A Pandit, J Kelly, L Joshi. (2011); A polysialic acid mimetic peptide modified collagen fibre conduit promotes peripheral nerve regeneration. September. XXXVIth Sir Peter Freyer Memorial Lecture and Surgical Symposium. Galway